Batteryboat

An effective solution
to store and transport
solar energy

R.Reiff

Batteryboat

An effective solution to store and transport solar energy

by

R. Reiff

in partial fulfillment of the requirements for the degree of

Master of Science
in Mechanical Engineering

at the Delft University of Technology,
to be defended publicly on Monday February 19, 2018 at 9:00 AM.

Chairman:	Prof. dr. ir. W. de Jong,	TU Delft
Thesis committee:	Prof. dr. ir. J. J. Hopman,	TU Delft
	Dr. A. Purushothaman Vellayani,	TU Delft
	Ing. D. Hoogendoorn,	DAMEN

This thesis is confidential and cannot be made public until December 31, 2022.

DAMEN

TU Delft Delft University of Technology

Preface

This thesis has been written to conclude the Master of Science program in Mechanical Engineering with the track Energy- & Process Technology (EPT) offered by the faculty of 3mE at the Delft University of Technology. Writing this thesis has given me a great inside in large-scale energy storage solutions, which is of huge importance to facilitate the energy transition.

During my Bachelor I saw a documentary about the Sahara Forest Project. This is a project that aims to provide fresh water, food and renewable energy in hot arid regions as the desert, which fascinated me. From this day on I got more and more attracted to creating a sustainable future. After my Bachelor, my passion for renewable energy solutions made me eventually switch from Aerospace Engineering to Energy- & Process Technology.

This research presents a feasibility study done on large-scale energy storage in combination with the transportation by tankers. It is satisfying to see the willingness of DAMEN to change and to create a sustainable future in such a conservative market.

I would like to express my gratitude to my supervisors Wiebren de Jong from the TU Delft and Don Hoogendoorn from DAMEN. Many hours of meetings, discussions and conversations over the last year have contributed to the final version of this report. Your experiences and insights gave me a great understanding in large-scale energy storage in combination with the mindset needed during a research process.

Abstract

Climate change, depletion of fossil fuels, and economic concerns are among the main drivers of sustainable energy transition. The Netherlands has drawn up ambitious goals in the energy transition. However, numerous studies have shown that there is a lack of space in the Netherlands to adapt to a 100% green economy. To solve this dilemma it is necessary to import renewable energy from other countries. Solar electricity prices are dropping rapidly in high solar irradiation areas and are currently the worlds cheapest source of electricity, likewise this is in places where space is often abundant. This thesis examines the techno-economical feasibility of importing solar energy from Morocco to the Netherlands. As subsidized solar electricity is bought by the Dutch government for 0.125 €/kWh, the target is to find a solution below this demand. All energy storage systems are analyzed thoroughly and an energy and cost analysis is performed for a cable, chemical energy storage, thermal energy storage and liquid air energy storage.

A HVDC submarine power cable between Morocco and the Netherlands is compared in proportion to the costs and distance of the NorNed cable. A HVDC submarine power cable over a distance of 2600 km results in a LCoE of 0.113 €/kWh. Other energy storage systems use a tanker to transport the stored energy. In this thesis liquid hydrogen, ammonia and methanol are analyzed as chemical energy storage systems. Liquid hydrogen is produced by cooling and expanding hydrogen, ammonia is produced by the Haber-Bosch process and methanol is formed by reacting H_2 and CO_2. Fuel cells are used to convert fuels back into electricity. The most efficient and cost effective solution for chemical energy storage is storing electricity in the form of liquid hydrogen. A round-trip efficiency of 27% with a LCoE of 0.491 €/kWh is obtained in 2015, from the predictions of 2030 a round-trip efficiency of 40% with a LCoE of 0.159 €/kWh is derived. The next concept is based on thermal energy storage with Solar Salt as energy carrier. Solar Salt is heated in the receiver of a solar tower where heat from the sun is concentrated to by heliostats. Hot Solar Salt is transported to the Netherlands by a tanker and a steam cycle is driven utilizing the heat of hot Solar Salt. The energy efficiency obtained from solar irradiation to electricity in the Netherlands is 28%, the output power is only 1% less than the output power should be if the power block was located in Morocco. An electricity price of 0.164 €/kWh is obtained, but if heat is delivered a heat price of 0.069 €/kWh can be realized. The final designed energy storage system combines liquid air with the heat of hot Solar Salt. Liquid air and hot Solar Salt are produced in Morocco and in the Netherlands electricity is produced with high efficiencies due to the large temperature differences. The system described results in a electricity price of 0.108 €/kWh with an energy efficiency of 58.7% from electricity and hot Solar Salt to electricity in the Netherlands.

It is concluded that storing electricity in chemical energy storage via the processes described in this thesis will lead to too high costs to be used as energy storage solution. There are possibilities in direct fuel conversion technologies due to high conversion efficiencies, only developments are still in its experimental phase. The combination of liquid air with Solar Salt complies to the cost requirement, some more research is required on the electricity generation process described, but the concept shows a lot of potential. Finally, heat of Solar Salt can be provided at a price of 0.069 €/kWh, subsidized solar heat is bought by the Dutch government for 0.095 €/kWh. This gives possibilities to effectuate a business case.

Contents

List of Figures

List of Tables

List of Symbols & Abbreviations

$\dot{m}$	Mass Flow
η	Efficiency
ρ	Density
AC	Alternating Current
ASU	Air Separation Unit
C	Cost
c_p	Specific Heat Capacity
$CAES$	Compressed Air Energy Storage
$CAPEX$	Capital Expenditures
CF	Capacity Factor
CRF	Capital Recovery Factor
CSP	Concentrated Solar Power
DHI	Direct Horizontal Irradiation
DWT	Deadweight Tonnage
E	Energy
ED	Energy Density
EXP	Turboexpander
GHI	Global Horizontal Irradiation
GNI	Direct Normal Irradiation
GTI	Global Tilted Irradiation
h	Enthalpy
HE	Heat Exchanger
HHV	Higher Heating Value
$HVDC$	High Voltage Direct Current
$J-T$	Joule-Thomson
LA	Liquid Air
$LAES$	Liquid Air Energy Storage
$LCoE$	Levelized Cost of Electricity
LHV	Lower Heating Value
m	Mass
MS	Molten Salt
$O\&M$	Operation & Maintenance
p	Pressure
PCM	Phase Changing Material
PEM	Proton Exchange Membrane
PV	Photovoltaics
Q	Heat
s	Entropy
$SDE+$	Stimulering Duurzame Energieproductie
SE	Specific Energy
SOE	Solid Oxide Electrolysis
$SOFC$	Solid Oxide Fuel Cell
T	Temperature
TES	Thermal Energy Storage
TRL	Technology Readiness Level
$ULCC$	Ultra Large Crude Carrier
W	Work

Chapter 1

Introduction

Since the beginning of the industrial revolution humanity is significantly influencing the climate, the emission of greenhouse gases has led to a significant temperature rise. According to NASA the global mean temperature in 2016 was 0.99 °C above the average temperature during the base period 1951-1980 [21]. Scientists have predicted that life on earth will be irreversibly changed if global warming passes the barrier of 2 °C. More and heavier natural disasters, major mass extinction and melting of the arctic (which will cause even more greenhouse gases to be released), are some of the expected consequences. To prevent this from happening, 195 countries signed the Paris climate agreement at the 21^{st} Conference of the Parties of the United Nations Framework Convention on Climate Change in Paris in December 2015.

1.1 Problem Statement

The target for the Netherlands set in the Paris climate agreement is to have 14% renewable energy of its total energy consumption in 2020. In 2014 and 2015 this was only 5.5% and 5.8% respectively [22], only a growth of 0.3 percentage point in one year. The Netherlands need to take more action to fulfill these requirements. The EU has set itself a long-term goal of reducing greenhouse gas emissions by 80-95% in 2050 [23].

To generate the total energy consumption of the Netherlands in a sustainable way will demand a lot of space. 17% of the total area of the Netherlands (land and sea) should be filled with solar panels or 104% of the total area needs to be occupied by wind turbines to obtain a 100% green economy, see Appendix A [24]. In these calculations energy storage is not taken into account and no spacing between solar panels is used. Together with the fact that space is already limited, it seems to be almost impossible to reach a 100% green economy using only land in the Netherlands.

Another problem is the intermittency of wind and solar power. There are different solutions for this problem; smart charging, oversize peak generation, interconnect geographically dispersed and technologically diverse renewable generation types, and of course energy storage. Creating a grid base load obtained by renewable energy sources is one of the challenges for the energy transition to a sustainable future. A solution to these problems could be to import sustainable energy.

1.2 Subsidized Solar Electricity in the Netherlands

The electricity price achieved in the Netherlands is dependent on the subsidy of the Dutch government. The subsidy program of the Netherlands is called SDE+. The SDE+ is an exploitation subsidy; this means that producers receive a subsidy for the renewable energy they generate, because the cost price of renewable energy is higher than that for energy from fossil fuels. SDE+ reimburses the difference between the cost price of renewable energy and the market value of the energy supplied: the unprofitable top. The subsidy is granted over a period of 8, 12 or 15 years. The amount of years and the amount of subsidy depends on the technology used and the quantity of renewable energy produced.

The Dutch government has a budget for all renewable energy sources; biomass, solar, hydro, geothermic and wind. The SDE+ program has two opening rounds in 2017, per opening round €6 billion is reserved for all categories together. Every round has three phases with all a maximum phase amount; for solar energy the first phase is sold for 0.09 $€/kWh$, the second phase for 0.11 $€/kWh$ and the third phase for 0.125 $€/kWh$. If the €6 billion budget is finished, no more subsidies are issued [25]. Last spring a part of the budget remained partially untapped [26]. The goal is to find a business case with a levelized cost of electricity (LCoE) of 0.125 $€/kWh$, but preferably lower to increase the opportunities of obtaining subsidies.

1.3 Market Potential

Solar energy is rapidly becoming the cheapest source of energy on this planet. In only 2 years the price in auctions of solar electricity has tumbled down from $6ct to $2.4ct per kWh in Abu Dhabi [27]. Solar energy can be produced worldwide, but the highest solar irradiation is found in areas around the equator. In the Netherlands subsidized solar electricity is bought from 0.09 $€/kW$ till 0.125 $€/kW$ [25]. This is done to stimulate cheaper renewable energy projects, since the possibility of the budget being finished is significantly lower in the 1^{st} round than the 3^{rd} round. This facilitates a market to transport sustainable energy from areas around the equator to the northern and southern latitudes in a similar manner as a conventional oil tanker. DAMEN would like to investigate the possibilities in this market. This thesis will investigate the market opportunities of importing solar energy.

1.4 Research Questions

The information given in the last sections lead to the following main research question of this thesis:

"Is it techno-economically feasible to store and transport solar energy using maritime shipping from areas with high solar irradiance to the Netherlands."

The corresponding subquestions are:

- *What area's will be considered?*
  What are existing and potential area's in the world where solar electricity can be cheaply generated, what systems are used to obtain the electricity. This is explained in Chapter 2.
- *At what order of power is the project operating?*
  The state-of-the-art solar power plants power outputs are discussed in Chapter 2. On behalf of these power outputs, the energy imported for this project is determined. The power output in the Netherlands depends on the round-trip efficiency of the relevant energy carrier.

- *What are promising energy carriers?*
  In Chapter 3 and Chapter 4 all the potential energy carriers to store and transport electricity are obtained.
- *How to select the right energy carrier?*
  In Chapter 3 and Chapter 4 the energy carriers will be analyzed on the costs, specific energy and round trip efficiency to obtain the cheapest and most efficient energy storage system.
- *Which components are needed?*
  What components are needed to fulfill the operation, and what are the corresponding costs of those components.
- *What are the energy conversions through out the whole chain?*
  An energy diagram is given for all the selected concepts. The losses from electricity to energy storage, transport losses and the losses from energy storage to electricity are calculated.
- *Which concept will lead to the lowest CAPEX and LCoE?*
  The CAPEX and LCoE of the final concepts will be calculated, from this a potential business can be derived to store and transport energy at this moment, or in the future.

1.5 Report Structure and Methodology

In Chapter 2 the processes to generate electricity from solar energy are investigated. The area's with high solar irradiance with corresponding state-of-the-art prices and power sizes are shown. In Chapter 3 all energy storage concepts are surveyed and selected by means of their specific energy and round-trip efficiencies. The chemical energy storage concepts are analyzed in Chapter 4. For thermal energy storage the specifications of CSP are used as input, because this is more efficient. For all other energy storage options, electricity obtained by PV systems is used. The most promising energy storage systems obtained with chemical energy storage are liquid hydrogen, methanol and ammonia. Chapter 2 describes these synthesizes processes, the costs are calculated and block diagrams and energy flows of the process are given. In Chapter 5 a design will be made where molten salt is used as energy carrier and finally in Chapter 6 a design will be made with liquid air and molten salt combined. For an overview of the report structure, see Figure 1.1.

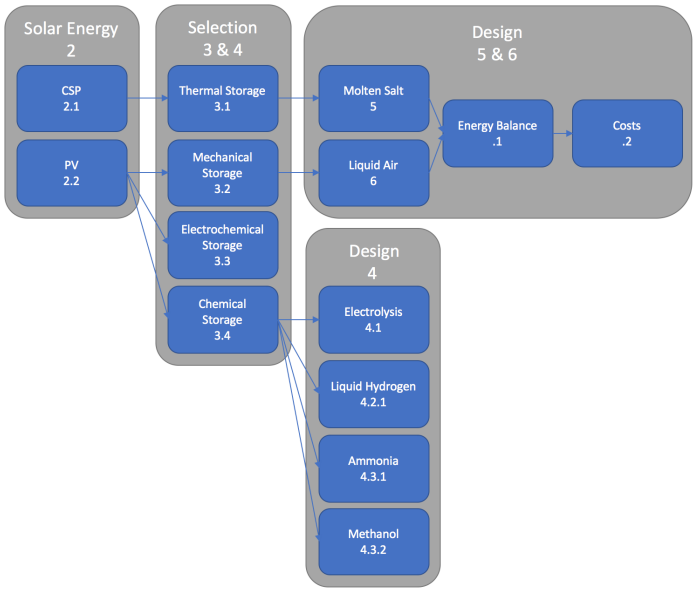

Figure 1.1: Overview of the report structure

Chapter 2

Solar Energy

The sun provides the earth with a staggering quantity of energy. In one hour the sun radiates more energy to the earth than the world consumes in one year. The energy is used by all living organisms in the world. Solar energy can be used passively; by heating and lighting a room. Or actively; by capturing, storing and converting solar energy into electricity. The two main systems used to produce electricity from solar energy are: Concentrated solar power (CSP) and photovoltaics (PV). In Section 2.2 and Section 2.3 the working principle of these systems are described, also an overview of the state-of-the-art power capacities and electricity prices is given. CSP will only be used for thermal energy storage concepts in further chapters, for chemical and cryogenic energy storage, always electricity obtained from PV systems is taken as input. In Section 2.1 all the potential geographical areas where CSP and PV systems can be profitable are displayed. The area with the best characteristics for CSP and PV and the shortest distance to the Netherlands will be taken as area where the solar energy will be imported from. In Section 2.4 the costs of a submarine high voltage direct current (HVDC) cable are calculated to find out if this is a viable solution, otherwise ships will be used.

2.1 High Irradiation Areas

There are different types of irradiance; direct normal irradiance (DNI), diffuse horizontal irradiance (DHI) and global horizontal irradiance (GHI). DNI is the amount of radiation received by a surface that is always held perpendicular to the sun. DHI is the amount of radiation received on a horizontal plane which does not come from a direct path of the sun, but is scattered by for instance clouds or buildings. GHI is the sum of DNI and DHI received on a horizontal plane, this means that the DNI has to be corrected for the zenith angle of the sun, see Equation (2.1).

$$GHI = DNI \cdot cos(\theta) + DHI \tag{2.1}$$

To look for appropriate areas with respect to CSP systems, the direct normal irradiation (DNI) is essential. For PV systems also the diffuse horizontal irradiation is important. This is due to the fact that heliostats reflect only the direct normal irradiation, while for PV systems also indirect radiation is converted into electricity. To obtain the total irradiation used by PV plants, the GHI is not used because the GHI is calculated using a fixed horizontal plane, while PV plants have solar tracking systems which will point the PV system into the direction where the irradiation is the highest at a specific moment. To calculate the total irradiance on a PV system, the DNI and DHI are added without multiplying the DNI with the zenith angle of the sun, this is called the global tilted irradiation (GTI), see Equation (2.2). The

assumption made is that the DHI is the same for a horizontal plane as a tilted plane, since the diffuse irradiation comes from all directions.

$$GTI = DNI + GHI \tag{2.2}$$

Looking at Figure 2.1 it can be seen that the areas around the world with the highest solar irradiance are; Chile, North Africa, South Africa, Australia, Middle East and Central America. See Appendix B for more GHI and DNI maps of the world and zoomed in on Africa and the Middle East.

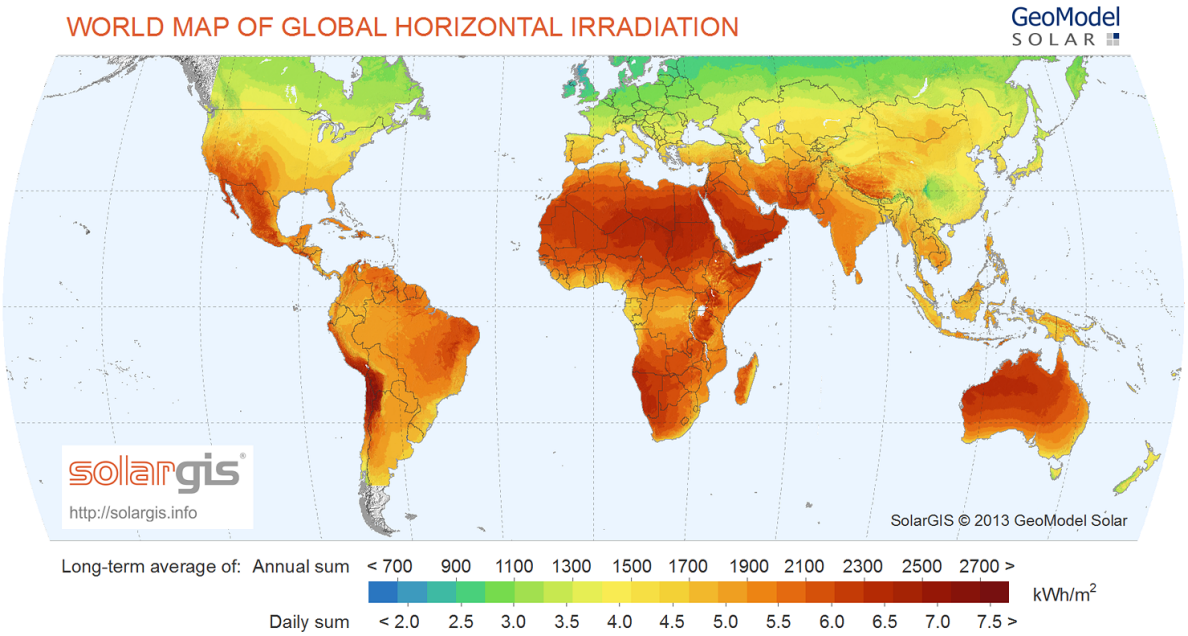

Figure 2.1: Global Horizontal Irradiation World [1]

2.1.1 Geographic Location Selection

Without looking at the efficiencies and costs for the energy storage system used, two other inputs are of great importance to obtain low cost electricity in the Netherlands; the purchase price of electricity and the distance the stored energy has to be transported over. Obviously, importing electricity to the Netherlands would be the cheapest if the purchase price is the lowest and the transported distance is the shortest. Looking at Table 2.3 and Table 2.4, most of the project are situated in the Arab Gulf States. Comparing regions in Figure 2.1 with the GHI of the Arab Gulf States, it can be seen that Morocco is the country closest to the Netherlands with an irradiation comparable to that of the Arab Gulf States. Also the political situation in Morocco is stable compared to the other countries in Africa and the Middle East. At this moment, only the NOOR III CSP project is situated in Morocco and it is expensive compared to other projects, see Table 2.3. Most of the recent projects being built are in the United Arab Emirates and at this moment the largest solar park of the world is being built in Dubai [28]. The goal is to generate 5000 MW of solar power by 2030, with PV and CSP power combined. PV systems are cheaper than CSP plants, but not able to produce electricity at night.

Nowadays the largest and cheapest CSP plants and PV systems are realized among others in Dubai, see Table 2.3 and Table 2.4. Comparing Dubai to Agadir, the solar irradiation in Morocco is better, see Figure 2.2. Agadir is chosen because it is a city with high solar irradiation in Morocco with direct access to the sea. Using the Solargis Imaps App it is found that the average DNI and DHI of Agadir is 2281

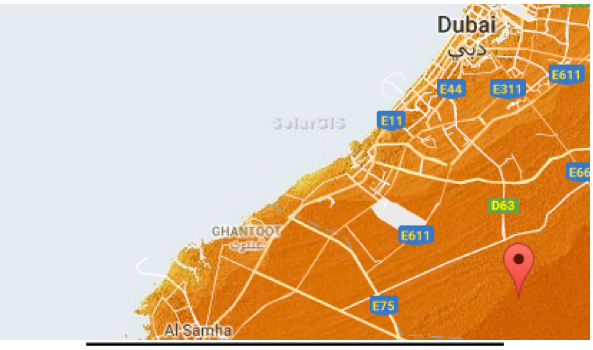

Solar irradiation (yearly average)		
GHI	2195	kWh/m^2
DHI	867	kWh/m^2
DNI	1975	kWh/m^2

(a) Solar irradiation Dubai [1]

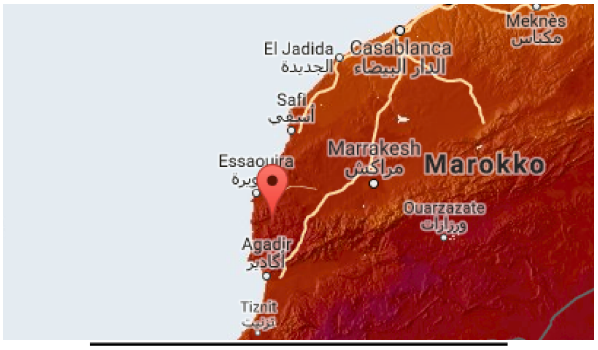

Solar irradiation (yearly average)		
GHI	2088	kWh/m^2
DHI	640	kWh/m^2
DNI	2281	kWh/m^2

(b) Solar irradiation Agadir [1]

Figure 2.2: Solar irradiation Agadir and Dubai [1]

$kWh/m^2/year$ and 640 $kWh/m^2/year$ respectively, while for Dubai the average DNI and DHI are 1975 $kWh/m^2/year$ and 867 $kWh/m^2/year$ respectively, see Figure 2.2. CSP plants have more potential in Agadir then Dubai, because the DNI is higher in Morocco. Also PV plants have more potential in Agadir than in Dubai if a solar tracking system is used, because the GTI is higher in Morocco. Morocco is also busy expanding there solar energy production [29], therefore the potential route Morocco - the Netherlands is chosen, or more precise: Agadir - Rotterdam.

2.1.2 Irradiation Variation

It is also important to know the monthly DNI and GHI throughout the year. In Figure 2.3 it can be seen that the DNI and GHI in Morocco are only 60% in the winter compared to the summer. Figure 2.3 gives an overview of the DHI and DNI in Ouarzazate, a city in the centre of Morocco where CSP projects are situated. It is assumed that the monthly irradiation variation is the same in Agadir. Less energy will be stored and transported during the winter and it is reasoned that in autumn and spring the power plants will produce 80% of their full power per day and during the winter this will only be 60%.

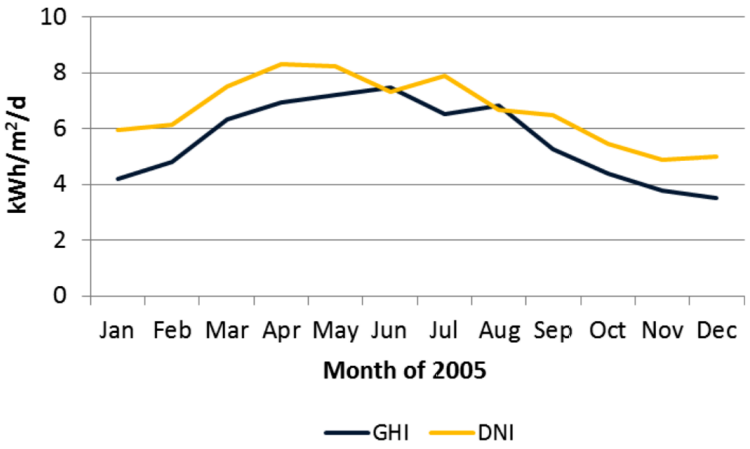

Figure 2.3: Monthly variation DNI and GHI in Ouarzazate, Morroco 2005 [2]

2.2 Concentrated Solar Power

There are three different systems that make use of concentrated solar power; the parabolic trough system, the power tower systems and the dish engine system. At this moment the power tower system and the parabolic trough system are produced on commercial scale, the maturity of dish engine systems is lower. The cheapest and most energy efficient option at this moment is the power tower system [30], since it is able to reach higher temperatures which results in higher Rankine cycle efficiencies. Whenever concentrated solar power is mentioned, the power tower system is used.

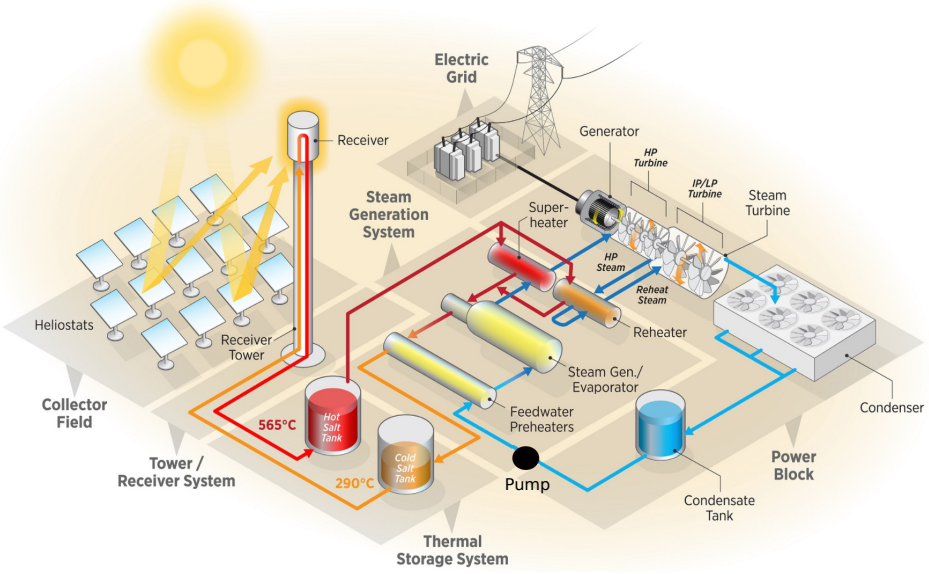

Figure 2.4: Solar power tower system [3]

The solar power tower system consists out of a collector field, wherein over a 100,000 heliostats are placed for a 150 MW system, a receiver system, a thermal storage system and a power block. The collector field concentrates sunlight onto the receiver. In the receiver the concentrated sunlight heats molten salt from 290 °C to 565 °C, where molten salt always stays in the liquid phase. The molten salt used is known as 'solar salt' and the mixture consists out of 60wt% sodium nitrate ($NaNO_3$) and 40wt% potassium nitrate (KNO_3). The heated molten salt can be stored in storage tanks. Hot molten salt is then used to convert pressurized water into pressurized steam, for this several heat exchangers are used. The pressurized and heated steam runs through a steam turbine where it generates electricity. The low pressure, low temperature steam which leaves the steam turbine is condensed into water in the condensate tank. Water is pressurized using a pump and the cycle starts all over again. This process can be seen in Figure 2.4. The big advantage of concentrated solar power over photovoltaics is the ability to store the heated molten salt. The steam turbine system is therefore also able to operate at night, which results in a more reliable base load electricity source.

2.2.1 Electricity Price & Power Capacity

In Table 2.3, an overview of different concentrated solar power projects is given. Comparing Table 2.3 and Figure 2.1, it can be seen that the countries of the projects all have a high irradiation. The typical power capacity of a single solar tower system lies between 100 - 150 MW; for the project in Dubai this was not clarified. Another point worth mentioning is the high capacity factor of the Copiapo plant in Chile. The plant will operate for a large part of the year 24 hours per day, with a capacity factor over the whole year of 80%. The capacity factor is the ratio of the actual electrical output of the CSP plant

per year to the maximum possible electrical output of the CSP per year. If the storage capacity of a CSP plant is enlarged, the capacity factor of the CSP plant will also increase since the CSP plant will operate for more hours during the night at full power. The prices of CSP are rapidly dropping every year. Although the prices in Morocco are high compared to Dubai, the solar irradiation conditions are better in Morocco: The direct normal irradiation in Dubai is 1975 $kWh/m^2/year$, while Noor III obtains a direct normal irradiation of 2600 $kWh/m^2/year$ [31]. One of the explanations of this difference is the large price drop in the period 2015 to 2018; in 2015 the Noor III project started, while the project in Dubai starts in 2018. In Chile the auction price in 2014 for a CSP plant was 0.11 €/kWh [32], while in 2017 the auction price tumbled down to 0.057 €/kWh [30].

Table 2.3: Overview specifications CSP plants

Project	**Country**	**Power** [$\mathbf{MW}_e$]	**Capacity** [$\mathbf{GWh}_e$/**yr**]	**Storage** [**hr**]	**Operating** [**yr**]	**Auction Price** [**€/kWh**]
NOOR III [33]	Morocco	150	500	8	2017	0.136
Redstone [34]	South Africa	100	480	12	2018	0.113
Copiapo [35]	Chile	260 ($2 \cdot 130$)	1800	13	2019	0.057
Dubai [36]	UAE	700 ($5 \cdot 140$)	-	15	2020	0.066
Port Augusta [37]	Australia	150	495	7	2020	0.055

A significant growth in global CSP capacity is foreseen, rising from the current 4.7 GW to reach a capacity between 10 GW and 22 GW by 2025 [38]. With the increase in CSP capacity and the decreasing price trend of the last years, see Table 2.3, it is reasoned that in high irradiance areas a CSP plant with an electricity price between 0.055 and 0.066 €/kWh is realistic. Because the conditions in Morocco are better than the conditions in Dubai, a price of **0.057** €/kWh is taken.

The state-of-the-art CSP systems are able to reach a power output of 150 MW of electricity. It is assumed that 2 CSP plants are operating next to each other generating a total power of **300** MW. The amount of 2 CSP plants is taken because nowadays it is common to build 1 or 2 CSP plants at one site. With a capacity factor the same as in Chile (80%), the annually produced energy will be **2100** GWh. Correcting this for the irradiation variation, this leads to a power output of 300 MW during summer, 240 MW during autumn and spring, and 160 MW during winter.

Heat Price

The goal of the energy storage based on CSP is to transport thermal energy from Morocco to the Netherlands. Therefore it is necessary to calculate the cost to heat molten salt right after the thermal storage system, because from this point the molten salt can be transported. This is done by dissecting the CSP tower system into multiple sections. In Figure 2.5 the cost breakdown of a CSP tower system is shown. The energy efficiency of the power block is 42% [39], this is also confirmed by Thomas Bauer from the German Aerospace Center (DLR).

Looking at Figure 2.5, it can be seen that around 75% of the total costs are the receiver system, heliostat field, thermal energy storage system, tower and a part of the costs for engineering and site preparation, contingencies and owners costs. The other 25% are the costs of the power block, balance op plant and the other part of the costs for engineering and site preparation, contingencies and owners costs. It is assumed that the O&M, personnel and other variable costs are divided in the same proportion. So the costs to heat molten salt including storage are 75% of the total costs. Also the ratio of kWh_{th} to kWh_e needs to be accounted for; with an energy efficiency of the power block of 42%, 1 kWh of heat is needed to produce 0.42 kWh of electricity. Therefore the price per kWh of heat drops by a factor of 0.42. This leads to a price of 0.018 €ct/kWh to heat and store molten salt, see Equation (2.3).

$$Price_{heat} = 0.0573 \cdot 0.75 \cdot 0.42 = 0.018€/kWh \tag{2.3}$$

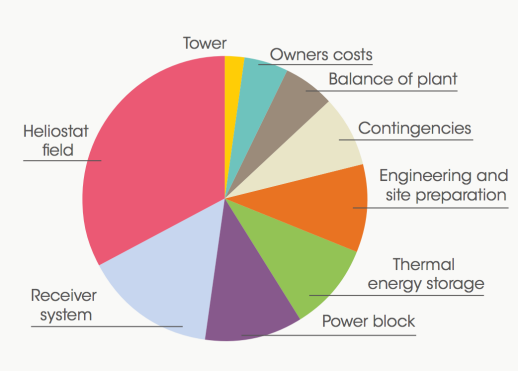

Figure 2.5: Cost breakdown CSP tower South Africa 100 MW 15hr storage [4]

2.3 Photovoltaic system

A photovoltaic (PV) cell is an electronic device which directly converts photons into electricity. If the energy of a photon is large enough, the semiconducting material absorbs the photon and creates an electron-hole pair. This is the energy needed for an electron to break free from its bond. When an electron breaks free this leaves an empty space which is called a hole, a hole is similar to an electron, but with a positive charge. The electron runs through the external load creating a current, after passing through the load the electron meets up with a hole completing the circuit, see Figure 2.6.

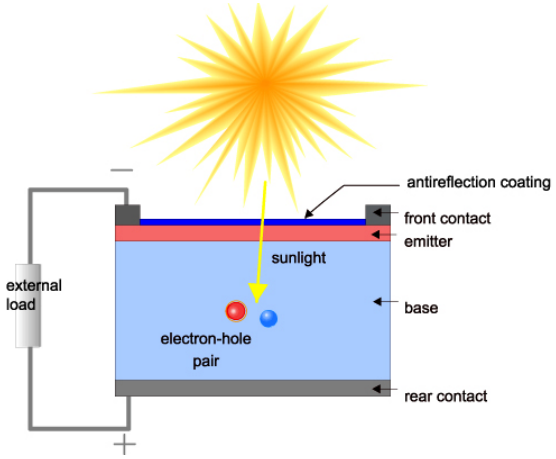

Figure 2.6: PV cell [5]

A PV system consists of several components, except for a PV cell it also contains mounting and cabling of the whole system. For large PV projects solar tracking systems are often used to improve the systems performance by pointing the PV panels to the direction with the most irradiation.

2.3.1 Electricity Price & Power Capacity

In Table 2.4 an overview of some operating and under construction standing PV systems is given. The prices are significantly lower than for CSP projects, but for PV systems no storage is included. In Abu Dhabi a large PV project is under construction, at this site 1177 MW of power will be generated. In China and India there are already existing PV sites with a power of 900 - 1500 MW [40], they are not mentioned in the overview because no prices are known.

Table 2.4: Overview specifications PV plants

Project	**Size [MW]**	**Operating [yr]**	**Auction Price [€/kWh]**
Zambia [41]	47	2017	0.0545
Dubai [42]	800	2018	0.0272
Abu Dhabi [43]	1177	2019	0.0220
Saudi Arabia [44]	300	2019	0.0163
Chile [45]	242	2024	0.0195

With the large amount of new PV projects issued and the prices which continues to drop, see Table 2.4, it is assumed that the maximum power capacity in high solar irradiance areas is 800 MW with an electricity price of 0.022 €/kWh. A capacity factor of 30% is taken, this capacity factor is obtained in the US and Libya [46] [47], it is assumed the same for Morocco. This results in **2100** GWh electricity production per year. In the summer the PV system will produce 7200 MWh/day of electricity, taking the irradiation variation into account, which corresponds to 9 hours of operation at peak-load. In the autumn and spring the capacity of the PV system is 7.2 peak-load hours/day and in the winter this becomes only 5.4 peak-load hours/day.

2.4 Cable or Ship

The first solution which comes to mind to transport electricity is to use cables. In this section the possibility of cables is discussed. For long distance transmission, a high-voltage direct current (HVDC) electric power transmission system is normally used instead of the more common alternating current (AC) systems. HVDC transmission systems are less expensive over large distances and suffers lower electrical losses. However, they need to have an AC-DC and a DC-AC converter, therefore HVDC transmission lines are only used for larger distances [48]. HVDC power cables can be used over land or underwater. Cables over land will be difficult, because cables have to pass three countries (Spain, France and Belgium) before it reaches the Netherlands. These countries will not allow such transmission lines through their territory for free. The exact price is impossible to calculate, but it is assumed to be too high to suffice the 0.125 €/kWh criteria set in Section 1.2.

Table 2.5: Cable Morocco - the Netherlands in ratio with NORNED

	Cable NorNed [49]	Cable MarNed
Length [km]	580	2600
Efficiency [%]	95.8%	82.5%
CAPEX [M€]	600	2690
O&M (0.4%) [M€]	2	11
Power output [MW]	670.6	577.5
Lifetime [yr]	20	20
CRF_{30year} (r=5%) [-]	1.605	1.605
$C_{cable30year}$ [M€]	1011	4532
$E_{30year,PV}$ [TWh]	35.3	30.4
$E_{30year,CSP}$ [TWh]	94.0	81.0
$LCoE_{cable,PV}$ [€ct/kWh]	2.87	14.92
$LCoE_{cable,CSP}$ [€ct/kWh]	1.07	5.60
$LCoE_{cable}$ + $LCoE_{PV}$ [€ct/kWh]	5.07	17.12
$LCoE_{cable}$ + $LCoE_{CSP}$ [€ct/kWh]	6.80	11.33

Submarine power cables are used to interconnect countries over large distances underwater. One

of the largest submarine power cable in the world is the NorNed cable, this cable interconnects the electrical grids of the Netherlands and Norway. To estimate the costs of such a cable from Morocco to the Netherlands (MarNed), the costs of the NorNed cable are proportionally taken over the distance, see Table 2.5. The NorNed cable has a length of 580 km, while the MarNed cable should have a length of 2600 km, this is the distance between Morocco and Agadir over sea. Therefore all the costs of the MarNed cable are 2600/580 = 4.48 times the costs of the NorNed cable. The efficiency of the NorNed cable is 95.8%, to obtain the efficiency of the MarNed cable, the efficiency of the NorNed cable is done to the power of the distance ratio, this results in an efficiency of $0.958^{4.48} = 82.5\%$, the power output of the MarNed cable is lower than the power output for NorNed. The O&M costs are taken at 0.4% of the CAPEX per year [50], and the lifetime is set at 20 years [50]. In Equation (2.4) the capital recovery factor (CRF) is calculated. The CRF is the ratio of a constant annuity to the present value of receiving that annuity for a given length of time. In this case this is the factor by which the capital costs have to be paid back for over a lifetime (n) of 20 years with a discount rate (r) of 5%. The CRF over 30 years becomes 1.952.

$$CRF_{30year} = \frac{r(1+r)^n}{(1+r)^n - 1} \cdot n = 1.952 \tag{2.4}$$

The levelized cost of electricity of the cable ($LCoE_{cable}$) is calculated by dividing the total cost over 30 years ($C_{cable30year}$) by the total amount of energy over 30 years ($E_{30years}$). To calculate $E_{30years}$, a capacity factor of 80% and 30% is taken for respectively CSP and PV, as these are the capacity factors obtained for CSP and PV. The maximum power input of both CSP and PV are 700 MW, this is not corrected to the power of 300 MW and 800 MW reasoned in Section 2.2 and Section 2.3, because the prices for such cables are not known. It is assumed that the scale-up benefits of a longer cable for CSP weigh up against the scale-down of the power input. The LCoE of a cable becomes 11.33 €ct/kWh, which is lower than the 0.125 €/kWh criteria set in Section 1.2, which could make it a viable concept. However, it is not known if the 3 countries (Spain, France and Belgium) will allow such transmission lines through their sea territory. It is assumed that the countries will do this for free, so the maximum LCoE in the Netherlands using a ship should be lower than 0.113 €/kWh.

$$LCoE_{cable} = \frac{CAPEX \cdot CRF_{30year} + O\&M \cdot Lifetime}{E_{30year}} \tag{2.5}$$

2.5 Conclusion

There are two main technologies which are used to generate electricity from solar energy; CSP and PV systems. An overview of state-of-the-art CSP and PV systems is given in Table 2.4 and Table 2.3 which gives a maximum power of 300 MW with an electricity price of 5.73 €ct/kWh for CSP and a maximum power of 800 MW with an electricity price of 2.2 €ct/kWh for PV. The price to heat and store molten salt is calculated in Equation (2.3) and is 1.80 €ct/kWh.

Due to the high solar irradiation conditions, close distance and the fact that Morocco is a relatively stable country, Morocco is chosen to be the country where the solar energy will be imported from. The irradiation in the summer is 60% of the irradiation in the winter, this results in less energy which can be transported during the winter. A cable from Morocco to the Netherlands is possible if it is approved politically for free. Concepts where electricity is stored and then transported by ship need to have a LCoE in the Netherlands lower than 0.113 €/kWh to compete with the cable. In the next chapter all energy storage systems are obtained and critically reviewed. All the carefully chosen assumptions the system choice is based on in this chapter are:

Table 2.6: Overview of assumptions

Power CSP	$2 \cdot 150$	MW
Power PV	800	MW
Price electricity CSP	5.73	€ct/kWh_e
Price heat CSP	1.80	€ct/kWh_{th}
Price PV	2.20	€ct/kWh_e
Route	Morocco - the Netherlands	
Ratio summer : winter	0.6	-
Ratio summer : autumn or spring	0.8	-
Price Cable	11.3	€ct/kWh

Chapter 3

Energy Storage Systems & Selection

In this chapter all potential energy storage systems are discussed. After the principles of all the potential energy storage systems are explained, a selection is made in Section 3.4. In Figure 3.1 an overview of different energy storage systems and their typical energy capacities is shown. Flywheels and supercapacitors will not be treated in this chapter due to their low energy capacities. Also pumped hydro power will not be covered, because it is simply impossible to transport gravitational potential energy on a ship. Chemical energy storage will be discussed in Chapter 4, an entire chapter has been assigned to this due to their large energy capacity and large variety of solutions. An overview of all the energy storage methods with their specific energy is given in Table 3.6.

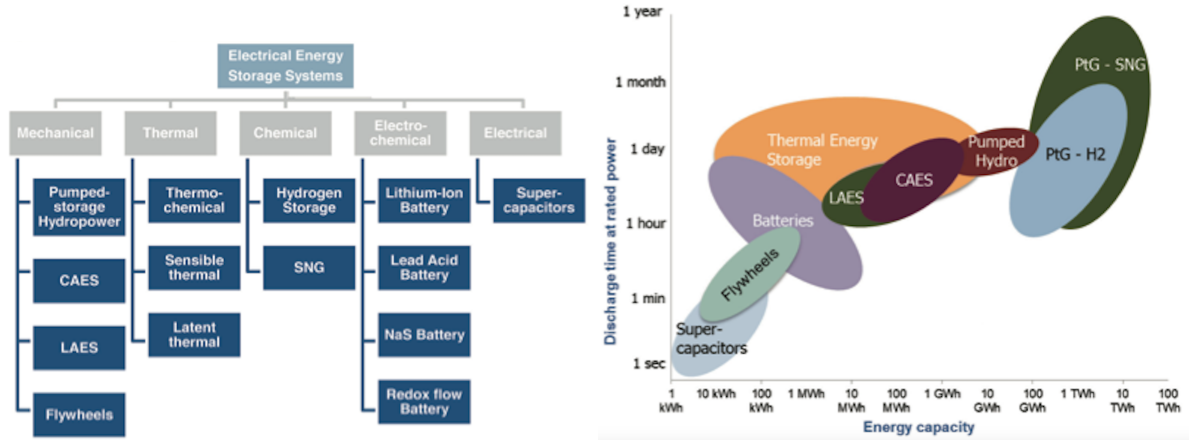

(a) Overview energy storage systems

(b) Energy capacity of storage technologies

Figure 3.1: Energy storage systems [6]

3.1 Thermal Energy Storage

One of the most important forms of energy storage is thermal energy storage. In thermal energy storage (TES) energy is used to heat or cool an energy carrier. This energy carrier can be used for space heating/cooling, water heating/cooling or electricity generation. Space and water heating/cooling is not the goal of this thesis, but it will be taken into account if it can be combined with electricity generation. To convert heat into electricity, steam turbines or heat pumps are often used. To find good thermal energy storage mechanisms it is important to find an energy carrier with the right characteristics. TES can be achieved by three different systems: latent heat storage (LHS), thermochemical heat storage and

sensible heat storage (SHS). In this thesis TES is always combined with CSP, the operating temperature of CSP is 565 °C.

3.1.1 Latent Heat Storage

Latent heat storage (LHS) is based on the heat release or heat absorption during the phase change of a material. This can be from solid to liquid or liquid to vapor, or vice versa. Energy storage in the form of liquid to vapor is not practical as the gas phase requires large volumes or high pressures. The main advantages of phase changing materials (PCM) over sensible heat storage (SHS) are higher energy densities and there is no temperature difference, also LHS is generally more energy efficient. Disadvantages are low thermal conductivity and large change in volume during phase transition, the technology readiness level is also lower. Typical PCM's are paraffin wax, salt hydrates, and fused salts.

When adding energy to a solid PCM, the material will start to increase in temperature as it absorbs the thermal energy. At a specific temperature, the material will start to melt and start its phase transition from solid to liquid, if heat is released the process is reversed. This phase transition will occur at (almost) constant temperature. The amount of energy released during melting is the total difference in enthalpy (h) in solid state and liquid state, see Equation (3.1).

$$q = \Delta_m h \tag{3.1}$$

Nowadays there are several PCM materials which are commercialized, however these materials have a phase change temperature in the range of 112 - 164 °C [16], which is too low to act as suitable energy carrier, because low temperatures will give low Carnot cycle efficiencies. There are a couple of PCM's which have a melting temperature between 500 - 600 °C, but these are not further evaluated due to the low technology readiness level, low thermal conductivity and problems with solid deposits on the heat transfer surface.

3.1.2 Thermochemical Heat Storage

Thermochemical heat storage is a promising concept of storing heat, higher energy densities can be obtained than for SHS and LHS and also there is no heat loss during storage, which makes it very suitable for long-term energy storage. The downside is that it is not sufficiently developed yet.

When adding sufficient heat to a thermochemical energy storage system, a reaction of chemical bonds at the molecular level will separate the thermochemical material. The heat will be stored if the materials are separated, this can be on ambient temperature. After adding the two materials together, the heat will be released again. Figure 3.2 illustrates this process. The energy density of the thermochemical material will depend on the specific enthalpy (h) change during the reaction, see Equation (3.2).

$$q = \Delta_r h \tag{3.2}$$

In Table 3.1 an overview of reactions that have been investigated to be used as thermochemical heat storage is given. When looking for an energy carrier which is suitable for CSP, the temperature should be in the range of 500-600 °C. The reaction with calciumhydroxide ($Ca(OH)_2$) and calciumoxide (CaO) stands out above the rest due to the high energy density, the right reaction temperature and low material costs.

The dehydration/hydration cycle of calciumhydroxide/calciumoxide is shown in Figure 3.3. The idea

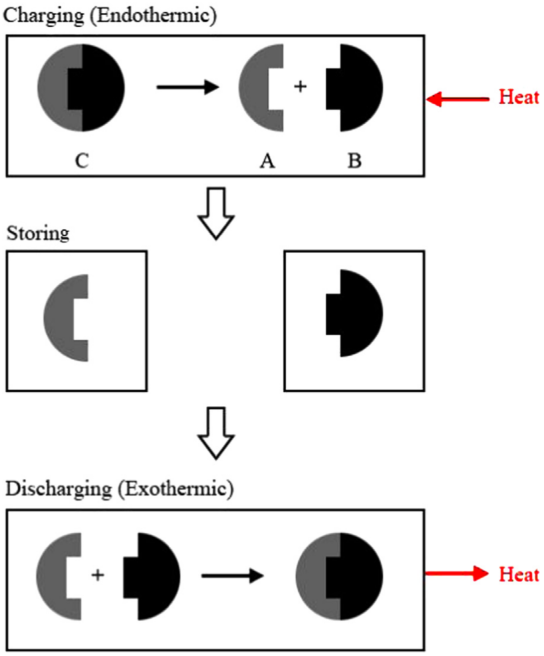

Figure 3.2: Charging, discharging, and storing process of thermochemical heat [7]

Table 3.1: Chemical storage materials and reactions [16]

Compound	Reaction	Material energy density	Reaction temperature [°C]
Ammonia [50]	$NH_3 + \Delta H \leftrightarrow 1/2N_2 + 3/2H_2$	67 kJ/mol	400–500
Methane/water [51]	$CH_4 + H_2O \leftrightarrow CO + 3H_2$	n.a.	500–1000
Hydroxides, e.g. [51]	$Ca(OH_2) \leftrightarrow CaO + H_2O$	3 GJ/m^3	500
Calcium carbonate [51,52]	$CaCO_3 \leftrightarrow CaO + CO_2$	4.4 GJ/m^3	800–900
Iron carbonate [53]	$FeCO_3 \leftrightarrow FeO + CO_2$	2.6 GJ/m^3	180
Metal hydrides [51]	Metal $xH_2 \leftrightarrow$ metal $yH_2 + (x-y)H_2$	4 GJ/m^3	200–300
Metal oxides (Zn and Fe) [54]	e.g. 2-step water splitting using Fe_3O_4/FeO redox system	n.a.	2000–2500
Aluminium ore alumina [55]	n.a.	n.a.	2100–2300
Methanolation–demethanolation [56]	$CH_3OH \leftrightarrow CO + 2H_2$	n.a.	200–250
Magnesium oxide [57]	$MgO + H_2O \leftrightarrow Mg(OH)_2$	3.3 GJ/m^3	250–400

is to transport $Ca(OH)_2$ at 25 °C from the Netherlands to Morocco. Heating the $Ca(OH)_2$ to 510 °C with the use of CSP will start the endothermic reaction to obtain CaO and H_2O at 510 °C, this uses $94.6 + 54 = 148.6$ kJ/mol of heat. The heated water will run through a steam turbine in Morocco, while the cooled CaO is shipped to the Netherlands. In the Netherlands CaO is brought into contact with H_2O to start an exothermic reaction where 63.6 kJ/mol of heat is released. This heat will feed a steam turbine in the Netherlands and the $Ca(OH)_2$ will be transported to Morocco again.

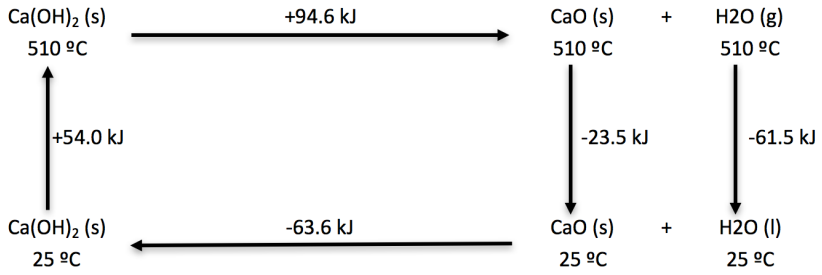

Figure 3.3: $Ca(OH)_2/CaO$ dehydration/hydration cycle [8]

At the German Aerospace Center (DLR) there is a prototype with 20 kg of $Ca(OH)_2$. At this moment it is not possible to achieve full reversibility at the dehydration step, which results in a limited number

of cycles from about 20 and also the order of power nowadays is low [8]. Therefore this process is not selected to be used as energy carrier, but it will be very interesting when all drawbacks are overcome, because shipping and storing CaO is very easy.

3.1.3 Sensible Heat Storage

Sensible heat storage (SHS), is an energy storage method where energy is added to increase the temperature of a material without changing its phase. In SHS a solid or a liquid material is used as a storage medium, examples of storage mediums for SHS are: water, metals, concrete, bricks, sand, rock beds, oil, molten salt, molten glass, soil, etc. There are thousands of materials which are suitable for SHS, however less are suitable for high temperatures. The energy density of a certain medium is dependent on the heat capacity coefficient (c_p) and the temperature difference, see Equation (3.3).

$$q = c_p \cdot (T_{Hot} - T_{cold}) \tag{3.3}$$

To achieve high energy densities, materials with high temperature differences in one phase combined with a high heat capacity coefficient have to be found. There are some problems with solid sensible heat storage, first of all the ability to store the heat for a longer period of time is difficult, also the heat transfer is difficult to manage and finally the purity of the solid often degrades after a number of cycles. Therefore the focus is put on liquid SHS, in Table 3.2 an overview of different liquid SHS materials with corresponding temperature ranges is given.

Table 3.2: Sensible heat liquid materials [16]

Storage medium	Temperature		Average density (kg/m^3)	Average thermal conductivity (W/m K)	Average heat capacity (kJ/kg K)	Volume specific heat capacity (kWh_t/m^3)	Media costs per kg (US$/$kWh_t$)	Media costs per kWh_t (US$/$kWh_t$)
	Cold (°C)	Hot (°C)						
HITEC solar salt	120	133	–	–	–	–	–	–
Mineral oil	200	300	770	0.12	2.6	55	0.30	4.2
Synthetic oil	250	350	900	0.11	2.3	57	3.00	43.0
Silicone oil	300	400	900	0.10	2.1	52	5.00	80.0
Nitrite salts	250	450	1825	0.57	1.5	152	1.00	12.0
Nitrate salts	265	565	1870	0.52	1.6	250	0.50	3.7
Carbonate salts	450	850	2100	2.0	1.8	430	2.40	11.0
Liquid sodium	270	530	850	71.0	1.3	80	2.00	21.0

Nitrate salt is chosen as thermal energy carrier because it has the lowest costs and it comes out of the CSP plant, therefore the temperature range is the same. More advantages of nitrate salts are the high thermal stability, high heat capacity, high density, non-flammability and low vapor pressure. Due to the low vapor pressure pressurized vessels are not required. There are 3 nitrate salts primarily used in thermal energy storage: (1) Hitec Salt, a ternary mixture of 7% sodium nitrate ($NaNO_3$), 53% potassium nitrate (KNO_3) and 40% sodium nitrite ($NaNO_2$). (2) Calcium nitrate salt (Hitec XL), a ternary mixture of 7% $NaNO_3$, 45% KNO_3 and 48% calcium nitrate ($Ca(NO_3)_2$). (3) Solar Salt, a binary mixture of 60% $NaNO_3$ and 40% KNO_3 [51]. Hitec Salt is in liquid phase between 142 °C and 535 °C at atmospheric pressure, Hitex XL is in liquid phase between 120 °C and 500 °C at atmospheric pressure, and Solar Salt has a liquid phase between 220 °C and 600 °C at atmospheric pressure. The heat capacities of all 3 nitrate salts are close to each other, but the prices of the salts differ. The cost of Hitec Salt is $0.93, the cost of Hitec XL is $1.19 and the cost of Solar Salt is $0.49. Combining the specifications on all 3 salts it is concluded that Solar Salt is the best option since it can reach the highest temperature for a more efficient Rankine cycle and also the cost is the lowest. Only the liquid temperature range is slightly in favor of Hitec Salt. However the better performance on the temperature range do not weigh up against the advantages of Solar Salt. Therefore Solar Salt is chosen as thermal energy carrier. If molten salt is mentioned further in the report, Solar Salt is the type of molten salt used.

3.2 Mechanical Energy Storage

There are several energy storage systems which make use of mechanical energy storage. Only compressed air energy storage (CAES) and cryogenic energy storage (CES) will be treated in this section, because the other mechanical energy storage systems are not viable to be used on a ship.

3.2.1 Compressed Air Energy Storage

Compressed air energy storage (CAES) stores its energy as pressure difference. Air is compressed to high pressures with a turbo-compressor when electricity is abundant. When electricity is needed, the compressed air is heated and expanded through a turbo-expander to generate energy. Nowadays compressed air is stored in rock mines, salt caverns, aquifers or depleted gas fields. CAES can obtain a specific energy of 0.2 MJ/kg and an energy density of 21.6 kJ/L at a pressure of 100 bar [52]. A 500,000 m^3 large tanker would only ship 3 GWh of energy. The energy density of CAES is too low to be a viable energy storage solution on a tanker.

3.2.2 Liquid Air Energy Storage

Liquid air energy storage (LAES) is a long duration, large scale energy storage solution that can be located at the point of demand. The LAES system can be divided into three parts; the charging part, storage part and discharging part. At the charging part, air is taken out of the atmosphere and impurities such as water and carbon dioxide are removed. The cleaned air is compressed to very high pressures, where the air is intermediately cooled to obtain high pressurized air at atmospheric temperature. The high pressurized air will be expanded through an turboexpander to drastically decrease the temperature until the air liquefies.

The liquid air can now be stored in well insulated storage tanks. Liquid air is stored at very low temperatures so there will be some standing losses. A liquid air system loses its stored energy through heat leakage into the main cryogenic storage tank which causes boil-off. These losses are nowadays lower than 0.2wt% per day [53].

To regenerate electricity, the liquid air is pumped to high pressures. The liquid air will be evaporated and superheated to ambient temperature or higher temperatures with the use of the heat stored in the first step or waste heat. Now the air is a high pressurized gas at high temperature, which will run through a turbine and generate electricity, in Figure 3.4 the process is visualized. The efficiency of the cycle can be raised if the heat obtained by compression is stored and used to heat the pressurized air before it runs through a turbine to generate electricity. Also the cold which is removed during the evaporation of liquid air can be stored and used to cool the compressed air to low temperatures before expansion. With these heat and cold storage, energy densities of 0.66 MJ/kg, 0.51 MJ/L, and round-trip efficiencies over 50% can be achieved [54].

3.3 Electrochemical Energy Storage

There are two kinds of electrochemical energy storage systems, batteries and flow batteries. Batteries are produced in many sizes and are the oldest and most commonly known form of energy storage. Batteries have a wide spectrum of power supply, which varies from watts to hundreds of kilowatts.

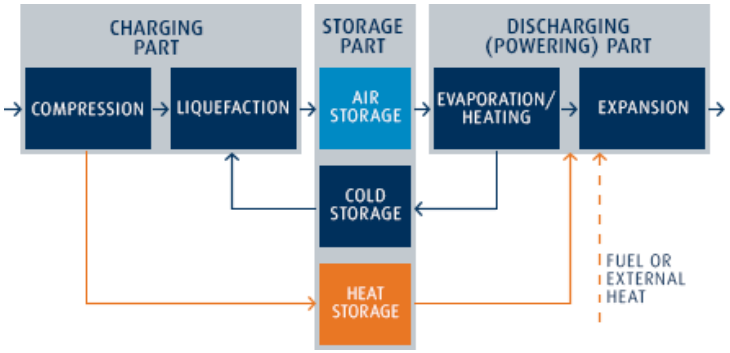

Figure 3.4: Liquid air energy storage process [9]

3.3.1 Batteries

Batteries consist out of an anode, cathode and electrolyte, which allow a chemical reaction to take place so a current can be produced when required. If the chemical reaction is reversed by adding a current, the battery charges. The two main batteries used for medium scale energy storage are the lead-acid and Lithium-ion batteries. There are also batteries available which can not be charged, these kind of batteries are obviously not used.

3.3.2 Flow Batteries

A flow battery is a type of electrochemical cell where chemical energy is provided by two chemical components dissolved in liquids contained within the system and separated by a membrane. Ion exchange occurs through the membrane while both liquids circulate in their own respective space. When electricity is needed, ions flow through the membrane and an electric current is generated by redox reactions. If excess electricity is available, the flow battery is charged by running an electric current through the circuit and the reverse redox reaction will occur so the ions will flow back through the membrane, see Figure 3.5. The advantages of flow batteries are the low cost of the system and the high round trip efficiency, the main disadvantage is the low specific energy of the system. Four different flow batteries are considered in this report; the zinc-iodine bromide flow battery, the vanadium flow battery, the polysulphide bromide flow battery and the iron flow battery, the corresponding specific energies are stated in Table 3.6.

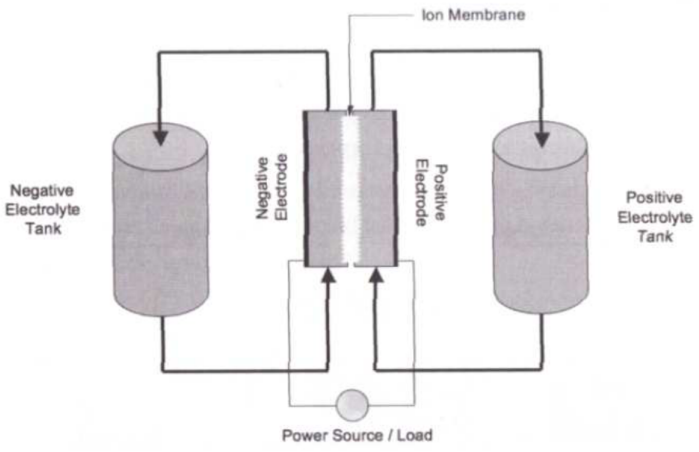

Figure 3.5: Flow Battery [10]

3.3.3 Chemical Energy Storage

Chemical energy storage is receiving world attention due to its potential to replace petroleum products and reduce greenhouse gas emission significantly. One of the most popular chemical energy storage is hydrogen energy storage. Hydrogen is not easy to store and transport due to its high volatility and low specific energy, therefore it is is necessary to pressurize, liquefy or adsorb hydrogen. Another possibility is to convert hydrogen with a chemical reaction into other fuels, such as ammonia, methanol, methane or formic acid. It is also possible to convert ammonia, formic acid or methane directly from electricity, however these processes are still in a stage of infancy. The energy density of chemically generated fuels is high. In Chapter 4 this topic will be elaborated on.

3.4 Selection

In this section the costs of transportation are calculated for differently sized ships, see Section 3.4.1. The maximum profit per trip is also calculated on the basis of the specific energy and efficiency. Combining the costs of transportation and profit per trip, the minimum specific energy combined with efficiency needed is calculated, see Section 3.4.2. The energy carriers obtained in the previous sections with their specific energies are displayed in Table 3.6, these energy storage systems will be evaluated and a selection will be made in Section 3.4.3.

3.4.1 Specific Cost per Ton

In this section the price per ton cargo for different sized tankers is determined. Energy carriers with high specific energy only need ships with a small DWT, and vice versa. In Table 3.4 the data of different sized tankers is shown. The specifications and assumptions of the route are shown in Table 3.3. LHV_{ED} is the lower heating value of the energy density and LHV_{SE} is the lower heating value of the specific energy.

Table 3.3: Specifications and Assumptions Morocco - the Netherlands

Distance	2600	km
harbour time*	48	hr
Engine efficiency [55]	47	%
$LHV_{diesel,SE}$ [56]	42.7	MJ/kg
ρ_{diesel} [57]	880	kg/m^3
$LHV_{diesel,ED}$	37.6	MJ/L
$Cost_{diesel}$ [58]	0.27	€/L
CRF_{30year}**	1.952	-
Lifetime*	30	yr
Crew*	100,000	€/yr

* DAMEN Shipyards
** See Equation (2.4)

All data from the tankers and container vessels is taken from [17], except for the crew size and ship costs. The crew size and ship costs are determined proportional to the ship costs and crew size of an ultra large crude carrier (ULCC) with a deadweight tonnage (DWT) of 560000 ton. The crew size of the 560000 DWT ULCC is 38 and the ship cost is 120 million euro, this data is obtained from DAMEN Shipyards. The largest ship has a DWT of 560000 ton, this is in the same range as the largest tankers nowadays.

Table 3.4: Data Tankers [17]

Name		**Small**	**Handysize**				**Aframax**		**Suezmax**	
Ship size	DWT	5000	10000	20000	40000	60000	85000	105000	115000	125000
Speed	knots	13.5	14.5	15.5	15	15	15	15	15	15
SMCR power	MW	2.34	4.1	7.1	8.5	10.1	12.3	13.4	14.3	15.2
Crew	#	2	3	4	5	7	9	10	11	12
Cost Ship	M€	5	6	8	12	16	22	26	28	30
Name		**Suezmax**		**VLCC**				**ULCC**		
Ship size	DWT	150000	165000	260000	280000	300000	319000	360000	440000	560000
Speed	knots	15	15	15	15	15	15	15.5	15.5	15.5
SMCR power	MW	16	16.8	21.8	22.6	23.5	24.6	27.8	231.1	36.7
Crew	#	14	15	22	24	26	27	30	37	46
Cost Ship	M€	35	38	58	62	66	70	79	95	120

First the amount of days needed for one round trip is calculated with use of the speeds defined in Table 3.4 and the harbour hours defined in Table 3.3; this lays between 11 and 13 days. This results in a range of total round trips of 840 to 1000 in 30 years. With the assumptions and data known from Table 3.3 and Table 3.4, all the costs are calculated; fuel costs, crew costs, ship costs and harbour costs. With all the costs known the cost of cargo per ton per round trip is obtained, see Figure 3.6.

The large range of DWT is important for this thesis, energy carriers with high specific energy only need small DWT and vice versa, because the energy input is a constraint. As can be seen in Figure 3.6 the costs continue to fall for higher DWT. Especially for low DWT the costs rise rapidly.

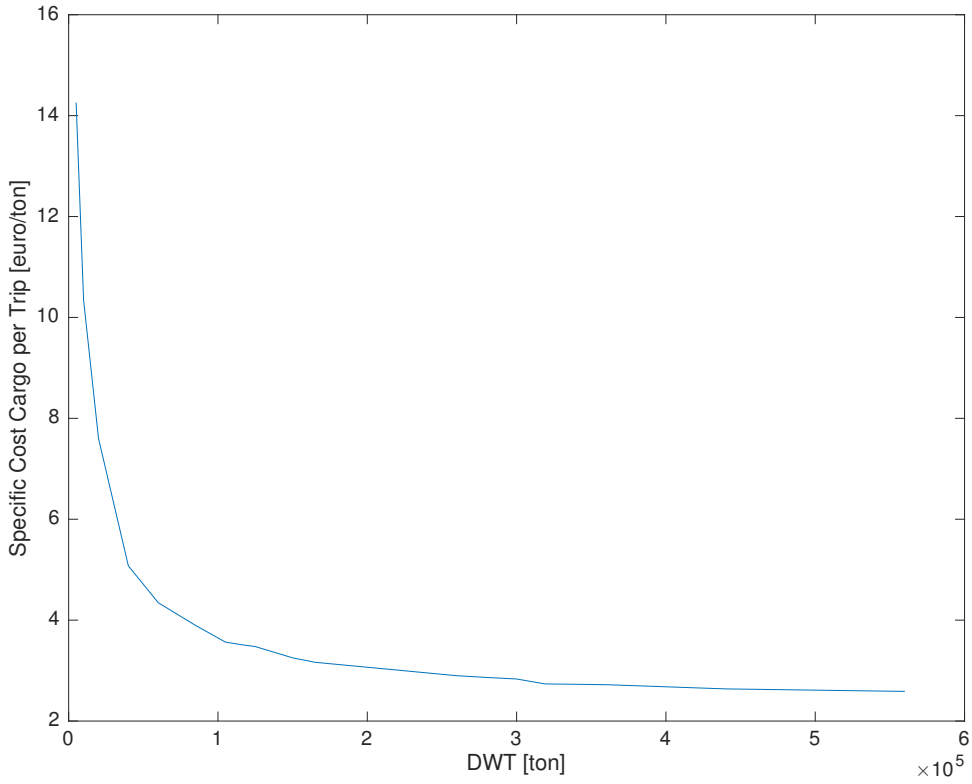

Figure 3.6: Price of transporting one ton of cargo per round-trip for differently sized tankers

3.4.2 Minimum Specific Energy

In this section the minimum specific energy is calculated, this is done by comparing the cost of ton cargo per trip from the previous section with the revenue of the energy carrier with the variables conversion and specific energy. The revenue per trip is calculated in Equation (3.4) for PV systems and Equation (3.5) for CSP systems, where η is the round-trip efficiency, this is the efficiency of electricity to the energy carrier and back to electricity again. SE is the specific energy of the specific storage system. The DWT of 560000 ton is taken because the cost per ton is the lowest for a tanker with a DWT of 560000 ton. The revenue is calculated by multiplying the SE (kWh/kg) with the profit obtained from selling one kWh at 0.125 €/kWh minus the costs of the energy carrier of 0.022 €/kWh for PV or 0.018 €/kWh for CSP divided by the round-trip efficiency of the specific energy carrier. To obtain the total revenue per trip, this is multiplied with the total amount of kg on one tanker ($DWT \cdot 1000$). The dashed lines and the points A,B,C and D are explained in Section 3.4.3.

$$Revenue_{PV} = (0.125 - 0.022/\eta) \cdot DWT \cdot 1000 \cdot SE \tag{3.4}$$

$$Revenue_{CSP} = (0.125 - 0.018/\eta) \cdot DWT \cdot 1000 \cdot SE \tag{3.5}$$

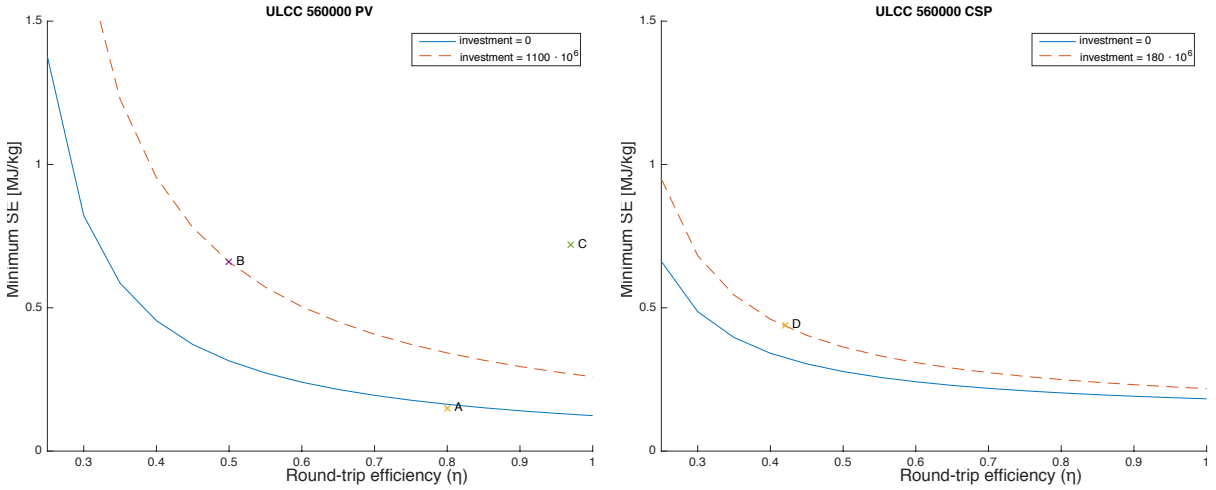

(a) PV minimum specific energy

(b) CSP minimum specific energy

Figure 3.7: Specific energy of an energy carrier compared with the round-trip efficiency of the energy carrier and costs of a 560000 DWT ULCC

As can be seen in Figure 3.7, the blue solid line represents the minimum SE combined with efficiency, but without any investment costs. No costs for the equipment to transfer electricity into the specified energy carrier and back is taken into account at this point. Equation (3.4) is compared to the cost of one trip.

3.4.3 Selection

The minimum SE at 100% conversion is 0.11 MJ/kg. So all concepts which have a lower energy density than 0.11 MJ/kg are eliminated. As can be seen in Table 3.6, except for chemical energy storage, 4 concepts have a higher energy density than 0.11 MJ/kg. These concepts are shown in Table 3.5.

When looking at Figure 3.7a, the ZIBB flow battery (A) is just below the blue solid line and therefore eliminated. The SE and conversion of the lithium ion battery (C) are very good. However, a battery is

Table 3.5: Description points Figure 3.7

Point	Process	Specific Energy [MJ/kg]	Efficiency [%]
A	Flow Battery ZIBB	0.15	70
B	Liquid Air	0.66	50
C	Li-ion Battery	0.72	97
D	Molten Salt	0.48	42

designed to be able to run over 100000 cycles in his lifetime, this has no advantage in this case. Over a lifetime of 30 years, the maximum number of cycles of a ship is 1000. The price of batteries is often displayed in $/kWh, where the lowest price at this moment is 200$/kWh. With 1000 cycles, this comes down to an energy price per kWh of 0.2$/kWh. This is already higher than the 0.125 $/kWh sold in the Netherlands, so the lithium ion battery is also eliminated.

For the thermal energy storage concept, molten salt (D) is used as show case, see Figure 3.7b. The solid line in Figure 3.7a and Figure 3.7b represent the break even point of the specific energy combined with the round-trip efficiency of the energy carrier with a selling price of 0.125 €/kWh in the Netherlands, but without any investment costs. In the dashed line also the investment costs are added which are necessary to buy turbines or compressors etc. For the molten salt concept, 180 million euro can be invested to reach the break-even point. For the molten salt concept only the costs of molten salt and the power block in the Netherlands have to be realized. Because the costs of heating and storing molten salt in Morocco are already included in the heat price of 0.018 €/kWh, see Section 2.2.1. In Equation (3.6) the specific energy of molten salt is calculated. See Chapter 5 for an elaboration on this concept.

$$q = c_p \cdot (T_{Hot} - T_{cold}) = 1.6 \cdot (565 - 290) = 440 \text{ kJ/kg} \tag{3.6}$$

Point B, liquid air, in Figure 3.7a is the other concept which lies above the break-even line without investments. For liquid air an investment of 1100 million euros can be made to break even, this includes the equipment cost of conversion from electricity to liquid air and from liquid air back to electricity. In Chapter 6 this concept will be treated extensively. See Table 3.6 for an overview of all the energy storage systems and if they are selected or not.

3.5 Conclusion

All kinds of energy storage were explained and critically reviewed in this chapter. All the fuels obtained by chemical energy storage passed the selection due to their high energy densities. In Chapter 4 these concepts will be worked out. Two other concepts are left; thermal energy storage and energy stored as liquid air. Thermal energy storage will be discussed further in Chapter 5 and the liquid air energy storage concept will be elaborated in Chapter 6. As can be seen in Table 3.6, thermochemical heat storage and latent heat storage are selected with an 'o'. The processes which are selected with an 'o' are processes which have a low technology readiness level. So they will not be treated extensively, but they are promising for the future.

Table 3.6: Concepts

Energy Storage			**SE [MJ/kg]**	**Selected**
Chemical		Hydrocarbon (methane)	55.5 [59]	✓
		Formic acid	6.2 [60]	✓
		Hydrogen	142 [59]	✓
		Liquid hydrogen	142 [59]	✓
		Methanol	22.7 [59]	✓
		Ammonia	22.5 [59]	✓
Thermal	Thermochemical heat	Calciumoxide	1.1 [8]	o
	Sensible heat	Molten salt	0.44 [52]	✓
	Latent heat (PCM)		0.2 - 2.0 [61]	o
Mechanical		Compressed air	0.2 [52] (21.6 kJ/L)	x
		Liquid air	0.66 [52]	✓
Electrochemical	Flow battery	Zinc iodine bromide	0.15 [52]	x
		Vanadium redox	0.1 [52]	x
		Aquabattery	0.015 [52]	x
		PSB	0.0675 [52]	x
		Iron	0.05 [52]	x
	Rechargeable battery	Lead acid	0.18 [52]	x
		Lithium ion	0.72 [52]	x

o Technology readiness level is too low
x Concept is eliminated
✓Concept is selected

Chapter 4

Chemical Energy Storage

In this chapter all the chemical energy storage concepts are explained and evaluated. An overview of the energy flow is given in Figure 4.1; PV solar panels generate electricity which is converted into a fuel, the fuel is transported and finally electricity is generated in the Netherlands. Only PV systems are considered because the electricity from PV systems is cheaper than electricity from CSP.

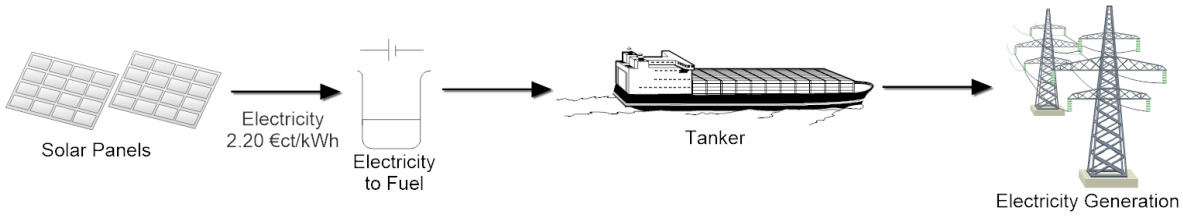

Figure 4.1: Overview energy flow

The electricity obtained by the solar panels is converted into hydrogen with the use of electrolysis. Hydrogen is not easy to store and transport due to its high volatility and low specific energy, therefore it is is necessary to pressurize, liquefy or adsorb hydrogen, these processes are analyzed in Section 4.2. Another possibility is to convert hydrogen with a chemical reaction into other fuels, such as ammonia, methanol, methane or formic acid, see Section 4.3. It is also possible to convert ammonia, formic acid or methane directly from electricity, however these processes are still in its infancy.

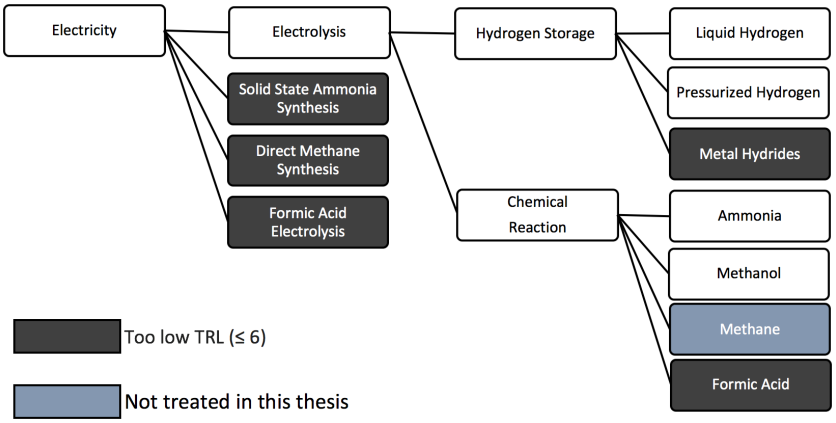

Figure 4.2: Electricity to storage

An overview of the processes of electricity to storage is given in Figure 4.2, the boxes marked in black are promising processes, however the technology readiness level (TRL) of these processes are ≤ 6 [62] [63]. If the TRL is 6, the development of the system is still in its technology demonstration phase. To become commercially viable for large-scale energy storage a lot of research and testing is still required, which will take too much time to be achieved in the near future. So the black marked processes will not be discussed in this report. Methane is marked blue, this is done because methane is not included in this report. The process of producing methane can be done with the sabatier reaction:

$$CO_2 + 4H_2 \rightleftharpoons 2H_2O + CH_4 \tag{4.1}$$

$$CO_2 + H_2 \rightleftharpoons H_2O + CH_3OH \tag{4.2}$$

The processes of producing methane and methanol with the use of carbon dioxide and hydrogen are very much alike. As can be seen in Equation (4.1) 50% of the hydrogen is lost by the formation of water, and for methanol this is 33%, see Equation (4.2). Because the production of hydrogen is a very energy intensive process, it is chosen to elaborate on the synthesis of methanol and not on the synthesis of methane.

4.1 Electrolysis

To produce hydrogen from electricity, electrolysis is used. There are a number of different types of electrolysis, but the most important three are: Alkaline electrolysis, proton exchange membrane (PEM) electrolysis and solid oxide electrolysis (SOE). These types of electrolysis will be analyzed in the following sections.

4.1.1 Alkaline Electrolysis

Alkaline is the oldest and most mature form of electrolysis. The alkaline electrolyzer is characterized by two electrodes operating in a liquid electrolyte. The electrolyte used in the conventional alkaline water electrolyzers is aqueous potassium hydroxide (KOH), with solutions of 20-30wt%. At the cathode, water is converted into hydrogen and hydroxide. The hydrogen is captured and the hydroxide travels through the diaphragm to the anode, where the hydroxide converts into oxygen and water.

The advantage of alkaline electrolyzers is the maturity of the process. Alkaline electrolyzers work on large scale and at this moment the lifetime and efficiency of alkaline electrolyzers is better than for PEM electrolysis and SOE. However, big disadvantages are the low current densities and the low turndown ratios. The turndown capability of an alkaline electrolyzer is 60 - 80% [64], which means that the alkaline electrolyzer needs to operate at a minimum of 20 - 40% of its capacity, it can not be shut down completely. So for an electrolyzer in Morocco, where the average daily sunshine hours is 7.2 hours, the electrolyzer has to operate for 16.8 hours a day at a minimum of 20 - 40% of its capacity.

If the alkaline electrolyzer runs on fossil fuels during a period of 16.8 hours at 20% of its capacity, the operation would not run on renewable energy anymore which is one of the requirements. Therefore a fuel cell has to be used to convert the hydrogen obtained during the day into electricity needed during the night. In Table 4.1 a quick calculation is made to obtain the total efficiency of the alkaline electrolyzer during night and day. During the day the power input of the alkaline electrolyzer is 800 MW for 7.2 hours, and during the night the power input becomes $800 \cdot 0.2 = 160$ MW for 16.8 hours. The hydrogen produced during the day is lower than the hydrogen needed to run the electrolyzer during the night. The

Table 4.1: Energy needed during day and night for the Alkaline Electrolyzer

H2_LHV	33.33	kWh/kg				
Alkaline eff	63%	LHV [65] [66]				
Elec_in	53.3	kWh/kg				
Fuel cell eff	50%	LHV [65]				
Elec_out	16.7	kWh/kg				
7.2	hours/day	100%	800	MW	5760	MWh
16.8	hours/day	20%	160	MW	2688	MWh
108155	kg hydrogen	produced during the day				
161296	kg hydrogen	needed during the night				

difference has to be compensated with fossil fuel based electricity and also the efficiency of the alkaline electrolyzer becomes very low. Therefore using the alkaline electrolyzer is not a viable option.

4.1.2 Proton Exchange Membrane Electrolysis

With PEM electrolysis two electrodes are separated by a proton exchange membrane. The proton exchange membrane is permeable to hydrogen ions, so it conducts protons. At the anode water is split into oxygen and hydrogen ions. A water/oxygen mixture leaves the PEM stack and is then separated. The water is recycled and the oxygen is released in the atmosphere or stored to be used in another process. The hydrogen ions and a part of the water permeate through the membrane and at the cathode the hydrogen is formed from the hydrogen ions. A water/hydrogen mixture leaves the PEM stack and is then separated. The water is also recycled and the hydrogen needs to be stored, the storage of hydrogen is covered in the following sections. See Figure 4.3 for a visualization of the PEM electrolysis system.

The technology readiness level of PEM electrolysis is 9, which means it is operating on commercial scale. The two main advantages of PEM electrolysis over alkaline electrolysis are the ability of the PEM electrolysis to operate on high current densities and the high turndown ratio. PEM electrolyzers are able to operate from 0% to 100% [67].

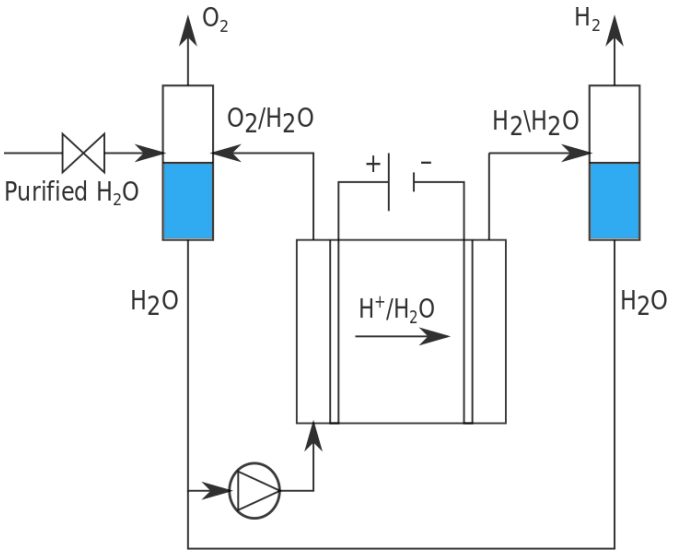

Figure 4.3: PEM electrolysis

In Table 4.2 all the specifications and costs of PEM electrolysis in 2025 are shown which are obtained from an excel sheet provided by the department of energy of the USA[68] [69].In this excel sheet the

capacity of the power plant is set on 52.3 ton of hydrogen per day, with a capacity factor of 30 % this becomes 15.69 ton/day. The capacity factor is the same as the capacity factor of the PV systems. The LHV efficiency of the total system usage per kg of hydrogen is 70%, which results in a total electricity usage of 47.7 kWh/kg hydrogen. This includes the total stack electrical usage and balance of plant electrical usage. See Appendix D.1 for a more elaborated overview of the total electricity needed per kg H2. To produce 15.69 ton/day with an electricity usage of 47.7 kWh/kg, the total electricity needed per day becomes 748 MWh. This is less than the electricity generated by the PV systems, therefore it is assumed that the PEM electrolysis can be scaled up in the same proportion.

Costs

In the right part of Table 4.2 the costs of hydrogen are shown. The capital recovery factor (CRF) with an interest rate of 5% has been calculated in Section 2.4. In Appendix D.2 and Appendix D.3 the cost breakdown of the capital costs (Cap_{cost}) can be found. The fixed operational costs (C_{FoC}) are specified in Appendix D.4. The replacement costs (C_{repl}) are 12% of the capital costs every 10 years, which results in a price of €415.000/year. It is assumed that the water which is not converted into oxygen and hydrogen will be recycled. The mass ratio of water : hydrogen becomes 1 : 9 ($2H_2O \rightarrow 2H_2 + O_2$). The cost of process water is 3€/ton [70], which leads to a process water cost (C_{water}) per year of 155,000 €. 748 MWh/day of electricity is needed to obtain 15.69 tonnes of hydrogen per day (H2_{day}). Combining this with an electricity price of 2.2 €ct, the total electricity costs (C_{elec}) per year become 6.8 M€. Now all the costs and the total amount of hydrogen produced are known, the price per kg hydrogen becomes 1.89 €/kg, see Equation (4.3).

Table 4.2: Specifications and costs PEM Electrolysis

	Values	Units		Values	Units
Lifetime	30	yr	Interest rate	5	%
Capacity factor	30	%	CRF_{30year}	1.952	-
Specific energy H2_{LHV}	33.3	kWh/kg	Capital cost	38.0	M€
Efficiency	63	%	Capital cost with CRF	74.1	M€
Design capacity	2.18	ton_{H2}/hr	Fixed operational costs	1.8	M€/yr
Process water : hydrogen	9	kg/kg	Replacement costs	415,000	€/yr
Process water cost	3	€/ton	Electricity costs	6.0	M€/yr
			Process water cost	155,000	€/yr
Hydrogen produced	15.69	ton/day	Price H2 per kg	1.89	€/kg
Electricity	846	MWh/day			

$$
\begin{aligned}
H2_{kg,PEM} &= \frac{\text{Total costs 30 yr}}{\text{Total kg produced 30 yr}} \\
&= \frac{Cap_{cost,CRF} + (C_{FoC} + C_{Repl} + C_{elec} + C_{water}) \cdot Lifetime}{H2_{day} \cdot days_{year} \cdot Lifetime} \\
&= \frac{74.1 \cdot 10^6 + (1.8 + 0.415 + 6.0 + 0.155) \cdot 10^6 \cdot 30}{15.69 \cdot 10^3 \cdot 365.25 \cdot 30} \\
&= 1.89 \text{ €/kg}
\end{aligned}
\tag{4.3}
$$

4.1.3 Solid Oxide Electrolysis

SOE is not yet commercially available as PEM electrolysis and alkaline electrolysis is. The technology readiness level at this moment lies between 5 and 6 [11]. SOE cells operate at high temperatures and

use a solid electrolyte. At the cathode water is split into hydrogen and oxide with the use of electricity, oxide and permeates through the electrolyte and the oxide ions form oxygen at the cathode. Steam is used as sweep gas to enhance performance by lowering the oxygen partial pressure and limit corrosion. An oxygen/steam and a hydrogen/steam mixture will leave the stack. The heat of the mixtures is used to preheat process and sweep water, and the two mixtures will thereafter be separated to create oxygen, hydrogen and water. Water will be cycled back into the systeem. The preheated process water will be heated further by an external heat source to 800 °C and fed to the stack. See Figure 4.4 for a visualization of the process. In this picture the external heat source is a natural gas burner, but the heat can also be obtained by use of electricity or the sun. The big advantage of solid oxide electrolysis over PEM electrolysis is its very high energy efficiency, it is able to reach almost 100% without the external heat source. Another advantage is its chemical flexibility, there are possibilities to create syngasses when CO_2 is added, however the technology readiness level for these processes is even lower. One of the disadvantages is the high operating temperature, this causes long start-up times and mechanical compatibility issues. Also the low technology readiness level is a big disadvantage, it is not operational on large scale yet.

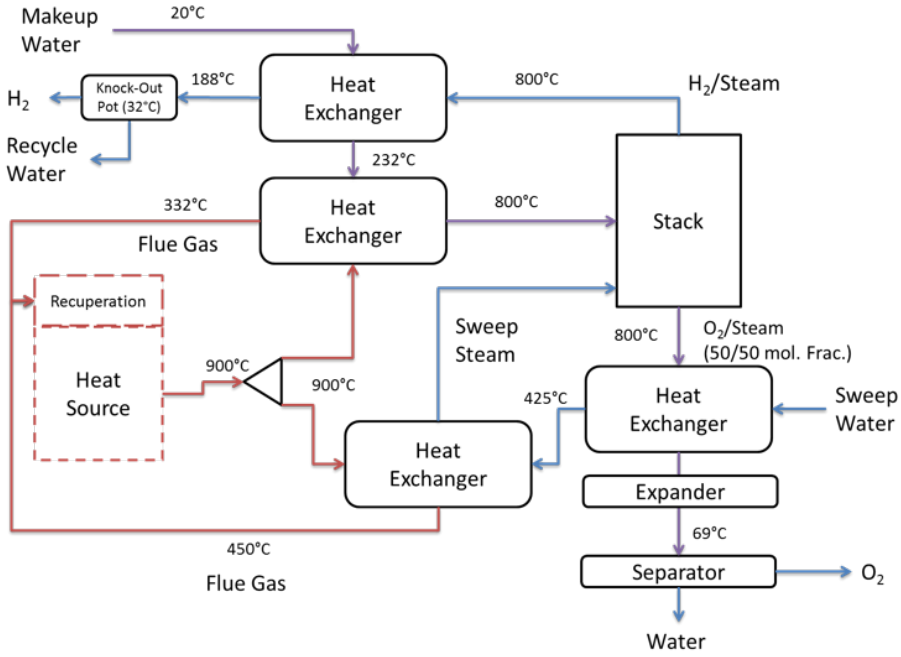

Figure 4.4: Solid oxide electrolysis [11]

In Table 4.3 the specifications and costs obtained for SOE are shown. These data is also obtained from an excel sheet provided by the department of energy of the USA [68] [11]. The lifetime, capacity factor, design capacity, process water : hydrogen ratio and process water costs are the same as for PEM electrolysis. The LHV efficiency of the SOE stack is very high, this is 95% [71]. But the input of the stack is hot steam with a temperature of 800 °C. To heat the sweep water and process water to 800 °C, in the way Figure 4.4 depicts it, 11.5 kWh/kg of heat needs to be added to the system.

Costs

In the right part of Table 4.3 the costs of hydrogen created with SOE are shown. The capital recovery factor (CRF) with an interest rate of 5% becomes 1.952, see Section 2.4. The cost breakdown of the capital costs (Cap_{cost}) is shown in Appendix C.1 and Appendix C.2. The stack costs are 7.5 million euro. Due to the high operational temperatures the stack has to be replaced every 4.5 years, this comes down to a replacement cost (C_{repl}) of 7.5/4.5 = 1.7 M€per year. The fixed operational costs (C_{FoC}) are

specified in Appendix C.3. The cost of process water is 3€/ton [70], which leads to a process water cost (C_{water}) per year of 155,000 €. 551 MWh/day of electricity is needed to obtain 15.69 ton of hydrogen per day. Combining this with an electricity price of 2.2 €ct, the total electricity costs (C_{elec}) per year become 4.0 M€. Now all the costs and the total amount of hydrogen produced are known. The price per kg hydrogen, excluding the heat price, is calculated in Equation (4.4) and is 2.07 €/kg. The price per kilogram of hydrogen is shown with and without heat addition, because it is not specified how the heat is generated. For the hydrogen price with heat included, the heat is generated with use of electricity, the additional heat price per kilogram hydrogen is $2.2 \cdot 11.5 = 25$ €ct.

Table 4.3: Specifications and costs SOE

	Values	Units		Values	Units
Lifetime	30	yr	Interest rate	5	%
Capacity factor	30	%	CRF_{30year}	1.952	-
Specific energy $H2_{LHV}$	33.3	kWh/kg	Total investment	41.9	M€
Efficiency	95	%	Total investment with CRF	81.8	M€
Heat needed per kg H2	11.5	kWh/kg	Fixed operational costs	3.3	M€/yr
Design capacity	2.18	ton_{H2}/hr	Replacement costs	1.7	M€/yr
Process water : hydrogen	9	kg/kg	Electricity costs	4.0	M€/yr
Process water cost	3	€/ton	Process water costs	155,000	€/yr
Hydrogen produced	15.69	ton/day	Price H2 per kg	2.07	€/kg
Electricity	551	MWh/day	(Price H2 per kg incl. heat	2.33	€/kg)

$$
\begin{aligned}
H2_{kg,SOE} &= \frac{\text{Total costs 30 yr}}{\text{Total kg produced 30 yr}} \\
&= \frac{Cap_{cost,CRF} + (C_{FoC} + C_{Repl} + C_{elec} + C_{water}) \cdot Lifetime}{H2_{day} \cdot days_{year} \cdot Lifetime} \\
&= \frac{81.8 \cdot 10^6 + (3.3 + 1.7 + 4.0 + 0.155) \cdot 10^6 \cdot 30}{15690 \cdot 365.25 \cdot 30} \\
&= 2.07 \text{ €/kg}
\end{aligned}
\tag{4.4}
$$

4.1.4 Overview

As can be seen in Table 4.4, PEM electrolysis is cheaper than SOE, also if the heat needed for SOE is free. Also the technology readiness level of PEM electrolysis is higher than for SOE. The costs to produce one kg of hydrogen is €7.28 in 2015 and becomes €2.20 in 2030. As a comparison; hydrogen is nowadays mostly produced with natural gas reforming, this has a price of 1 €/kg [72]. The price of hydrogen produced with natural gas is still a lot cheaper, but new regulations due to the energy transition will drive up natural gas prices and CO2 emissions in the future. If the technology readiness level of SOE becomes higher and the materials used are better able to withstand the high operational temperatures, the high efficiencies and especially the fuel flexibility become very interesting. But for now there is no benefit in the near future to use SOE over PEM electrolysis and therefore PEM electrolysis will be used to convert electricity into hydrogen. In the following sections the different possibilities of hydrogen storage are stated.

Table 4.4: Types of Electrolysis [18]

Electrolysis Technology	**Alkaline Electrolysis**	**PEM Electrolysis**	**Solid Oxide Electrolysis**
Anode Reaction	$4OH^- \rightarrow O_2 + 2H_20 + 4e^-$	$2H_2O \rightarrow O_2 + 4H^+ + 4e^-$	$2O^{2-} \rightarrow O^2 + 4e^-$
Cathode Reaction	$H_2O + 2e^- \rightarrow H_2 + 2OH^-$	$2H^+ + 2e^- \rightarrow H_2$	$H_2O + 2e^- \rightarrow H_2 + O^{2-}$
Charge Carrier	OH^-	H^+	O^{2-}
Operating Temperature	40 - 90 °C	20 - 100 °C	700 - 1000 °C
TRL	9	9	5-6
Cost [€]	-	1.89	2.07 (2.33)

4.2 Physical Hydrogen Storage

Hydrogen is a gas with a very high specific energy, but a very low energy density. It is a difficult gas to store since it is the lightest gas of all gases, and therefore very volatile. Nowadays the three main technologies used to store hydrogen without using a chemical reaction are: compressed hydrogen storage, liquid hydrogen storage and storage in metal hydrides. Compressed hydrogen storage and liquid hydrogen storage are used for large-scale stationary applications. Compressed hydrogen storage includes metal tanks in addition to underground compressed hydrogen storage. Metal hydrides may be suitable for mobile applications, but they are not yet commercially viable for large systems as they are still in the research stage [73].

4.2.1 Compressed Hydrogen

Compressed hydrogen storage is a technology that is well developed and popular. The energy density of compressed hydrogen is low: to store 4 kg of hydrogen at a pressure of 200 bar, a 225 liter tank is needed. The energy required to compress hydrogen to 200 bar consumes around 8% of the HHV of hydrogen [14]. However, the advantage is that the process is simple with only a compressor train and a pressure vessel required.

Small-scale hydrogen storage is often used for mobile applications; hydrogen is compressed to pressures exceeding 600 bar and stored in carbon fiber reinforced tanks. For large-scale hydrogen storage, stationary applications use spherical or cylindrical storage tanks. Cylindrical containers with pressures of 50 bar and capacities of 400 kg ($\pm$ 350 m^3) are currently used in European countries [73]. This is equal to an energy density of 38 kWh/m^3, which is a factor of 62 lower than the energy density of liquid hydrogen. To transport the amount of hydrogen produced in 12 days (round-trip time of tanker), the volume of the tanker needs to exceed 1,400,000 m^3. Tankers with these large volumes do not exist yet. Due to the low energy density and huge additional costs that this entails, pressurized hydrogen storage is not seen as a viable option to store and transport solar electricity.

4.2.2 Liquid Hydrogen

Another storage solution for hydrogen is to liquefy it, liquid hydrogen (LH_2) is obtained at extremely low temperatures; 21.2 K. The critical temperature of hydrogen is 33 K, therefore it is common to store liquid hydrogen in open systems since there is no liquid phase above the critical temperature and the critical temperature and melting point of liquid air are close to each other. The density of liquid air is 70.8 kg/m^3 which leads to an energy density of 2359 kWh/m^3 (LHV). In the US there are some companies with large scale liquefaction plants, the largest is from Praxair and has production rates of 35 ton LH_2 per day.

Electricity to Liquid Hydrogen

The process consists out of 3 heat exchangers, before hydrogen enters the first heat exchanger, hydrogen is compressed. Before hydrogen can be cooled by means of expansion, hydrogen needs to be cooled down to the inversion temperature of hydrogen, which is 224 K. If the temperature of a gas lies above the inversion temperature, the expansion of a gas will lead to a temperature rise of the gas and if the temperature of a gas lies below the inversion temperature the gas will cool when expansion occurs. In the first heat exchanger hydrogen is cooled with nitrogen gas, hydrogen gas which is recycled and an external refrigeration cycle. Hydrogen is split into two flows before entering the second heat exchanger, both flows are cooled with liquid nitrogen to 180 K [12], this is below the inversion temperature of hydrogen. One flow of hydrogen is used to cool the other hydrogen flow by the use of expansion through expansion turbines. The cooling flow is split into three, the first part is expanded through a turbine and still flows through the second heat exchanger. The second part is also cooled by expansion and cools the third heat exchanger, the third part runs through a Joule-Thomson (J-T) valve and also cools the third heat exchanger. A J-T valve decreases the temperature of a gas by forcing the gas through the valve while keeping it insulated so no heat is exchanged with the environment. The enthalpy remains the same during the expansion through the valve. J-T valves are used when a phase change occurs and no turboexpanders, which are more efficient, can be used anymore. The other flow is cooled by the heat exchangers and is still pressurized. The pressurized hydrogen is liquefied due to the enthalpic expansion of two J-T valves and then stored in thermally insulated storage tanks.

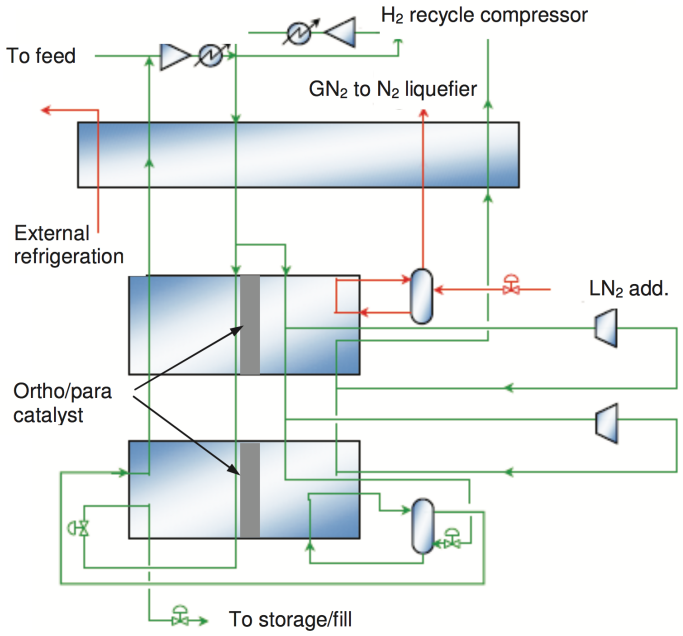

Figure 4.5: Praxair hydrogen liquefaction process [12]

Hydrogen molecules exist in two forms, para and ortho, this depends on the electron configuration in the individual hydrogen atoms. At the boiling point of hydrogen, 21.2 K, the concentration of hydrogen is almost 100% para-hydrogen. But at room temperature the concentration is around 25% para-hydrogen and 75% ortho-hydrogen [74]. The conversion of ortho-hydrogen to para-hydrogen is very slow if no catalyst is used. The problem with liquefied hydrogen which contains a high percentage of ortho-hydrogen is the reaction of ortho-hydrogen to para-hydrogen which is a exothermic reaction, the hydrogen will heat up and evaporate again. The ortho/para catalysts are used to obtain a higher parahydrogen fraction in the the ortho- to parahydrogen mixture. An overview of the whole liquefaction process is given in Figure 4.5.

In Table 4.5 the specifications and costs of producing liquid hydrogen in 2015 and 2030 are displayed. The electricity used is coming from PV systems and not from CSP plants due to the lower LCoE costs. PV systems have an average operation time of **7.2** hours per day, therefore PEM electrolysis and the liquefaction process will also operate for 7.2 hours per day. In 2015 **52** kWh of electricity is needed to obtain 1 kg of hydrogen, in 2030 this will be improved to **47** kWh [66]. The lifetime of the electrolysis system is **40,000** and **75,000** hours in 2015 and 2030 respectively [65] and the investment costs are **1700** €/kW in 2015 and **750** €/kW in 2030 [66]. The capital recovery factor (CRF) is calculated with use of Equation (2.4). The O&M costs for electrolysis are set at **1.53**%, this is estimated by Bertucciolli (2014) for a system between 250 MW and 1000 MW [66]. Finally the costs of purified water are set at **3**€/ton [70]. Liquefaction plants are able to operate around 10 kWh/kg nowadays [12]. While capital costs are around 2270 €/kW [74]. In the future it will be possible to accomplish an efficiency of 5.9 kWh/kg, according to Etternavn (2013) [12]. The O&M costs are set at 4% [75] and the lifetime is 30 years [76].

The electricity costs per kg ($C_{electricity}$) are simply calculated by multiplying the cost of electricity (2.2 €ct/kWh) by the amount of electricity needed per kg (52 kWh in 2015 and 47 kWh in 2030). The investment costs per kg ($C_{investment}$) are obtained in Equation (4.5); I is the investment cost per kW, L is the lifetime in hours and $Elec_{in}$ is the electricity needed to produce one kg of (liquid) hydrogen.

$$C_{investment}[€/\text{kg}] = \frac{I \cdot CRF}{L} \cdot Elec_{in} \tag{4.5}$$

In Equation (4.6) the O&M costs per kg ($C_{O\&M}$) are calculated: the O&M costs per year are calculated by multiplying the O&M fraction by the investment in kW. This is divided by the total amount of operating hours per year, which is the capacity factor (CF) times the total amount of hours in a year. To obtain the O&M per kg this has to be multiplied with the amount of electricity needed per kg of (liquid) hydrogen.

$$C_{O\&M}[€/\text{kg}] = \frac{O\&M \cdot I}{365.25 \cdot 24 \cdot CF} \cdot Elec_{in} \tag{4.6}$$

There is 9 kg of water needed to obtain 1 kg of hydrogen ($2H_2O \rightarrow 2H_2 + O_2$), therefore the cost of water (C_{H_2O}) to produce 1 kg of hydrogen is 27 €/ton (0.03 €/kg). To obtain the liquid hydrogen costs, the electrolysis costs and the liquefaction costs are added. The price per kg of liquid hydrogen (C_{LH_2}) becomes **6.02** €/kg in 2015 and **2.82** €/kg in 2030.

Storage and transport

To transport liquid hydrogen, one tanker is used which sails back and forth. The time to sail from Morocco to the Netherlands with a speed of 15 knots takes 4 days, with a harbour time of 2 days the round-trip time of the ship becomes 12 days. The capacity of the storage tanks on shore and on the tanker need to be able to store 12 days of liquid hydrogen produced. With a maximum power input per day of $800 \cdot 9 = 7200$ MWh during the summer, see Section 2.3.1, 86.4 GWh of electricity needs to be

Table 4.5: Specifications Liquid Hydrogen

Electricity to Liquid Hydrogen						
	PEM Electrolysis [65] [66]		Liquefying Hydrogen [12] [74] [76]		Liquid Hydrogen	
Year	2015	2030	2015	2030	2015	2030
Hour per day	7.2	7.2	7.2	7.2		
LHV [kWh/kg]	33.33	33.33	33.33	33.33	33.33	33.33
Eff [%]	64%	71%			54%	63%
$Elec_{in}$ [kWh/kg]	52	47	10.0	5.9	57.7	46.6
Lifetime [hr]	40000	75000	30 [yr]	30 [yr]		
Investment [€/kW]	1700	750	2270	2270		
CRF [-]	1.45	1.90	1.952	1.952		
O&M [%]	1.53	1.53	4	4		
H_2O [€/ton]	3	3				
C_{H_2O} [€/kg]	0.03	0.03				
$C_{electricity}$ [€/kg]	1.14	1.03	0.22	0.13	1.36	1.16
$C_{investment}$ [€/kg]	3.21	0.89	0.56	0.33	3.77	1.22
$C_{O\&M}$ [€/kg]	0.51	0.21	0.35	0.20	0.86	0.41
C_{LH_2} [€/kg]	4.89	2.16	1.13	0.67	6.02	2.82

converted into liquid hydrogen in 12 days. With an electricity input of 62.0 kWh/kg and 52.9 kWh/kg this results in a liquid hydrogen storage capacity of **1400** ton in 2015 and **1600** ton in 2030, respectively. Which results in a volumetric capacity of 19700 m^3 and 23000 m^3 respectively. The liquid hydrogen tanks are assumed to be **10** M€each. No data about the costs could be found, but it is assumed that the costs are 2 times the costs of a storage tank for ammonia, see Section 4.3.1. It is assumed that the storage tanks have a lifetime of 30 years, which results in a CRF of 1.952. Three storage tanks are needed; one in Morocco, one in the Netherlands and one on the tanker.

During the storage on shore and during transportation, the boil-off rate due to heat leaks has to be taken into account. The boil-off rate is a function of its size, shape and thermal insulation. Heat losses are proportional to the surface to volume ratio. Boil-off losses occur due to a variety of mechanisms such as ortho-para conversion, thermal stratification and self pressurization, heat leaks, sloshing and flashing. Boil-off losses are typically 0.4% per day for a volume of 50 m^3, 0.2% for a volume of 100 m^3, and 0.06% for a volume of 20000 m^3, for double-walled, vacuum insulated storage tanks [77]. This is in the same order as the storage volumes on shore and on the ship and therefore boil-off losses of 0.06% per day are taken. During one round-trip, liquid hydrogen has to be stored for 12 days on shore in Morocco, 8 days on the tanker ($2 \cdot 2$ days harbour time and 4 days sailing) and 12 days on shore in the Netherlands. This results in a total of 32 days with a boil-off loss of $1 - 0.9994^{32} = \mathbf{2}\%$

The round-trip costs for tankers with different DWT are calculated in Section 3.4.1. The round-trip cost for a tanker with a DWT of 1500 ton is approximately **50,000** €. The additional costs to transport one kg of liquid hydrogen ($C_{transport}$) becomes **0.21** €/kg in 2015 and **0.13** €/kg in 2030, see Table 4.6 for an overview of all the storage and transportation costs. Looking at Table 4.5, the costs to transport liquid hydrogen is low compared to the costs to produce liquid hydrogen.

Liquid Hydrogen to Electricity

There are 2 techniques to convert hydrogen in electricity; hydrogen turbines and fuel cells. For hydrogen turbines, the challenges are to run for 100% on hydrogen and to lower the high NO_x emissions. If hydrogen turbines are operative it is possible to achieve the same efficiencies obtained by combined-gas turbine

Table 4.6: Specifications Liquid Hydrogen storage & transportation

Storage & Transport		
DWT ship [ton]	1400	1600
Cost storage tanks shore and ship [M€] ([€/kg])	30 (0.05)	30 (0.04)
Cost round trip [€] ([€/kg])	50,000 (0.04)	50,000 (0.03)
Boil-off storage & transportation [%] ([€/kg])	2 (0.12)	2 (0.06)
$\mathbf{C_{transport}}$ **[€/kg]**	0.21	0.13

cycles, which is up to 60%. However, PEM fuel cells already have an efficiency of 51% nowadays, and the prediction is that in 2030 the efficiency becomes 64% [65]. For solid oxide fuel cells even efficiencies over 80% are predicted [65]. Nowadays the maturity of fuel cells is higher than for hydrogen turbines, and also the potential in the future is better, therefore fuel cells are chosen.

There are different kind of fuel cells which run on hydrogen; the alkaline fuel cell (AFC), the proton exchange membrane fuel cell (PEMFC), the solid oxide fuel cell (SOFC) and the phosphoric-acid fuel cell (PAFC). The most efficient fuel cell on MW scale nowadays is the PEMFC [78]. In the future it is possible that the SOFC, which is able to achieve higher efficiencies, will perform better than the SOFC, but for now the SOFC is not commercialized yet. Therefore the PEM fuel cell is chosen.

A PEM fuel cell works exactly the other way around as the PEM electrolyzer does. Hydrogen is fed to the PEM fuel cell and at the anode hydrogen is decomposed into hydrogen ions and electrons, the hydrogen ions permeate through the electrolyte and form water with oxygen added at the cathode. The electron runs through an electric circuit to generate electricity. PEM fuel cells usually operate at low pressures and low temperatures (50°C - 100°C). The electrolyte of a PEM fuel cell is a polymer, provided with catalysts, the catalyst usually used for the ionization of hydrogen is platinum or platinum ruthenium. An overview of the process is shown in Figure 4.6.

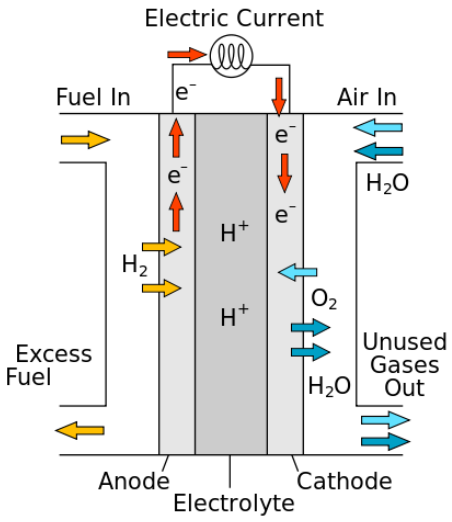

Figure 4.6: PEM fuel cell [13] [9]

In Table 4.7 an overview of all the specifications and costs of PEM fuel cells are given. PEM fuel cells operate **24** hours a day with an efficiency of **51**% (17.0 kWh/kg) in 2015 and **64**% (21.3 kWh/kg) in 2030 [65]. The lifetime of the PEM fuel cell is **60,000** hours and **80,000** hours in 2015 and 2030 respectively [65] and the investment costs are **2900** €/kW in 2015 and **750** €/kW in 2030 [65]. The O&M costs are assumed to be the same as for PEM electrolysis (**1.53**%). The costs of liquid hydrogen delivered in the Netherlands ($C_{LH_2,transport}$) is the liquid hydrogen cost produced in Morocco (C_{LH_2}) added with

the transportation costs ($C_{transport}$), which is **6.23** €/kg in 2015 and **2.95** €/kg. To obtain the costs per kWh ($C_{LH_2,out}$), $C_{LH_2,transport}$ is divided with the amount of electricity produced by the PEM fuel cell with one kg of hydrogen (17.0 kWh/kg in 2015 and 21.3 kWh/kg in 2030). The energy which can be obtained from the low liquid hydrogen temperature with for example waste heat is not taken into account. To get a feeling, the enthalpy difference between liquid hydrogen and hydrogen at ambient temperature is $2700kWh/kg = 0.75kWh/kg$. If 50% of the energy can be converted into electricity, 17.4 kWh/kg of electricity could be obtained in stead of 17.0 kWh/kg. This is a small increase in efficiency, but a large investment is needed to achieve this.

To obtain the investment costs of the PEM fuel cell $C_{invest,PEMFC}$ Equation (4.7) is used; The investment costs per kW (I) of the fuel cell are multiplied with the CRF and divided by the lifetime (L) times the efficiency of the fuel cell.

$$C_{investment}[€/\text{kg}] = \frac{I \cdot CRF}{L \cdot Eff} \tag{4.7}$$

The O&M costs of the fuel cell $C_{O\&M,PEMFC}$ are calculated with Equation (4.8), the O&M fraction is multiplied with the investment costs per kW, this is divided with the amount of hours in a year times the efficiency of the fuel cell. It is assumed that the capacity factor is 100%, so the fuel cell runs 24 hours a day.

$$C_{O\&M}[€/\text{kg}] = \frac{O\&M \cdot I}{365.25 \cdot 24 \cdot Eff} \tag{4.8}$$

The levelized cost of electricity (LCoE) of the liquid hydrogen concept become 0.491 €/kWh in 2015 and 0.159 €/kWh in 2030 with an round-trip efficiency of 27% and 40% respectively. This is, even in 2030, significantly above the criteria set of 0.125 euro/kWh. Therefore this option will at least not be viable until 2030 with the assumptions and predictions made in this report.

Table 4.7: Specifications Liquid Hydrogen Storage & Transportation

Liquid Hydrogen to Electricity		
	PEM Fuel Cell [65]	
hr per day	24	24
LHV [kWh/kg]	33.33	33.33
Eff [%]	51%	64%
Electricity out [kWh/kg]	17.0	21.3
Lifetime [hr]	60000	80000
CRF [-]	1.21	1.27
Investment [€/kW_out]	2900	750
O&M [%]	1.53%	1.53%
$C_{LH_2,transport}$ [€/kg]	6.23	2.95
$C_{LH_2,out}$ [€/kWh]	0.366	0.138
$C_{invest,PEMFC}$ [€/kWh]	0.115	0.019
$C_{O\&M,PEMFC}$ [€/kWh]	0.010	0.002
LCoE [€/kWh]	**0.491**	**0.159**
Round-trip efficiency	**27%**	**40%**

Energy Overview

In Figure 4.7 and Figure 4.8 a block diagram and an energy flow diagram of the liquid hydrogen concept is given. The values are from the year 2015. First hydrogen is produced by PEM electrolysis with an efficiency of 64%. Liquid hydrogen is created in the liquefaction plant with an energy consumption of 10 kWh/kg. The electricity inputs in PEM electrolysis and liquefying hydrogen are obtained from PV systems. During storage in Morocco, the Netherlands and on the tanker 2% of the liquid hydrogen is lost due to boil-off losses. In the Netherlands a PEM fuel cell is used to obtain electricity again. The efficiency of the PEM fuel cell is 51%. This leads to an overall efficiency of 27%. In Figure 4.8 the first part represents the electricity to liquid hydrogen process, the second part shows the storage and transport of liquid hydrogen. Finally, the third part shows the process from liquid hydrogen to electricity.

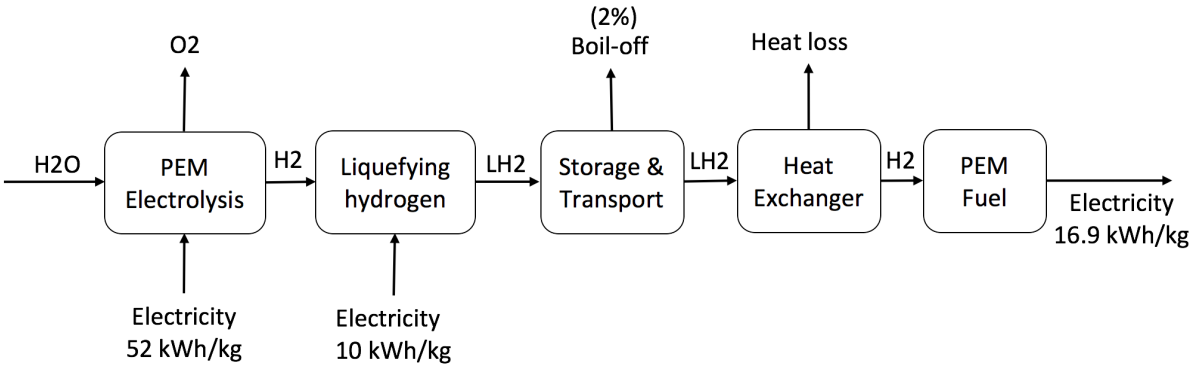

Figure 4.7: Liquid hydrogen block diagram

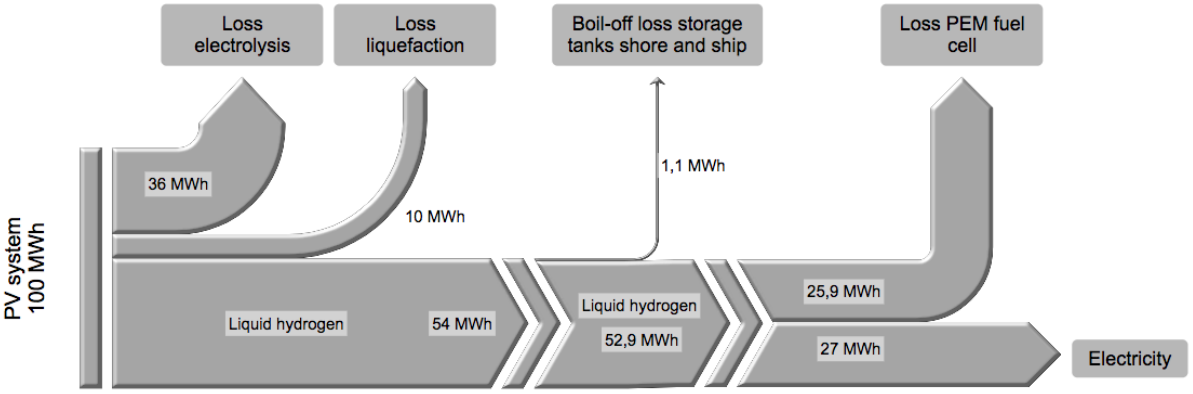

Figure 4.8: Liquid hydrogen energy flow

4.3 Chemical Hydrogen Storage

Hydrogen can also be stored as another fuel with the use of a chemical reaction. It is possible to create ammonia, methanol, hydrocarbons or formic acid from hydrogen, these are all fuels with a high energy density. The formation of formic acid is still in its infancy, it is a difficult process and a lot of research is done due to the high market price, but as an energy storage material methanol is a more viable option, therefore this method is not treated. For hydrocarbons the production of methane is considered.

4.3.1 Ammonia

Ammonia can be produced in two ways, with the Haber-Bosch process and by solid state ammonia synthesis. Solid state ammonia synthesis is a very promising concept, however the technology readiness level is still in its experimental phase. Because the technology readiness level of solid state ammonia synthesis is so low it is chosen to produce ammonia with electrolysis and the Haber-Bosch process.

Ammonia Production

Ammonia is produced with the over a century old Haber-Bosch process. The Haber-Bosch process is developed in 1909 by Fritz Haber and Carl Bosch. The most common way to produce ammonia nowadays is to convert natural gas into hydrogen (steam reforming) and obtain nitrogen from air. Nitrogen is combined with hydrogen to produce ammonia via the Haber-Bosch process. It is also possible to obtain hydrogen via electrolysis and produce ammonia with the Haber-Bosch process. An overview of producing ammonia with the use of electrolysis and the Haber-Bosch process is given in Figure 4.9.

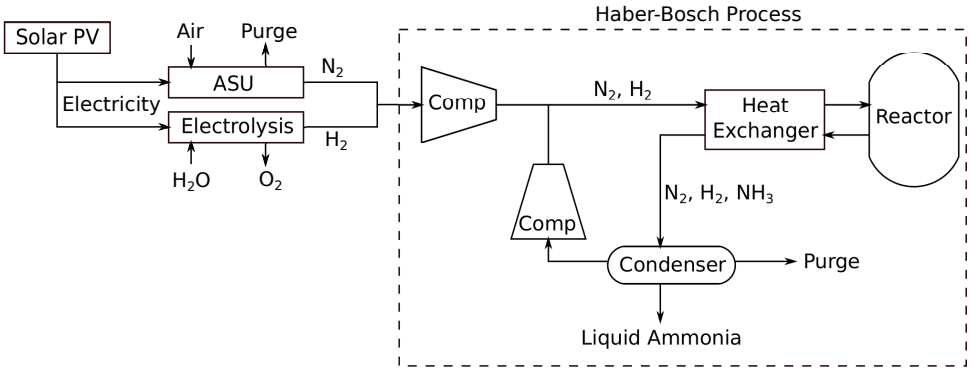

Figure 4.9: A schematic overview of ammonia production by electrolysis and Haber-Bosch

Electricity obtained from PV panels is used to run the air separation unit (ASU), electrolysis system and compressors. Air separation technologies separate air into pure nitrogen, argon and oxygen streams. There are three main processes to separate air; membrane separation, pressure swing adsorption and cryogenic air separation. Cryogenic air separation is the only separation process at this moment which can economically and realistically create large volumes of ultra-pure nitrogen [14]. First air is compressed and cooled to remove water vapor. The air is cooled further by a heat exchanger with the cold purified streams and expanded through a Joule-Thomson valve to obtain partially liquefied air, see Section 6.1.1 for more information on the liquefaction process of air. In a multiple column distillation tower pure nitrogen will boil-off due to its lower boiling point compared to oxygen and argon.

In the Haber-Bosch process the nitrogen (N_2) and hydrogen (H_2) streams are compressed and heated before they are fed into the reactor. In the reactor the reaction $N_2 + 3H_2 \rightarrow 2NH_3$ takes place. In the reactor catalysts are used to break up the strong triple bond of nitrogen. Typical catalysts are based on iron promoted with K_2O, CaO, SiO_2, or Al_2O_3. The reacted N_2, H_2 and NH_3 leave the reactor and enter the condenser. Because the boiling point of NH_3 is a lot lower than for H_2 and N_2, the liquid ammonia will be separated from the H_2 and N_2. The unreacted H_2 and N_2 streams are compressed and recycled. The reaction is strongly in favor of ammonia at room temperature, only the reaction rate is incredibly slow. The reaction rate increases at higher temperatures, only the reaction will shift towards nitrogen and hydrogen. Higher pressures will be in favor of ammonia as well, but high pressures cost energy too. The Haber-Bosch process acts optimally at pressures and temperatures between 150-250 bar and 400-500 °C respectively.

In Table 4.8 the specifications and costs of producing ammonia in 2015 and 2030 are displayed. The

Table 4.8: Specifications Ammonia Production

Electricity to Ammonia						
	PEM Electrolysis [65] [66]		Haber-Bosch & ASU [14]		Ammonia	
Year	2015	2030	2015	2030	2015	2030
Hour per day	7.2	7.2	7.2	7.2		
LHV [kWh/kg]	33.33	33.33	5.88	5.88	5.88	5.88
Eff [%]	64%	69%	88%	88%	59%	65%
$Elec_{in}$ [kWh/kg]	52	47	0.73	0.73	9.9	9.0
Lifetime [hr]	40000	75000	30 [yr]	30 [yr]		
Investment [€/kW]	1700	750	6800	6800		
CRF [-]	1.45	1.90	1.952	1.952		
O&M [%]	1.53	1.53	3.0	3.0		
H_2O [€/ton]	3	3				
$C_{electricity}$ [€/kg]	1.14	1.03	0.02	0.02	0.22	0.20
$C_{investment}$ [€/kg]	3.21	0.89	0.06	0.06	0.63	0.22
$C_{O\&M}$ [€/kg]	0.51	0.21	0.06	0.06	0.15	0.09
C_{H_2O} [€/kg]	0.03	0.03			0.005	0.005
$\mathbf{C_{NH_3}}$ **[€/kg]**	4.89	2.16	0.14	0.14	1.00	0.52

electricity used is coming from PV systems due to the lower LCoE costs. PV systems have an average operation time of **7.2** hours per day, therefore PEM electrolysis, ASU and the Haber-Bosch process will also operate for 7.2 hours per day. In 2015 **52** kWh of electricity is needed to obtain 1 kg of hydrogen, in 2030 this will be improved to **47** kWh [66]. The lifetime of the electrolysis system is **40,000** and **75,000** hours in 2015 and 2030 respectively [65] and the investment costs are 1700 €/kW in **2015** and **750** €/kW in 2030 [66]. The capital recovery factor (CRF) is calculated with use of Equation (2.4). The O&M costs for electrolysis are set at **1.53**%, this is estimated by Bertucciolli (2014) for a system between 250 MW and 1000 MW [66]. Finally the costs of purified water are set at **3**€/ton [70]. For the Haber-Bosch process and ASU the values are the same in 2015 and 2030, this is done because the Haber-Bosch process is responsible for most of the costs and little improvement in efficiency and costs is expected due to the maturity and well developed status of the process. The electricity needed for the ASU to produce enough nitrogen for one kg of ammonia is **0.088** kWh. The Haber-Bosch process consumes **0.64** kWh of electricity to produce one kg of ammonia [14]. The lifetime is set at **30** years and the investment costs are **6800** €/kg [14].

The electricity costs ($C_{electricity}$) are simply calculated by multiplying the LCoE of PV systems (0.022) with the electricity needed per kg. $C_{investment}$ and $C_{O\&M}$ are obtained with Equation (4.5) and Equation (4.6), respectively. There is 9 kg of water needed to obtain 1 kg of hydrogen ($2H_2O \rightarrow 2H_2 + O_2$), therefore the cost of water (C_{H_2O}) to produce 1 kg of hydrogen is 27 €/ton (0.03 €/kg). To obtain the ammonia costs, the electrolysis costs are multiplied by a factor of 3/17=0.18 ($N_2 + 3H_2 \rightarrow 2NH_3$) and the Haber-Bosch and ASU costs are added. The price per kg of ammonia becomes **1.00** €/kg in 2015 and **0.52** €/kg in 2030.

Storage & Transport

To transport liquid ammonia, one tanker is used which sails back and forth. The time to sail from Morocco to the Netherlands with a speed of 15 knots takes 4 days, with a harbour time of 2 days the round-trip time of the ship becomes 12 days. The capacity of the storage tanks on shore and on the tanker need to be able to store 12 days of liquid ammonia produced. With a maximum power input per day of $800 \cdot 9 = 7200$ MWh during the summer, see Section 2.3.1, 86.4 GWh of electricity needs to

be converted into ammonia in 12 days. With an electricity input of 9.9 kWh/kg and 9.0 kWh/kg this results in a liquid ammonia storage capacity of **8700** ton in 2015 and **9600** ton in 2030, respectively.

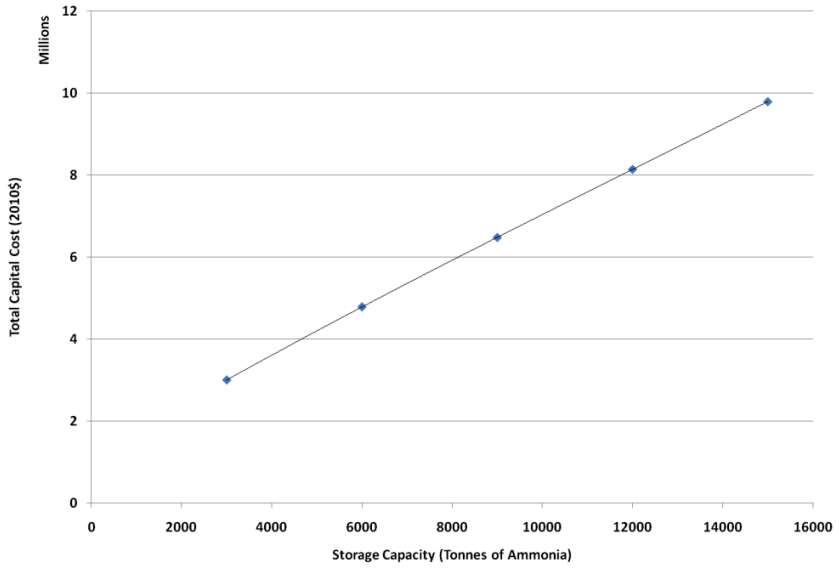

Figure 4.10: Ammonia storage costs including refrigeration loop [14]

Liquid ammonia is stored at 240 K and atmospheric pressure in an insulated storage tank. Due to the heat transfer to the atmosphere, boil off of ammonia occurs. Because the boil-off of ammonia harms the environment, it is necessary to include a refrigeration loop to liquefy the gaseous ammonia again. Morgan (2013) obtained a boil off rate of 0.03% per day for a storage tank with a capacity of 9000 tonnes of liquid ammonia. This is almost the same as the capacity used in 2015 and 2030, therefore the same values are taken. To liquefy this, 12.75 kW of electricity is needed to run the refrigeration loop [14]. In Morocco the electricity is generated by the PV system, but on board of the tanker and in the Netherlands the electricity is obtained by a fuel cell. An efficiency of 50% is assumed for the fuel cell and the fuel cell on board of the tanker only operates 50% of the time since it is empty when it sails from the Netherlands to Morocco. This results in an electricity addition of $12.75 \cdot 24 \cdot 12 + 12.75 \cdot 24 \cdot 6/0.5 + 12.75 \cdot 24 \cdot 12/0.5 =$ 14.7 MWh per round-trip. This is negligible compared to the electricity input of 86.4 GWh. The extra costs as a result of the extra fuel cells are also very small compared to the total costs and therefore also neglected. The costs of the storage tanks including refrigeration loop are respectively 6.2 M$ and 6.8 M$ per tank, see Figure 4.10. For 3 storage tanks this becomes **16.9** M€ in 2015 and **18.6** M€ in 2030. With the DWT and total number of trips in 30 years ($365.25 \cdot 30/12 = 900$) known, the induced cost in 2015 and 2030 becomes **0.004** €/kg.

The round-trip costs for tankers with different DWT are calculated in Section 3.4.1. The round-trip cost for a tanker with a DWT of 9000 ton is **100,000** €. The cost addition to transport one kg of ammonia becomes **0.01** €/kg in 2015 and 2030. Looking at Table 4.9, the cost to transport ammonia is low compared to the costs to produce ammonia.

Table 4.9: Specifications Ammonia Storage & Transportation

Storage & Transport		
DWT ship, size storage tanks [ton]	8700	9600
Cost storage tanks shore and ship [M€] ([€/kg])	16.9 (0.004)	18.6 (0.004)
Cost round trip [M€] ([€/kg])	0.10 (0.01)	0.10 (0.01)
$\mathbf{C_{transport}}$	0.01	0.01

Ammonia to Electricity

There are 2 techniques to convert ammonia in electricity; turbines and fuel cells. To convert ammonia into power by means of gas turbines is difficult, the auto-ignition temperature of ammonia is very high (651 °C) and the flame speed is low [79], therefore it is hard to obtain a stable efficient combustion. Another problem is the high production of NO_x emissions which harm the environment. Also the TRL is low as the largest ammonia turbines nowadays are 50 kW, which is low compared to normal gas turbines of several 100 MW. Due to all these disadvantages of ammonia turbines, fuel cells are used to convert ammonia into electricity.

Before the PEM fuel cell can be used, ammonia has to be cracked at high temperatures to obtain hydrogen and nitrogen. The dissociation of ammonia takes place at a temperature of 920 °C [80]. To maintain the heat added to the system, solid oxide fuel cells can be more efficient to use in the future. For now PEM fuel cells are used to convert electricity back from ammonia, since it is the most efficient fuel cell power plant operating at MW scale nowadays. To crack ammonia a heat addition of **14**% of the LHV of ammonia is needed ($E_{cracking,\%}$) [80], this results in an energy addition of **0.83** kWh/kg ($E_{cracking,kWh}$). It is assumed that the heat is obtained from burning ammonia with an efficiency of 100%. The specifications in Table 4.10 of the PEM fuel cell are obtained exactly the same as for the PEM fuel cells in the liquid hydrogen to electricity subsection, see Section 4.2.2. Also $C_{invest,PEMFC}$ and $C_{invest,PEMFC}$ are calculated in this same manner as in Section 4.2.2. Only $C_{NH_3,out}$ is obtained slightly different; The total costs of ammonia in the Netherlands ($C_{NH_3,transportation}$) is obtained by adding the ammonia production costs (C_{NH_3}) and the transportation costs ($C_{transporation}$). To obtain $C_{NH_3,out}$, $C_{NH_3,transportation}$ is divided by the amount of electricity the PEM fuel cell generates with one kg of hydrogen ($Elec_{out}$) times the fraction of ammonia left after cracking, which is $100 - 14 = 86\%$, see Equation (4.9).

$$C_{NH_3,out} = \frac{C_{NH_3,transportation}}{(100 - E_{cracking,\%})/100 \cdot Elec_{out}} \tag{4.9}$$

Table 4.10: Specifications Ammonia to Electricity

Ammonia to Electricity		
	Cracking [80]	
$E_{cracking,\%}$ [% of LHV]	14%	14%
$E_{cracking,kWh}$ [kWh/kg NH_3]	0.83	0.83
	PEM Fuel Cell [65]	
hr per day	24	24
LHV [kWh/kg]	5.88	5.88
Eff [%]	51%	64%
$Elec_{out}$ [kWh/kg]	3.0	3.8
Lifetime [hr]	60000	80000
Investment [€/kW_out]	2900	750
CRF [-]	1.21	1.27
O&M [%]	1.53%	1.53%
$C_{NH_3,transport}$ [€/kg]	1.015	0.531
$C_{NH_3,out}$ [€/kWh]	0.394	0.164
$C_{invest,PEMFC}$ [€/kWh]	0.058	0.012
$C_{O\&MPEMFC}$ [€/kWh]	0.005	0.001
LCoE [€/kWh]	**0.458**	**0.178**
Round-trip efficiency [%]	**26%**	**36%**

Energy Overview

In Figure 4.11 a block diagram of the ammonia concept is given. The values are from the year 2015 and the electricity inputs are based on the production of 1 kg of ammonia. First, hydrogen is produced by PEM electrolysis, which uses 9.18 kWh to produce 0.18 kg of hydrogen. 0.82 kg of nitrogen is obtained from an air separation unit (ASU) with an electricity consumption of 0.09 kWh. Hydrogen and nitrogen produce one kg of ammonia with use of the Haber-Bosch process. The losses during storage and transportation of ammonia are neglected. A part of the ammonia is burned to generate the heat necessary to crack ammonia into nitrogen and hydrogen. With use of PEM fuel cells 2.57 kWh of electricity is obtained.

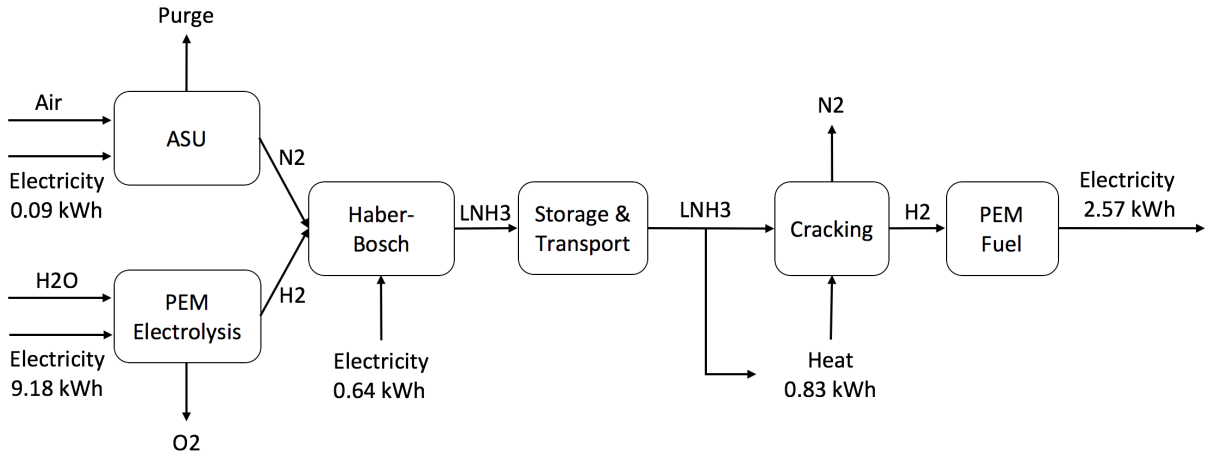

Figure 4.11: Ammonia block diagram

In Figure 4.12 an energy flow diagram with 100 MWh of electricity input from PV systems is shown. The first part represents the electricity to ammonia process. During electrolysis 35.9 MWh of electricity is lost, the Haber-Bosch process and ASU consume 4.7 MWh together. The second part shows the storage and transportation of ammonia, here no losses are shown because they were so low they are neglected. In the third part the process from ammonia to electricity is shown. First the ammonia is cracked into hydrogen and nitrogen, this process consumes 8.4 MWh of heat. Finally the PEM fuel cell is used to obtain electricity again. The efficiency of the PEM fuel cell is 51%. This leads to an electricity output of 26 MWh and a round-trip efficiency of 26%.

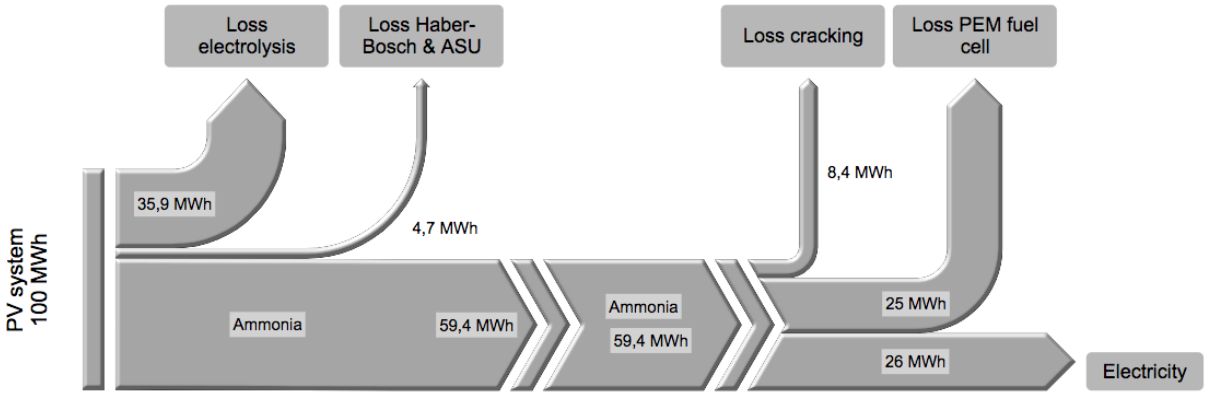

Figure 4.12: Ammonia energy flow

4.3.2 Methanol

To store electricity in methanol, methanol is produced by reacting hydrogen with carbon dioxide. The process described in Perez-Fortes (2016) [15] is used to obtain all the efficiencies and costs of the methanol production process. Methanol is converted into electricity with the use of PEM fuel cells. CO_2 is captured in the Netherlands during methanol reforming and transported to Morocco to feed the methanol production process.

Methanol Production

In Figure 4.13 a schematic overview of the methanol production process is shown, in Appendix E the full methanol production process flow diagram used in Perez-Fortes (2016) is shown [15]. H_2 and CO_2 are compressed to a pressure of 78 bar and mixed with the recycle stream coming from the flash vessel. The mixed stream is heated up to 210°C before it enters the reactor. The two main reactions that occur in the reactor are:

$$CO_2 + 3H_2 \rightleftharpoons H_2O + CH_3OH \tag{4.10}$$

$$CO_2 + H_2 \rightleftharpoons H_2O + CO \tag{4.11}$$

The stream leaving the reactor has a temperature of 290°C with a volume fraction of 4.7% of methanol, it also contains CO_2, H_2O, H_2, and CO. Reaction Equation (4.10) produces methanol, while Equation (4.11) is undesired because it consumes the feed meant to produce methanol. The selectivity is pushed towards methanol production by recycling CO and the unreacted hydrogen after the flash vessel. The stream is cooled to 35°C before entering the flash vessel. In the flash vessel the liquid and vapor phases are separated. The vapor stream contains CO_2, H_2, and CO and is recycled, about 1% of the recycle stream is purged to avoid accumulation. The liquid stream only contains methanol and water. The methanol/water mixture is preheated and partially evaporated before it is fed to the distillation tower where the mixture is separated. The top gas stream of the distillation tower is partially condensed and the liquid stream is fed back to the distillation tower. Finally, methanol is condensed at 35°C and the remaining inert gases are purged. The heat addition and heat removal during the process are integrated with heat exchangers, the heat which is left is used to run an organic Rankine cycle to obtain electricity for the compressors.

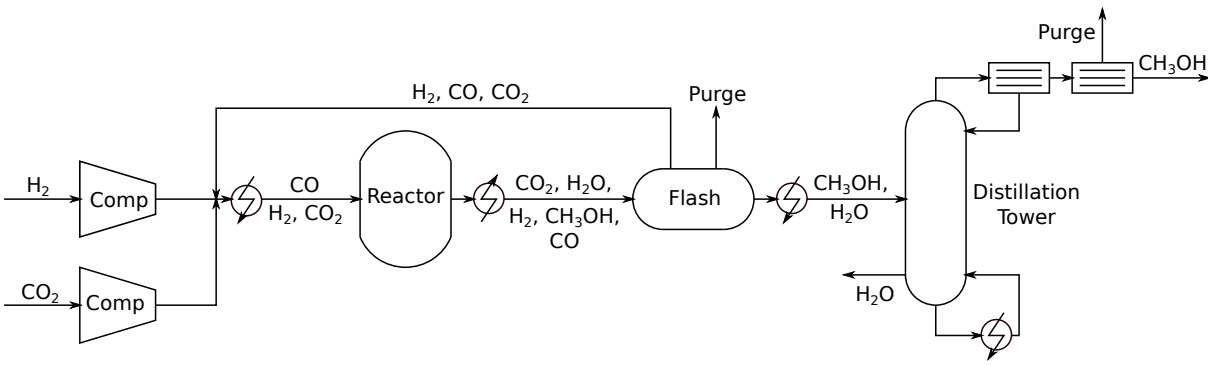

Figure 4.13: Schematic overview of the methanol production process

In Table 4.11 the specifications and costs of the methanol production are shown. The method to obtain the PEM electrolysis costs and specifications are explained in Section 4.2.2 and Section 4.3.1, also

the method to obtain the costs for methanol synthesis and methanol production are obtained in the same manner as the production of ammonia and the production of liquid hydrogen. In Appendix E two tables out of Perez-fortes (2016) are stated [15]. Here it can be seen that the total energy consumption is **1.49** kWh of electricity and heat per kg methanol. It is assumed that the heat input can also be fulfilled by electricity with an efficiency of 100%. It is also assumed that the efficiency of the entire process increased with 10% in 2030. The investment costs are 451 €/(t_{MeOH}/yr). Rearranging this with an LHV of 5.53 kWh/kg and average operation hours of 7.2 hours per day, the investment costs become **950** €/kW. This leads to a methanol production cost of **0.88** €/kg in 2015 and **0.42** €/kg in 2030.

Table 4.11: Specifications Methanol Production

Electricity to Methanol						
	PEM Electrolysis [65] [66]		Methanol Synthesis [15]		Methanol	
Year	2015	2030	2015	2030	2015	2030
Hour per day	7.2	7.2	7.2	7.2		
LHV [kWh/kg]	33.33	33.33	5.53	5.53	5.53	5.53
Eff [%]	64%	71%			49%	54%
$Elec_{in}$ [kWh/kg]	52	47	1.47	1.32	11.2	10.2
Lifetime [hr]	40000	75000	30 [yr]	30 [yr]		
CRF	1.45	1.90	1.952	1.952		
Investment [€/kW_{in}]	1700	750	950	950		
O&M [%]	1.5%	1.5%	3.0%	3.0%		
H20 [€/ton]	3	3				
$C_{electricity}$ [€/kg]	1.14	1.03	0.03	0.03	0.22	0.20
$C_{investment}$ [€/kg]	3.21	0.89	0.02	0.02	0.55	0.17
$C_{O\&M}$ [€/kg]	0.51	0.21	0.02	0.02	0.10	0.05
C_{H_2O} [€/kg]	0.03	0.03			0.005	0.005
C_{CH_3OH} [€/kg]	4.89	2.16	0.07	0.06	0.88	0.42

Transport

As described in Section 4.3.1, the total amount of electricity generated in 12 days (round-trip time of tanker) is 86.4 GWh. With 86.4 GWh of electricity, 7700 ton methanol is produced in 2015 and 8500 ton of methanol is produced in 2030 using the production process described in Figure 4.13. Methanol can be stored at ambient temperature and atmospheric pressure, to store methanol is less complex and no recycle loop is needed in comparison with ammonia storage. However, the CO_2 recovered in the Netherlands needs to be transported to Morocco. 1.37 kg CO_2 is needed per kg of methanol, see Appendix Chapter E, therefore the capacity of the tanker should be **10000** ton in 2015 and **11000** ton in 2030. Liquid CO_2 is shipped at 7.5 bar with a temperature of -53°C [81]. It is assumed that the costs for ammonia storage and CO_2 storage are the same. In Figure 4.10 it can be seen that the cost of a 10000 ton storage tank is **7** M€and the cost for a 11000 ton storage tank is **7.5** M€. A tanker with a DWT of ±10500 has a round-trip cost of **110,000** €. For the specification and assumptions made on the tanker, see Section 3.4.1. The additional cost of transporting methanol becomes **0.016** €in 2015 and **0.014** in 2030, see Table 4.12 for an overview of the transportation costs.

Methanol to Electricity

To obtain electricity from methanol, it is chosen to reform methanol into H_2 and CO_2. The hydrogen is used to run a PEM fuel cell and the CO_2 is captured, stored and transported back to Morocco. Reforming

Table 4.12: Specifications Methanol Storage & Transportation

Storage & Transport		
DWT ship, size storage tanks [ton]	10000	11000
Cost storage tanks shore and ship [M€] ([€/kg])	21 (0.004)	22.5 (0.004)
Cost round trip [€] ([€/kg])	110,000 (0.01)	110,000 (0.01)
$\mathbf{C_{transport}}$	0.016	0.014

methanol into hydrogen involves a reaction with gaseous methanol and steam on heterogeneous catalytic surfaces; first methanol is decomposed into hydrogen

$$H_2O + CH_3OH \rightleftharpoons CO + H_2 \tag{4.12}$$

and the second reaction is the water shift reaction.

$$H_2O + CO \rightleftharpoons CO_2 + H_2 \tag{4.13}$$

The reaction operates at 200°C (473K), because at this temperature with a suitable catalyst and ideal operating conditions nearly 100% conversion of methanol can be achieved [82]. The two reactions combined give the total reaction:

$$H_2O(l) + CH_3OH(l) \rightleftharpoons CO_2(g) + 3H_2(g) \qquad H_{473} = 58.4kJ/mol \tag{4.14}$$

The theoretical heat needed to convert 1 kg of methanol into hydrogen and carbon dioxide is the difference in enthalpy of water and methanol at atmospheric temperature and 473 K plus the heat addition during the endothermic reaction. The enthalpy of water and methanol at ambient temperature and atmospheric pressure are respectively 1.5 kJ/mol and -3.8 kJ/mol [83]. The enthalpy at 1 bar and 473 K is 51.8 kJ/mol for water and 43.5 kJ/mol for methanol[83]. The heat addition during the endothermic reaction is 58.4 kJ/mol [82]. To obtain the units in kJ/kg, the formula is divided by the molar mass of methanol ($MM_{methanol}$), see Equation (4.15).

$$\begin{aligned} E_{heat} &= \frac{(H_{H_2O,293} - H_{H_2O,473}) + (H_{CH_3OH,293} - H_{CH_3OH,473}) + H_{reaction,473}}{MM_{methanol}} \\ &= \frac{((51.8 - 1.5) + (53.5 - -3.8) + 58.4)}{0.032} \\ &= 5187.5kJ/kg = 1.44kWh/kg \end{aligned} \tag{4.15}$$

Methanol is burned to achieve the heat needed, the efficiency is assumed to be 90% and no use is made of heat recovery. This leads to an energy addition of 1.44/0.9 = **1.60** kWh/kg. With a LHV of methanol of 5.53 kWh/kg, 1.60/5.53=**0.289** kg of methanol has to be burned to convert 1 kg of methanol into hydrogen and carbon dioxide, so 22.4% of all the methanol has to be burned to provide heat for the methanol reforming process.

Now hydrogen and carbon dioxide have to be separated; hydrogen will be fed to the PEM fuel cell and carbon dioxide will be liquefied, stored and transported to Morocco. This is done by cryogenic distillation because the carbon dioxide has to be liquefied anyway. It is an energy intensive process

estimated to consume 0.6 kWh per kg of liquefied carbon dioxide recovered [84]. Electricity obtained from the fuel cell is needed to cool the gases. To cool the carbon dioxide and hydrogen obtained by 1 kg of methanol, $0.6 \cdot 44/50$ (molar mass carbon dioxide / molar mass methanol) = **0.53** kWh of electricity is needed. This includes the CO_2 produced by burning the methanol and the production of CO_2 by the methanol reforming process.

Table 4.13: Specifications Methanol to Electricity

Methanol to Electricity		
	Reforming [82]	
Reforming [kWh/kg CH_3OH]	1.60	1.60
	Carbon Capture [84]	
Carbon Capture (CC) [kWh/kg CH_3OH]	0.53	0.53
	PEM Fuel Cell [65]	
hr per day	24	24
LHV [kWh/kg]	5.53	5.53
Eff [%]	51%	64%
$Elec_{out}$ [kWh/kg]	2.8	3.5
Lifetime [hr]	60000	80000
Investment [€/kW_out]	2900	750
CRF [-]	1.21	1.27
O&M [%]	1.53%	1.53%
$C_{CH_3OH,transport}$ [€/kg]	0.897	0.436
$C_{CH_3OH,out}$ [€/kWh]	0.542	0.197
$C_{invest,PEMFC}$ [€/kWh]	0.114	0.019
$C_{O\&MPEMFC}$ [€/kWh]	0.010	0.002
LCoE [€/kWh]	**0.666**	**0.217**
Round-trip efficiency [%]	**14%**	**20%**

In Table 4.13 the specifications and costs for the methanol to electricity process are given. The operation and capital costs for methanol reforming and carbon capture are not included. No data could be found and even without the extra costs of these processes, the LCoE of the methanol concept is large compared to the other concepts. The LCoE in 2015 becomes **0.666** €/kWh and in 2030 the LCoE is **0.217** €/kWh. Almost everything is calculated the same as in Section 4.3.1, only $C_{CH_3OH,out}$ is calculated according to the following formula:

$$C_{CH_3OH,out} = \frac{C_{CH_3OH,transport}}{Elec_{out} \cdot (1 - F_{burned,methanol}) - CC} \tag{4.16}$$

$F_{burned,methanol}$ is the extra methanol fraction burned to provide the heat necessary for the reforming process and CC is the electricity needed for the carbon capture process. The costs of water used by the reforming process are neglected.

Energy Overview

In Figure 4.14 a block diagram of the methanol concept is given. The values are from the year 2015 and the electricity inputs are based on the production of 1 kg of methanol. To produce 1 kg of methanol 0.199 kg of hydrogen is needed, see Appendix Chapter E, which consumes 10.3 kWh/kg. 1.5 kWh is needed to synthesize 1 kg of methanol by reacting hydrogen and the recovered carbon dioxide following the scheme

given in Figure 4.13. Methanol is transported and 22.4% of the methanol is burned to provide the heat necessary for methanol reforming, this process consumes 1.6 kWh. To capture the carbon dioxide produced during burning and reforming methanol, 0.53 kWh of electricity is needed. The total electricity produced by the fuel cell which can be delivered to the customer is 1.7 kWh.

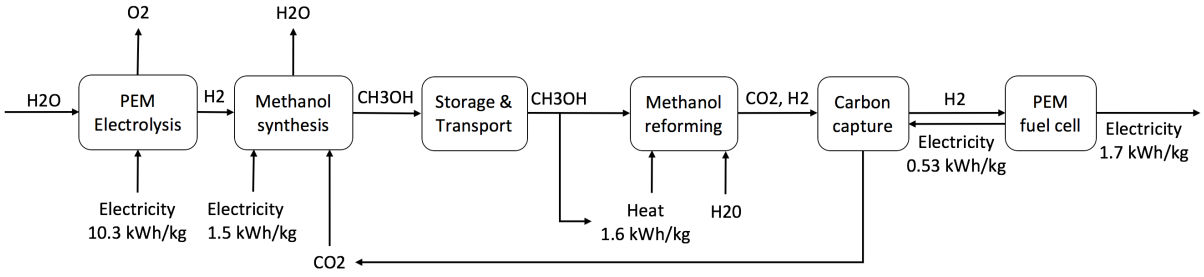

Figure 4.14: Methanol block diagram

In Figure 4.15 an energy flow diagram with 100 MWh of electricity input from PV systems is shown. The first part represents the electricity to methanol process. During electrolysis 40.5 MWh of electricity is lost and the losses of methanol synthesis obtain 12.6 MWh. The second part shows the storage and transportation of methanol, there are no heat losses since methanol is a liquid at ambient temperature and atmospheric pressure. In the third part the process from methanol to electricity is shown. First the methanol is reformed into hydrogen and carbon dioxide, this process consumes 10.5 MWh of heat. The carbon dioxide produced during burning and reforming methanol has to be captured and stored, this process consumes 8.8 MWh of electricity. The PEM fuel cell is used to obtain electricity again. The efficiency of the PEM fuel cell is 51%. This leads to an electricity output of 14 MWh and a round-trip efficiency of 14%.

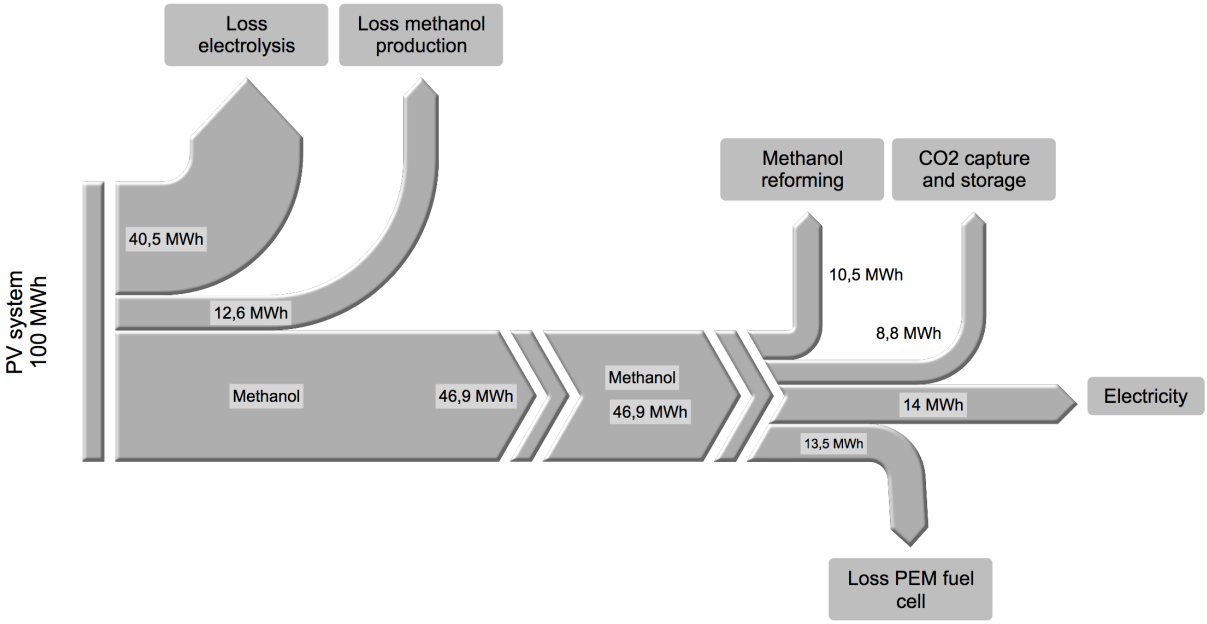

Figure 4.15: Methanol energy flow

4.4 Conclusion

The direct formation of ammonia, methane or formic acid from electricity are all very interesting due to high conversion efficiencies, only the developments are still in its experimental phase; all the direct fuel conversion technologies have a TRL lower than 6. All the processes are very promising but it will take a lot of time before these processes are commercially available.

It is found that the best way to produce hydrogen is by PEM electrolysis; SOE is simply more expensive and less mature, while the inability to turn off the electrolysis process completely is the cause of failure for alkaline electrolysis. The costs to produce one kg of hydrogen with PEM electrolysis is €7.28 in 2015 and becomes €2.20 in 2030. Nowadays hydrogen is mostly produced with natural gas reforming, this has a price of 1 €/kg. So the market price of hydrogen from renewable sources can not compete with hydrogen produced from natural gas.

In this thesis 3 hydrogen storage solutions are worked out: Liquefying hydrogen, producing ammonia with the Haber-Bosch process and producing methanol by reacting H_2 with CO_2. Liquid hydrogen is obtained by cooling and expansion, it needs to be stored at extremely low temperatures which results in boil-off losses and expensive ships and storage tanks. To obtain electricity in the Netherlands, PEM fuel cells are used. A round-trip efficiency of 27% with a LCoE of 0.491 €/kWh is obtained in 2015, from the predictions of 2030 a round-trip efficiency of 40% with a LCoE of 0.159 €/kWh is derived. Ammonia is produced with the Haber-Bosch process, this is an energy intensive process. The costs to produce ammonia is 1.00 €in 2015 and 0.52 €in 2030. To generate electricity again in the Netherlands, ammonia has to be cracked first before it runs through a fuel cell. The efficiencies obtained in 2015 and 2030 are 26% and 35% respectively. The LCoE is 0.458 €/kWh in 2015 and 0.178 €in 2030. Methanol is produced by reacting H_2 with CO_2, a lot of energy is lost by the production of water. Methanol is obtained at a price of 0.88 €/kg and 0.42 €/kg in 2015 and 2030 respectively. To obtain electricity from methanol, methanol has to be reformed and the CO_2 needs to be captured and used in the methanol production process again. Methanol reforming and CO_2 capture are energy intensive processes. A round-trip efficiency of 14% with a LCoE of 0.666 €/kWh is obtained in 2015, the predictions in 2030 result in a round-trip efficiency of 20% with a LCoE of 0.217 €/kWh.

The most efficient and cost effective solution in this chapter is storing electricity in the form of liquid hydrogen. Looking at the LCoE of all the fuels evaluated it is concluded that storing electricity in chemical energy storage via electrolysis is not profitable. The market price for methanol is 0.38 €/kg and the market price for ammonia is 0.32 €/kg [85]. The price of methanol synthesis in 2030 via electrolysis are coming close to the market price, assuming the market price will be the same in 2030. It has to be remarked that no CO_2 costs are included in the methanol production prices.

Chapter 5

Thermal Energy Storage (Solar Salt)

5.1 Operation

In Figure 5.1 an overview of the Solar Salt concept is given. First Solar Salt is heated by the use of CSP (left side of Figure 5.1). Hot Solar Salt is pumped onto a tanker and shipped to the Netherlands (centre of Figure 5.1). In Rotterdam the hot Solar Salt is used to power a steam turbine (left side of Figure 5.1). Finally, the cooled Solar Salt is fed back to the tanker and shipped to Morocco (centre of Figure 5.1).

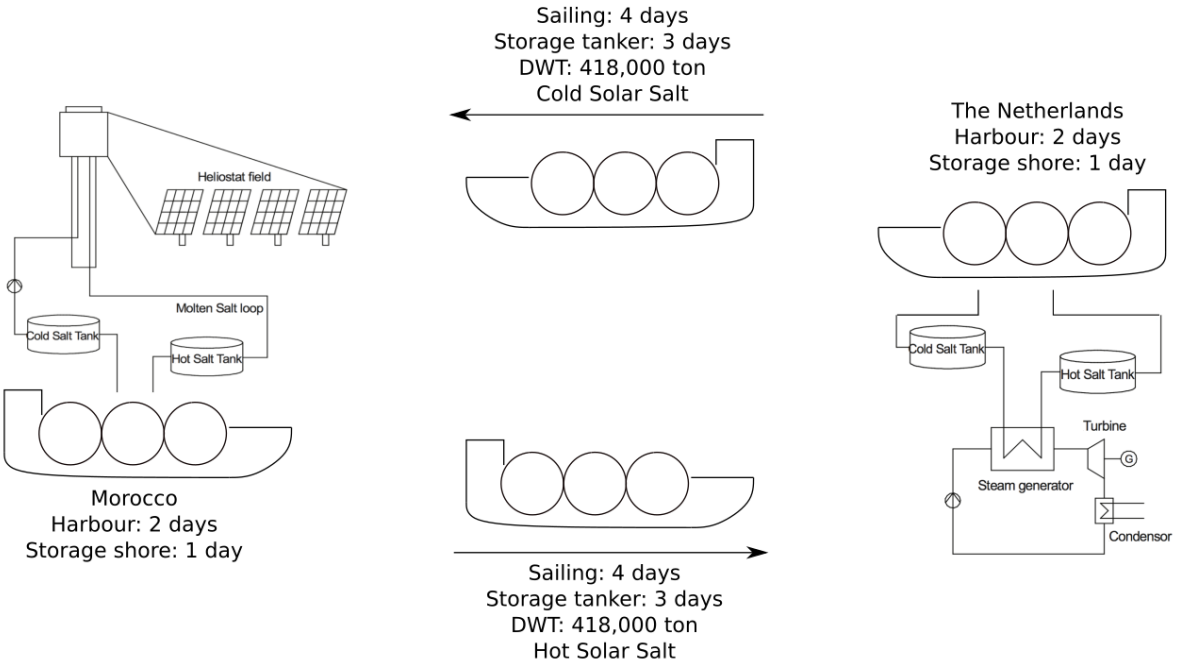

Figure 5.1: Operation Solar Salt concept with 4 ships

The total project exists out of 4 tankers which are sailing with an interval of 3 days between each other. Calculations were also done for different amounts of tankers; more tankers led to higher capital and fuel costs and less tankers led to less energy transported. It was found that the operation was the most cost effective with 4 tankers. The round trip time of one tanker is 12 days; sailing takes 4 days from and 4 days to Morocco, the harbour time in Morocco and in the Netherlands is both 2 days, see

Section 3.4.1. The storage tanks on shore in the Netherlands and in Morocco need to have a capacity of 1 full day of storage. This is needed because the interval between a tanker leaving the harbour and the next tanker arriving at the harbour is 1 day. When the tanker is in the harbour, the heated Solar Salt is pumped directly on the tanker. The storage tanks on the tanker need to be able to store the amount of Solar Salt heated in 3 days. The heat losses of each step are shown in Table 5.3 and Figure 5.4. Solar Salt always stays in liquid form to prevent solid deposits and keep it easy to pump around.

5.2 Energy Balance

In this section the energy balance of the Solar Salt concept is described. First the properties of Solar Salt are given and in the subsections following the heat losses in the storage tanks, pipes and during transportation are calculated. Finally the total power output in the Netherlands is calculated and an overview of the energy balance can be found in Figure 5.4.

5.2.1 Solar Salt properties

Solar salt is the energy carrier used for thermal energy storage, see Section 3.1.3 for the selection process. It is used because CSP plants also use Solar Salt and the characteristics of Solar Salt are very good. It is relatively easy to handle at such high temperatures, because no unwanted chemical reactions occur at high temperatures and there is no boil-off. Also the energy density is high compared to other sensible heat energy storage solutions. To prevent solidification the minimum temperature of Solar Salt is taken at 288 °C, this is 68 degrees higher than the solidification temperature of Solar Salt. Solar Salt stays in liquid form at all times, this is done te prevent volume expansion and solid deposits. In Table 5.1 the characteristics of Solar Salt are shown.

Table 5.1: Properties Solar Salt

Variable	Value	Unit
T_{hot}	565	$^{\circ}C$
T_{cold}	288	$^{\circ}C$
$T_{solidification}$	220-240	$^{\circ}C$
c_p	1.6	$kJ/kg \cdot K$
ρ	1840	kg/m^3

5.2.2 Solar energy to Solar Salt on ship

The energy from the sun is reflected by heliostats to heat Solar Salt in the receiver of the solar tower, this process is explained in Section 2.2. The efficiency of the heliostat reflection is 75%[86] of the DNI and the heat loss in the receiver is 7.5% of the DNI [86]. The hot Solar Salt reaches the hot storage tank with a temperature of 565 °C, as can be in Figure 2.4. The Solar Salt is pumped through a piping system to the ULCC.

Storage tank

The capacity of the storage tanks on shore in Morocco need to be designed to store energy for one full day, this is needed because the interval between a tanker leaving the harbour and the next tanker arriving at the harbour is 1 day. It is reasoned in Section 2.2 that the total electrical output of the CSP system

is 300 MW ($2 \cdot 150$) of electricity, this is equal to 714 MW of heat stored in Solar Salt. The CSP plant runs for 24 hours a day during the summer and the electricity is obtained by 2 solar tower systems. Each CSP system has one hot storage tank and one cold storage tank. The energy capacity of one hot storage tank must be able to store 3600 MWh of electricity, because the power block has an efficiency of 42%, see Equation (5.4), the storage tank must be able to hold 8570 MWh of heat stored in Solar Salt. The specific energy (SE) of Solar Salt is shown in Equation (5.1).

$$SE_{MS} = c_p \cdot \Delta T = 1.6 \cdot (565 - 288) = 443.2 kJ/kg \tag{5.1}$$

The storage tanks need to store $8570 \cdot 3600/0.4432 = 70,000$ ton of Solar Salt, this corresponds to 38,000 m^3. This results in a storage tank with a radius of 20 meter and a height of 30 meter. A cylindrical shape is chosen since internal stresses will be evenly distributed by the round shape of the storage tank and it is still convenient to place the storage tank on the ground. Because there are 2 CSP systems, there will be 2 hot storage tanks and 2 cold storage tanks in Morocco. For the heat losses in the storage tanks the following empirically derived formula is taken [87], see Equation (5.2). This formula is derived from storing Solar Salt in storage tanks with a capacity of 5,000 ton to 70,000 ton.

$$q_{loss} = 0.00017 \cdot T_{salt} + 0.012 \quad kW/m^2 \tag{5.2}$$

Where T_{salt} is the temperature (in °C) of the Solar Salt in the hot and in the cold tank, respectively. The total area of one storage tank is 6300 m^2, this results in a heat loss of 680 kW for the hot storage tanks and a heat loss of 384 kW for the cold storage tanks. In 24 hours the hot storage tank has lost **16 MWh** of energy and the cold storage tank has lost **9.2 MWh**.

Piping system

The solar tower of a CSP system stands in the middle of the heliostat field. To pump Solar Salt on and off the ship, it is assumed that the heliostat field is very close to the sea, as can be seen in Figure 5.2. A CSP plant with an electricity output of 150 MW requires an area of around 300 hectares [88], to obtain an area of 300 hectares the radius of the heliostat field would become 1 km. To reach the tanker from the middle of the heliostat fields, two piping systems with a length of 1.4 km are needed, see Figure 5.2, and every piping system has two pipes; one pipe which pumps cold Solar Salt from the tanker to the solar tower and one pipe which pumps hot Solar Salt from the solar tower to the tanker. The heat flow coming from the solar tower stored in molten salt is 150/0.42=357 MW, 357 MW of hot molten salt corresponds to a Solar Salt flow of 806 kg/s. It is assumed that the speed of Solar Salt through the pipes is 2 m/s, combining this with the density of Solar Salt results in a cross sectional area of 0.22 m^2 for the pipes and a circumference of 1.66 m. The total area of one pipe from the solar tower to the tanker is 2320 m^2. It is assumed that the heat loss of the pipes can also be modelled with Equation (5.2) of the storage tanks. Implementing the total area of the pipes in the equation results in a heat loss of 251 kW and 141 kW for one hot pipe and cold pipe respectively. To fill up one tanker takes 2 days, this is the time the tanker stays in the harbour and heat losses will occur. The heat losses of one piping system to load and unload one tanker with Solar Salt in Morocco become **12.0** MWh and **6.8** MWh respectively. Since there are 2 piping systems, the total heat loss of pumping Solar Salt on and off the tanker is $12 \cdot 2 + 6.8 \cdot 2 = 37.6 MWh$.

In Rotterdam it is assumed that the ship harbours immediately next to the power block. The piping system to the heat exchanger of the power block has a length of maximum 50 meters, the heat losses are so small that they are neglected.

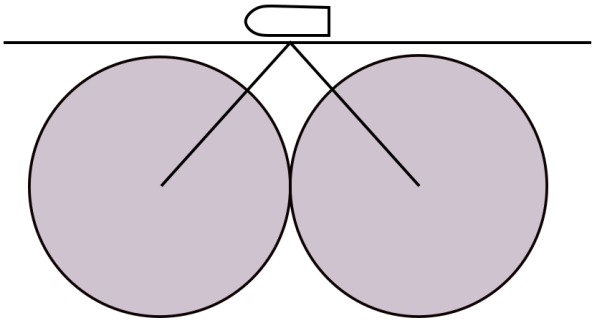

Figure 5.2: Heliostatic field and pipelines

5.2.3 Transport

The ship contains 3 spherical storage tanks, a spherical design is chosen because this results in low heat losses due to the high volume : surface ratio and the internal stresses will be evenly distributed. The tanker must be able to store the amount of Solar Salt heated in 3 days, this is because the round-trip time of one tanker is 12 days and there are 4 tankers sailing back and forth to Morocco. Because there are 3 full storage tanks on the tanker during sailing, each storage tank needs to store the amount of Solar Salt obtained in 1 day. In 1 day 139,000 ton of Solar Salt is heated by the 2 CSP plants, which is equal to 76,000 m^3. The radius of the sphere is 26.3 meter and the surface is 8700 m^2. This leads to an energy loss of 940 kW per storage tank for hot storage and an energy loss of 530 kW for cold storage, using Equation (5.2). Solar Salt will be stored on the ship for an average of 6 days, the total heat loss for the hot and cold Solar Salt on one trip will be **406 MWh** and **229 MWh** per trip, respectively.

With three fully loaded storage tanks the total DWT of the ship is $139,000 \cdot 3 = 418,000$ ton. This corresponds to a total thermal energy of $418,000,000 \cdot 1.6 \cdot 277 = 1.85e11kJ = 51.4GWh$. In Section 3.4.1 the specifications and assumptions of the tanker are shown.

5.2.4 Solar Salt on ship to electricity

The storage tank in the Netherlands needs to be designed to store energy for one full day, this is needed because the interval between a tanker leaving the harbour and the next tanker arriving at the harbour is 1 day. This results in a storage tank with twice the volume of the storage tanks on shore in Morocco ($2 \cdot 38000m^3$). The dimensions of the storage tank are 36m x 26m (height x radius). A cylindrical shape is chosen since internal stresses will be evenly distributed by the round shape of the storage tank and it is still convenient to place the storage tank on the ground. This leads to a surface area of 10000 m^2 with a heat loss of 1080 kW for the hot storage tank and 610 kW for the cold storage tank. Which results in an energy loss of **25.9 MWh** and **14.6 MWh**, respectively.

The total heat loss of the hot Solar Salt from the storage tanks in Morocco to the heat exchanger of the power block in the Netherlands is $16 \cdot 2 + 12 \cdot 2 + 406 + 25.9 = \mathbf{488}MWh$, which results in a temperature loss of 2.6 °C ($mc_p\Delta T$). The total heat loss of the cold Solar Salt from the Netherlands to Morocco is $2 \cdot 9.2 + 2 \cdot 6.8 + 229 + 14.6 = \mathbf{276}MWh$, this results in a temperature loss of 1.5 °C. The total heat transferred from Solar Salt to generate steam in the heat exchanger of the power block is 50.7 GWh, see Equation (5.3) (m=418,000 ton). A schematic overview of the entire process is given in Figure 5.3 and the heat losses obtained are stated in Table 5.3. Only the efficiency of the power block still has to be determined.

$$Q_{transfer} = m \cdot c_p((565 - 2.6) - (288 + 1.5)) = 50.7GWh \tag{5.3}$$

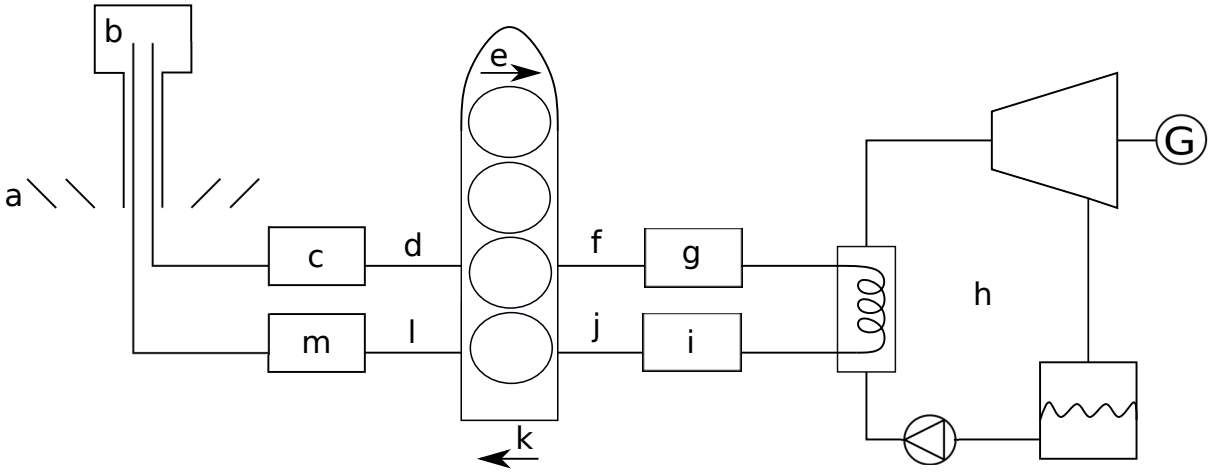

Figure 5.3: Overview Solar Salt concept

Power block

In Appendix F a simple reheat Rankine cycle is shown, this is the Rankine cycle used to obtain the efficiency of the power block. The temperatures, pressures, enthalpies and entropies of each specific point are calculated and the efficiency of the turbine is obtained. An overview of the Rankine cycle and the corresponding variables are shown in Appendix F. The efficiency of the total cycle is determined by Equation (5.4).

$$\eta_{cycle} = \frac{\dot{W}_{turbine} - \dot{W}_{pump}}{\dot{Q}_{in}} \cdot 100 = \frac{(h5 - h6) + (h3 - h4) + (h1 - h2)}{h3 - h2} \cdot 100 = 42\% \tag{5.4}$$

The isentropic efficiency of the pump and the turbine are assumed to be 90% [20], the temperature difference of hot Solar Salt entering the heat exchanger and hot steam leaving the heat exchanger is set at ΔT of 5°C [20]. The CSP plant is situated close to the sea, therefore seawater is used to condense the steam after the steam turbine, the water temperature at Agadir in the summer is 22 °C, a temperature difference of 14°C between the condenser and the water temperature is taken [89]. The maximum operational pressure used in steam turbines used for CSP made by Siemens is 165 bar [90]. An overview of the inputs and outputs of the Rankine cycle is given in Table 5.2.

Table 5.2: Input & output

	Input		Output
$\eta_{pump,isen}$	90% [20]	η_{cycle}	42%
$\eta_{turb,isen}$	90% [20]		
ΔT_{HE}	5 °C [20]		
T_{cond}	36 °C [20]		
p_{max}	165 bar [90]		

With a power block efficiency of 42% the total electricity generated by the freight of one tanker will be $50.7 \cdot 0.42 = 21.3 GWh$. The tanker stays in the harbour for 2 days and there is a storage capacity on shore to store the heat used by the steam turbine in 1 day. Therefore the electricity capacity of 21.3 GWh is spread out over 3 days (72 hours), which results in a power size of the power block in the Netherlands of 296 MW. This power will only be met in the summer, in the winter the power output will be 60% (178 MW), see Section 2.1.2. In Table 5.3 all the energy efficiencies and energy losses are shown through the whole system. An overview of the heat losses and electricity obtained by the freight

of one tanker transported in one trip is shown in Table 5.3.

Table 5.3: Heat losses Solar Salt concept

Point	Description	Efficiency [%]	Energy loss [GWh]	Electricity [GWh]	Energy [GWh]
input	Solar irradiation				76.2
a	Heliostats	75	19.1		57.1
b	Receiver	90	5.73		51.4
c	Hot storage MA		$2 \cdot 0.016$		51.4
d	Hot Pipes MA		$2 \cdot 0.012$		51.4
e	Transport to NL		0.406		51.0
f	Hot pipes NL		negl.		51.0
g	Hot storage NL		0.026		51.0
h	Power block	42	29.4	21.3	0.3
i	Cold storage NL		0.015		0.3
j	Cold pipes NL		negl.		0.3
k	Transport to MA		0.229		0.0
l	Cold pipes MA		$2 \cdot 0.007$		0.0
m	Cold storage MA		$2 \cdot 0.009$		0.0

In Figure 5.4 a sankey diagram is given, the input of heated Solar Salt is set at 100 MWh. This is done so it easier to compare with the Sankey diagrams obtained in Chapter 6 and Chapter 4. The Solar Salt instead of the solar irradiation is set at 100 MWh, because in the other Sankey diagrams the first step from solar irradiation to electricity is not included. It can be seen that the efficiency from Solar Salt to electricity is 41.4% and the efficiency of the whole cycle starting by solar irradiation is 27.9%.

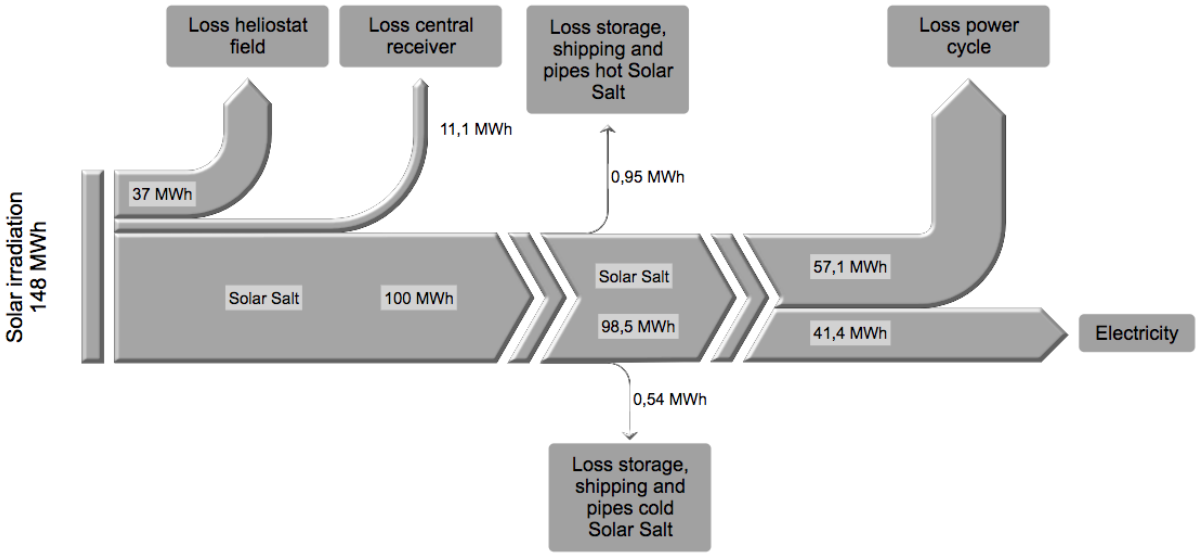

Figure 5.4: Sankey diagram Solar Salt concept with 100 MWh of heated Solar Salt

5.3 Costs

In this section the levelized costs of electricity (LCoE) of the Solar Salt concept are calculated. First, all the capital costs and O&M costs are determined, see Table 5.6, with use of the inputs which are stated in Table 5.5. The annualized capital costs are calculated with the capital costs, see Equation (5.5), and

the LCoE is calculated by dividing the total costs per year with the total amount of electricity generated in one year, see Equation (5.6).

According to Mancini (2011) the costs to store 8140 MWh of Solar Salt in thermal storage tanks is approximately 14.4 €/kWh$_{th}$ Table 5.4. In this paper the LCoE of the CSP plant is 0.075 €/kWh$_e$, the LCoE of the CSP plant in this thesis taken are 0.057 €/kWh$_e$, see Section 2.2. This is a cost reduction of 24%. It is assumed that the costs of the components of the storage tank over the years have also decreased by 24%. In Table 5.4 the costs of all the components of the storage tanks are stated. It is assumed that the costs of the cold storage tank are 80% of the costs of the hot storage tank and consist out of the costs for the tanks and foundations. The costs of hot storage and cold storage become respectively **2.7** €/kWh$_{th}$ and **2.2** €/kWh$_{th}$. The cost of Solar Salt in €/kWh is calculated with the Solar Salt price and energy density. The rest storage costs are the costs which are installed on shore to control the storage tanks.

Table 5.4: Cost of TES subsystems [€/kWh$_{th}$] [19]

Storage system component	Abengoa Study 8140 MWh Storage	
	Study [€/kWh$_{th}$]	Corrected [€/kWh$_{th}$] (24% reduction)
Tanks & foundation	6.4	4.9
Salt media	4.1*	4.1*
Rest storage	3.9	3.0
Total capital costs	14.4	12.0
LCoE	0.075	0.0573

* Calculated with Solar Salt price of 0.5 €/kg & energy density of 0.123 kWh/kg (0.443 kJ/kg)

The capital recovery factor (CRF) is calculated in Equation (2.4). This factor represents the increase of capital costs which have to be paid back over a lifetime of 30 years with a discount rate of 5%. A discount rate of 5% is taken which is realistic for low-carbon investments [91]. The lifetime of a CSP plant is set by most studies at 30 years [92], although estimations for 40 years are also done [93]. For tankers the lifetime lies between 25 and 30 years [17]. Due to the lifetime of tankers and CSP plants, the lifetime of the entire system is 30 years. The capacity factor of the CSP power plant is 80 %, see Section 2.1.2, this results in a capacity capacity factor of 80% by the entire system. The LCoE of CSP is 0.0573 €/kWh, see Section 2.2.1. The O&M costs of the storage systems is set on 1% per year [94] of the total capital costs of the storage tanks on shore, the storage tanks on the ships, Solar Salt and rest storage. The insurance and maintenance costs of the ship are set on 4% of the capital costs of the ship per year.

In Table 5.6 all the capital costs and O&M costs are stated. The CSP plant is split into two: The heliostat field, receiver and storage system are standing in Morocco and the power block is standing in the Netherlands. Therefore the O&M and capital costs for these components are included in the LCoE (0.0573 €/kWh) of the CSP plant. The heat obtained in Morocco comes from 2 CSP plants, therefore there are 2 heliostats etc. The pipes in Morocco are 1.2 km long and have a cost of 1.5 M€/km [95], it is assumed that the costs for Solar Salt pipelines are the same as for pressurized gas pipelines. There are 4 pipelines needed since the Solar Salt needs to be pumped on to the ship and back to the CSP plant.

The cost of a 418,000 DWT ship is approximately 100 M€, this does not include storage tanks which are able to operate at high temperatures. The storage of a ship consists out of three hot storage tanks, each hot storage tank is able to store 17 GWh of heat, this is the amount of energy generated by the CSP plant in one day. Thus the total storage costs on one ship becomes the amount of energy transported times the price of a hot storage tank per kWh (2.7), this becomes $51.4 \cdot 2.7 = 139$ M€. To store 51.4 GWh of energy, 418,000 ton Solar Salt is needed. The cost of 418,000 ton Solar Salt is 209 M€.

Table 5.5: Inputs/assumptions costs

Item	Unit	Value
Discount rate	%	5
CRF	-	1.952
Lifetime	yr	30
Capacity factor	%	80
LCoE CSP	€/kWh	0.0573
Insurance & maintenance tanker	%	4
O&M storage	%	1
Cost Solar Salt	€/kg	0.5
Hot storage	€/kWh	2.7
Cold storage	%	80% of hot storage
Rest storage	€/kWh	3.0

The storage system in the Netherlands needs to be able to store 17 GWh of energy, for this 140,000 ton of Solar Salt is needed which result in a cost of 70 M€. The price of the hot storage tanks is $17 \cdot 2.7 = 46$ M€and for the cold storage tank this is $17\dot{2}.2 = 37$ M€. Rest storage are all the components stated in Table 5.4 except for tanks, foundations and salt media. The costs of these components is 3.0 €/kWh, so 51 M€.

The total amount of electricity which is generated from a CSP plant with a power of 300 MW with a capacity factor of 80% is 2100 GWh, the total costs per year for the CSP plant become $2100 \cdot 0.0573 = 120$ M€. The O&M costs of all the inventory which is not included in the CSP plant result in $1607 \cdot 0.01 = 16$ M€per year. On the ship it is assumed that the crew consists out of 30 persons, the average salary is set at 100,000 €/yr so a total of 12 M€per year is needed to pay the crew on all 4 ships. The insurance and maintenance costs are 4% of the capital costs of the ship and are 16 M€.

Table 5.6: Capital costs

Capital costs								
Morocco			Transport			The Netherlands		
Component	Cost [M€]	#	Component	Cost [M€]	#	Component	Cost [M€]	#
Heliostats	$LCoE_{CSP}$	2	Ship	100	4	Power block	$LCoE_{CSP}$	1
Receiver	$LCoE_{CSP}$	2	Storage	139	4	Solar Salt	70	1
Hot storage	$LCoE_{CSP}$	2	Solar Salt	210	4	Cold storage	37	1
Cold storage	$LCoE_{CSP}$	2				Hot Storage	46	1
Rest storage	$LCoE_{CSP}$	2				Rest storage	51	1
Solar Salt	$LCoE_{CSP}$	2						
Pipes	1.8	4						
O&M costs (annually)								
$LCoE_{CSP}$*	120		Fuel	46				
O&M Storage	16	1%	Crew	12				
			Insurance & maintenance	16	4%			
LCoE	**0.16 €/kWh**							

* $LCoE_{CSP}$ includes capital costs and O&M costs for the CSP plant
** These are induced O&M costs due to the increase in size and number of storage tanks, larger quantities of Solar Salt and longer piping system

Now all the capital costs are known, the annualized capital costs can be calculated. This done by

adding all the capital costs (CAPEX) which are stated in Table 5.6 times the capital recovery factor (CRF) and divide this by the lifetime of 30 years. This is done in Equation (5.5) and results in a annualized CAPEX of 130.6 M€.

$$\begin{aligned} CAPEX_{annualy} &= \frac{CAPEX \cdot CRF}{lifetime} \\ &= \frac{((Pipes_{Morocco} + CAPEX_{transport}) \cdot 4 + CAPEX_{Netherlands}) \cdot CRF}{lifetime} \\ &= \frac{((1.8 + 100 + 139 + 210) \cdot 4 + 70 + 37 + 46 + 51) \cdot 1.952}{30} \\ &= 131 \ M€/yr \end{aligned} \tag{5.5}$$

With the annualized CAPEX known, the LCoE of the total system can be calculated. The annualized CAPEX and all the O&M costs are added and divided by the total electricity generated over one year, the electricity generated in one year is the power of the power block (296 MW) times the capacity factor (0.8) and the total amount of hours in a year (8766). The total LCoE becomes 0.164 €/kWh. This is higher than the requirement of 0.125 €/kWh. It can also be considered to sell heat in the Netherlands, the price of heat becomes $0.164 \cdot 0.42 = 0.069$ €/kWh, this even includes the costs of the power block. The subsidized solar thermal energy in the Netherlands is 0.09 - 0.095 €/kWh [25].

$$LCoE = \frac{CAPEX_{annually} + O\&M_{annually}}{Electricity_{annually}} = \frac{131 + 120 + 16 + 46 + 12 + 16}{0.296 \cdot 8766 \cdot 0.8} = 0.16 \ €/kWh \tag{5.6}$$

5.4 Conclusion

Thermal energy storage with Solar Salt as energy storage fluid is a technology with high maturity. Almost all the components during the process are well developed. Heating Solar Salt with the use of CSP plants is a conventional method and the Solar Salt is stored in thermally insulated storage tanks. There only needs to be done some research to the implementation of storage tanks on a tanker and the increase of the storage tanks size, which is a factor of 4 compared to storage tanks for a 150 MW CSP plant.

The efficiency from solar irradiation to the electricity output in the Netherlands is very high. This is 28%, which is even higher than the conversion of the sun into electricity by PV panels without storage (± 20%). Also the storage losses are very low compared to other concepts, only 1.5 % of the heat transported is lost during storage and transportation. However, the energy density of Solar Salt is low, so the costs to transport Solar Salt are relatively high.

The LCoE of the Solar Salt concept is 0.164 €/kWh. This is 31 % higher than the requirement of 0.125 €/kWh. To realize this the costs have to be reduced; most of the costs come from the storage tanks, Solar Salt and the LCoE of CSP.

Another option is to sell heat instead of electricity. The levelized cost of heat is 0.069 €/kWh, where the subsidized solar thermal energy in the Netherlands is 0.09 - 0.095 €/kWh [25]. This gives possibilities to effectuate a business case. The unendowed heat price is ± 0.043 €/kWh. Although the costs of heat will likely go up in the coming years: Gas prices are increasing and less gas can be pumped out of the Groninger gas-field. Also it is planned that the coal-fired power plants are shut down, which leaves a gap for waste heat.

Chapter 6

Liquid Air with Molten Salt Combined

In this chapter the liquid air concept is explained. Liquid air becomes more efficient if a heat source is added. Because waste heat is always received from grey energy sources and molten salt is found to be cheap per kWh of heat, it is chosen to combine liquid air with molten salt. In Figure 6.1 a schematic overview of the process is shown. Liquid air is obtained from PV electricity and molten salt is obtained from CSP, both fluids are pumped onto a tanker and shipped to the Netherlands, in the Netherlands electricity is generated from the high temperature differences of molten salt and liquid air. In Section 6.1 the energy balance of the whole process is determined and in Section 6.2 the component costs are obtained and the LCoE is calculated.

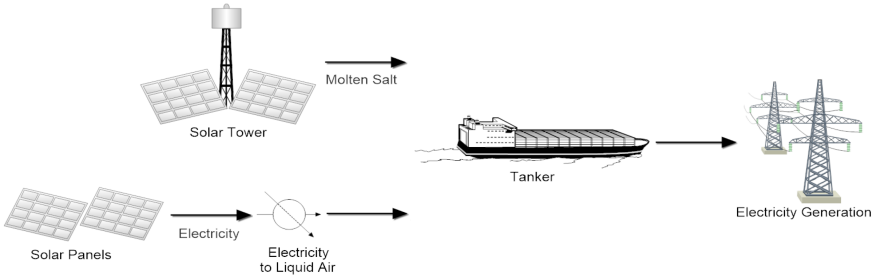

Figure 6.1: Insert caption

The operation of the liquid air with molten salt concept is shown in Figure 6.2. This is done in the same manner as for the molten salt concept in the previous chapter. The total project exists out of 4 ships which are sailing with an interval of 3 days between each other. The round trip time of the ships is 12 days; sailing takes 4 days from and 4 days to Morocco and the harbour time in Morocco and in the Netherlands is both 2 days. The storage tanks on shore in the Netherlands and in Morocco have a capacity of 1 full day of storage. This is done because the interval between a tanker leaving the harbour and arriving at the harbour is 1 day. This leaves a hot storage tank, cold storage tank and liquid air storage tank on shore in Morocco and on shore in the Netherlands with a capacity to produce one full day of power. The storage tanks on the tanker are able to store energy which is obtained by the CSP system and PV panels in 3 days. On the way from the Netherlands to Morocco no (liquid) air is returned, but the, still liquefied, cold molten salt is. To prevent mixing of hot and cold Solar Salt, the tanker consists out of 3 storage tanks to store Solar Salt. The storage tanks for Solar Salt on shore have the same size as one storage tank on the tanker. So before pumping hot Solar Salt on the ship, one storage tank containing cold Solar Salt on the ship is emptied to the cold storage tank on shore, or vice versa.

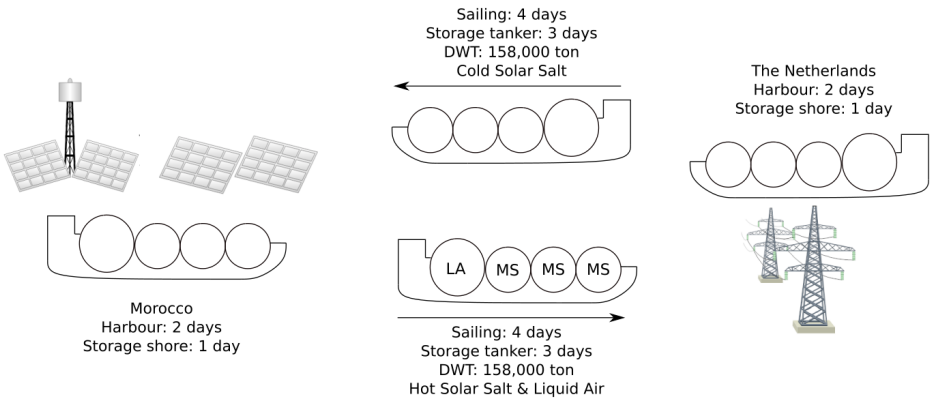

Figure 6.2: Operation 4 ships

6.1 Energy Balance

In this section the liquid air production process with corresponding energy efficiencies are determined. Also the losses during transportation are calculated. Finally the process to obtain electricity from liquid air and molten salt in the Netherlands is explained and the energy efficiencies are computed.

6.1.1 Production of Liquid Air

In Figure 6.3 and Table 6.2 the process of liquid air production is shown. First, air is compressed and cooled with seawater, this is done in four stages to increase the efficiency of compression, see Table 6.2. After the third stage, the air is now compressed up to 50 bar, the compressed air flow is split into two separate flows. Flow 11 is compressed to 147 bar and cooled to ambient temperature before it is expanded through a turboexpander (EXP). The turboexpander cools the air to a temperature of 122 K with a pressure of 4.5 bar, and also generates some electricity for the compressor. The cooled flow (14) runs through the large heat exchanger (LHE) and is fed back to the compressor at stage 2. The other flow, flow 15, is cooled in the large heat exchanger (LHE) by flow 14 and the vapor flow 19 which comes from the liquid-vapor separator. The cooled flow now has a temperature of 127 K and a pressure of 50 bar. The flow is forced through a Joule Thomson (JT) valve, where the air is partially liquefied. Now the flow enters the liquid-vapor separator (S2) with a high liquid fraction and at point 18 liquid air under a pressure of 20 bar is obtained.

The isentropic efficiency of the compressor is set on 85% [20] and the isentropic efficiency of the turbine and turboexpander are set on 90% [20]. For the heat exchangers a Δ T of 5 ° C is taken [20], for top temperature differences as well as bottom temperature differences. Finally the Joule Thomson valve is isenthalpic. An overview of the assumptions is stated in Table 6.1.

Table 6.1: Assumptions [20]

$\eta_{comp,isen}$	0.85
$HE_{\Delta T}$	5 °C
$\eta_{turb,EXP,isen}$	0.9
JT	Isenthalpic

The temperature, pressure, enthalpy and entropy are calculated with REFPROP and MATLAB and stated in Table 6.2 for each flow. In the MATLAB model different compressor pressure ranges, fractional mass flow separations and feed back temperatures and pressures are taken. The model with the highest efficiency is shown in this report.

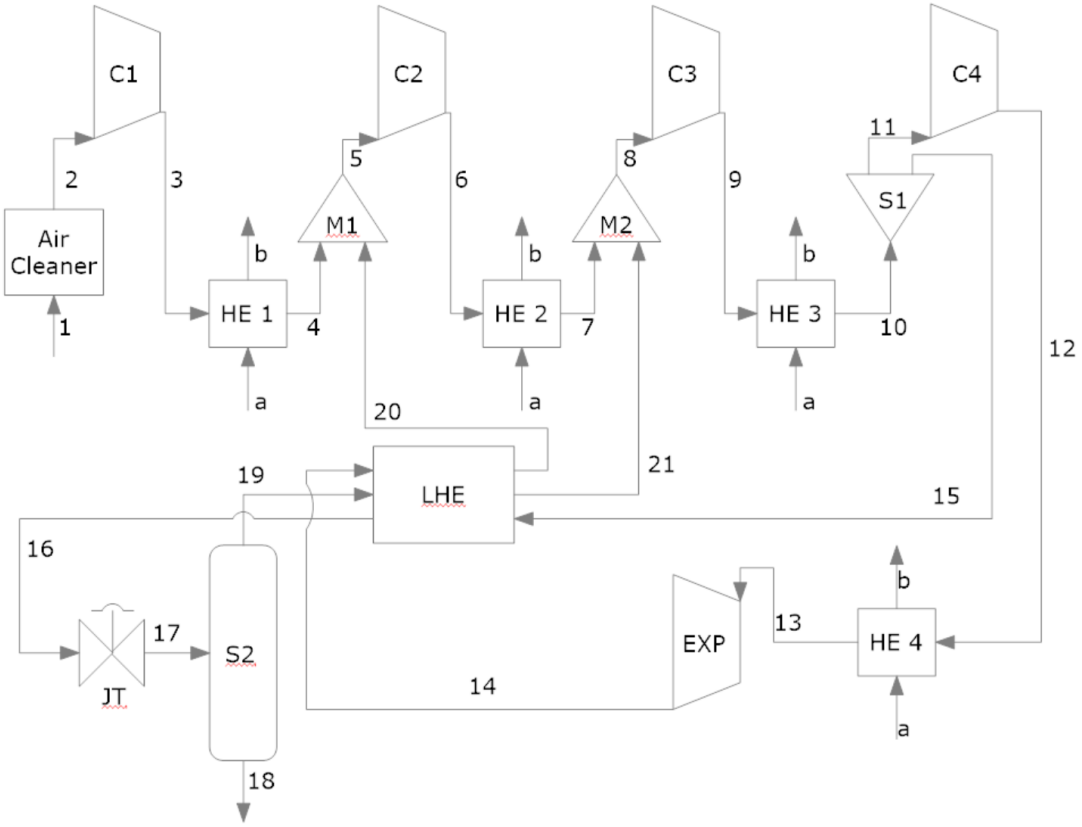

Figure 6.3: Liquid air production

Table 6.2: Liquid air production values with 609 MW input

nr	**T [K]**	**p [bar]**	**h [kJ/kg]**	**s [kJ/kg K]**	**ṁ [kg/s]**
1	300	1.01	426.3	3.89	610.5
2	300	1.01	426.3	3.89	610.5
3	486	4.5	614.6	3.95	610.5
4	300	4.5	425.5	3.46	610.5
5	300	4.5	425.5	3.46	1734
6	486	20	614.3	3.52	1734
7	300	20	614.3	3.52	1734
8	300	20	614.3	3.52	1836.6
9	406	50	528.6	3.06	1836.6
10	300	50	415.7	2.74	1836.6
11	300	50	415.7	2.74	1123.5
12	429	147	546.5	2.78	1123.5
13	300	147	398.6	2.37	1123.5
14	122	4.5	242.1	2.52	1123.5
15	300	50	415.7	2.74	713
16	127	50	105.2	0.97	713
17	119	20	105.2	1.01	713
18	119	20	86.7	0.86	610.5
19	120	20	211	1.9	102.5
20	295	4.5	420.5	3.44	1123.5
21	295	20	416.9	3	102.5
a	cold seawater				
b	warm seawater				

In Equation (6.1) the formula for the isentropic efficiency of the compressor is shown. Because the isentropic efficiency of the compressor is assumed to be 85%, the enthalpy in the point after a stage of the compressor can be calculated (h_{2r}). h_1 is the enthalpy in the point before the stage and h_{2s} is the enthalpy obtained with 100% isentropic efficiency, this enthalpy is calculated in REFPROP where the input is the entropy at h_1 and the pressure at point h_2.

$$\eta_c = \frac{h_{2s} - h_1}{h_{2r} - h_1} \tag{6.1}$$

With use of Equation (6.2) the enthalpy after the turboexpander is calculated, the same principle applies as for the compressor.

$$\eta_t = \frac{h_1 - h_{2r}}{h_1 - h_{2s}} \tag{6.2}$$

Equation (6.3) is used to determine all the mass flows around the LHE, it is assumed that no heat losses occur and the bottom and top temperature differences are 5 °C.

$$\sum(\dot{m}_i h_i)_{in} = \sum(\dot{m}_i h_i)_{out} \tag{6.3}$$

With all the properties calculated at each point, the work done by the compressor and the work obtained by the turboexpander are calculated following Equation (6.4), and stated in Table 6.3. The flow through the compessor and turbine is steady-state and the potential and kinetic energies of the fluid are neglected. The energy efficiency of the liquid air production ($\eta_{LAproduction}$) is calculated in Equation (6.5). The energy for 3 days is calculated because a tanker transports energy which is obtained in 3 days. The liquid air production runs for 9 hours per day during the summer, because this is also the amount of time the PV system is active, see Section 2.1.2. The energy of liquid air over 3 days is calculated with the specific energy, 0.66 MJ/kg [52], and mass flow.

$$W = \dot{m} \cdot \Delta h \tag{6.4}$$

Table 6.3: Work compressors and expanders liquid air production process

Components	**Power [MW]**	**Flow [kg/s]**	**Energy 3 days [GWh]**
Compressor 1	114.9	610.5	3.10
Compressor 2	327.3	1734	8.84
Compressor 3	195.6	1836.6	5.28
Compressor 4	146.9	1123.5	3.97
Expander	-175.8	1123.5	-4.75
Liquid air	–	610.5	10.89
Total work in	609	–	16.44

$$\eta_{LA,production} = \frac{W_{liqair}}{W_c - W_t} = \frac{10.88}{16.44} = 66.2\% \tag{6.5}$$

Joule Thomson Valve

A Joule Thomson (J-T) valve decreases the temperature of a gas by forcing the gas through the valve while keeping it insulated so no heat is exchanged with the environment. The enthalpy remains the same during the expansion through the valve. J-T valves are used when a phase change occurs and no turboexpanders, which are more efficient, can be used anymore because the high liquid fraction will damage the turbine blades.

After the LHE flow 16 has an enthalpy of 105.2 kJ/kg and a pressure of 5 MPa. In the JT-valve flow 16 is expanded from 5 MPa to 2 MPa. The horizontal lines in Figure 6.4 are the liquid to vapor lines at a certain pressure. If a gas lies more to the left on the horizontal line, the liquid fraction is higher. To show the difference compared to a flow with a higher enthalpy, the path of an extra line with a higher enthalpy is shown. More liquid air is created when air is expanded with an enthalpy of 105.2 than 129.2, because the enthalpy line of 105.2 kJ/kg intersects the horizontal line more to the left. However, obtaining air with a low enthalpy also requires more energy. Also it can be seen that the liquid fraction obtained is higher if liquid air is expanded to 20 bar instead of 1 bar. After an iterative process it is found that the optimum conditions to expand air is with an enthalpy of 105.2 kJ/kg from 5 MPa to 2 MPa.

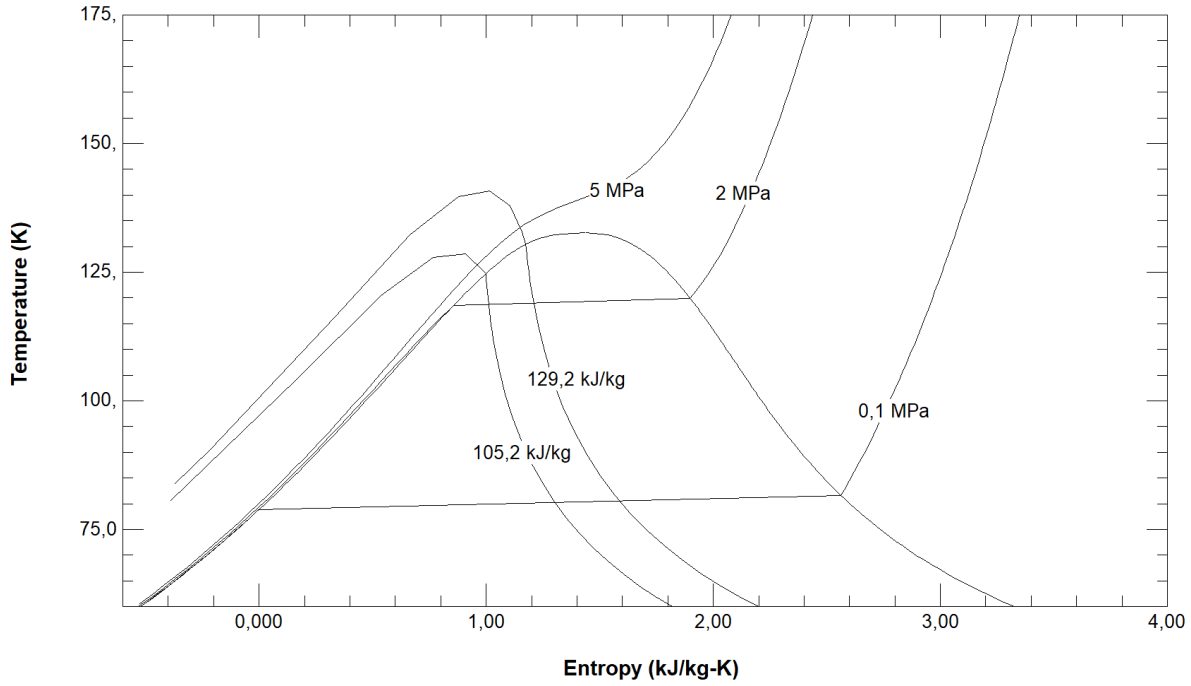

Figure 6.4: T-s diagram of air with pressure and enthalpy lines from REFPROP

6.1.2 Storage & Transportation

To calculate the heat losses and size of the tanker it is necessary to know the ratio of molten salt and liquid air. This is calculated in Section 6.1.3 and the mass ratio of liquid air : molten salt is 1 : 1.67. The maximum electricity a PV system can obtain is 2100 GWh per year and for a CSP plant the maximum electricity obtained is also 2100 GWh per year, see Section 2.3.1. For CSP, 2100 GWh of electricity becomes $2100/0.42 = 5000$ GWh of heat stored in Solar Salt. Those are only partly taken as input, so the total energy input does not rise above the 2100 GWh of electricity input (CSP and PV combined). A tanker must be able to transport 3 days of energy during the summer (more irradiation,

see Section 2.1.2), which leads to an energy input of 21.6 GWh. With the energy input, energy efficiency of liquid air production and mass ratio known, the DWT of the tanker is determined. The tanker will transport 99000 ton (12.0 GWh) of molten salt and 59000 ton (10.9GWh) of liquid air per trip, this leads to a DWT of 158000 ton. The liquid air production loss becomes 5.56 GWh. This leads to a CSP plant of 71 MW and a PV system of 609 MW in Morocco. An overview of the energy balance which can be transported by one tanker is given in Figure 6.6. On the left the energy losses during energy storage, in the middle the energy losses during transportation and at the right the energy losses during electricity generation are shown.

The storage tanks on shore need to have a capacity to produce electricity for one full day. This is a third of the total capacity of the tanker and results in a storage tank of 33,000 ton (4.0 GWh) for Solar Salt and 19,700 ton (3.6 GWh) for liquid air. The heat losses for molten salt during storage, pumping and transportation are taken the same as the losses taken in Chapter 5; a 2.6 °C temperature drop of hot molten salt from Morocco to the Netherlands and a temperature drop of 1.5 °C of cold molten salt from the Netherlands to Morocco. These temperature losses result in heat losses of 6.56 kJ/kg ($c_p \Delta T$), this is a loss of 0.18 GWh per trip. Because the losses are low and no research could be found on the heat losses of liquid air it is assumed that the losses of liquid air are in the same proportion as the losses of molten salt; 0.16 GWh per trip.

6.1.3 Electricity Generation

In this section the electricity generation is explained and calculated. Normally liquid air is pressurized, heated and fed through a turbine to generate electricity. A cold recycle loop is added to minimize the heat losses, cold energy is stored during electricity generation and is used again in the liquefaction process. In this case this is not possible because the two processes are not close to each other. Another method has to be found to deal with the cold recycle heat losses. Therefore a second cycle is added and this principle works as a heat engine. With this secondary cycle more electricity is obtained with a second compressor and turbine. Both cycles are explained in detail below.

The process of electricity generation with liquid air and molten salt is shown in Figure 6.5 and the corresponding values can be found in Table 6.4. At point 1, the liquid air obtained in Section 6.1.1 is pressurized with a cryogenic pump to 200 bar, cryogenic pumps which are currently available are not able to operate at higher pressures [96]. The pressurized liquid air is heated in heat exchanger (HE) 1 to 339 K, where the air comes out in gaseous phase. In HE 2 the pressurized air is heated further to 833 K by use of hot molten salt. Finally the hot pressurized air drives an air turbine which generates electricity.

In the second cycle, two options are shown; a cycle with air as working fluid and a cycle with a noble gas as working fluid. A noble gas is used because the specific heat to specific volume ratio is high and this leads to a more efficient Brayton cycle. The largest capacity, helium turbine built to date is a 50 MWe unit in Oberhausen, Germany [97]. Of the noble gases, argon is used. This is done because it is the cheapest of all noble gases. In HE 1, argon/air is cooled to 124 K. The cooled argon is compressed to 6.4 bar and the cooled air is compressed to 26 bar, the pressure ratio was put in the model as a variable and these values were the most efficient pressure ratios obtained. The compressed air/argon is heated to 833 K in a heat exchanger with hot molten salt. The hot pressurized air/argon drives the turbine. Air/argon which comes out of the turbine heats the liquid air in HE 1 and the circle is closed. The work obtained and delivered by this process is shown in Table 6.5. The enthalpy around the turbines and compressors are calculated in Equation (6.1) and Equation (6.2) in the same manner as for the production of liquid air. The mass flows around the heat exchangers are calculated with the energy balance equation, see Equation (6.3). The enthalpy change of molten salt is calculated with $\Delta h = cp \cdot \Delta T$, where cp is 1.6 kJ/kgK, the lower temperature of molten salt is 289.5 $°C$ and the maximum temperature is 562.4 $°C$, so the enthalpy change (Δh) of molten salt is $1.6 \cdot 272.9 = 436.6 kJ/kg$. In Table 6.4 the temperature (T), pressure (p), enthalpy (h), entropy (s) and mass flow $\dot{m}$ of each point is given. The enthalpy and entropy of molten salt were not needed for the calculations.

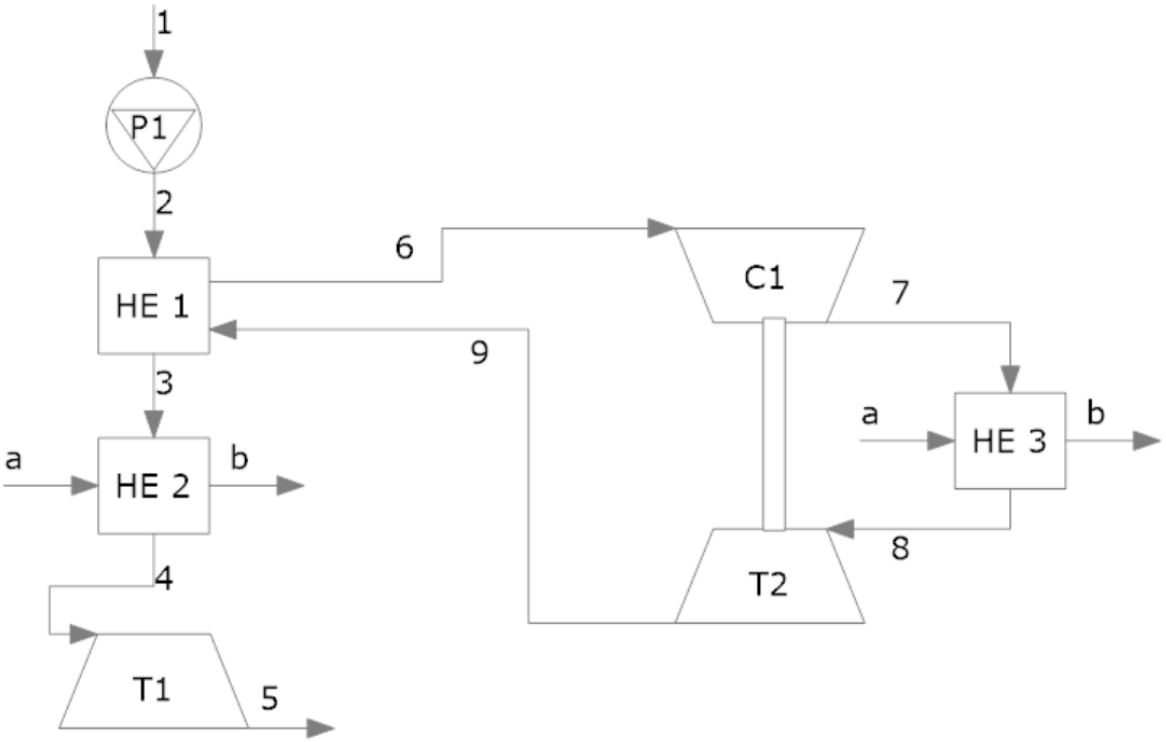

Figure 6.5: Electricity Generation with Liquid Air and a Brayton Cycle

Table 6.4: Properties flows electricity generation with argon as 2^{nd} cycle

nr	**T [K]**	**p [bar]**	**h [kJ/kg]**	**s [kJ/kg K]**	**ṁ [kg/s]**	**Fluid**
1	119	20	86.7	0.86	225.8	air
2	118	200	86.7	0.64	225.8	air
3	436	200	552.6	2.7	225.8	air
4	831	200	991.4	3.42	225.8	air
5	256	1.01	381.7	3.73	225.8	air
6	124	1.01	63.4	3.41	633.5	argon
7	281	6.38	144.8	3.46	633.5	argon
8	831	6.38	432.3	4.02	633.5	argon
9	441	1.01	229.4	4.08	633.5	argon
a	836	1.01	-	-	226.7	molten salt (1^{st} cycle)
b	563	1.01	-	-	226.7	molten salt (1^{st} cycle)
a	836	1.01	-	-	148.6	molten salt (2^{nd} cycle)
b	563	1.01	-	-	148.6	molten salt (2^{nd} cycle)

In Table 6.5 the power, mass flows and energy over 3 days through all the different components to produce electricity are shown. The liquid air cycle has an energy input of 10.73 GWh over 3 days, this is 0.16 GWh lower than the output of the liquid air production, which is lost during the storage and transport of liquid air. Also it can be seen that the flow of argon is higher than the flow of air through the second cycle, this is caused by the lower pressure ratio of argon with respect to air. Therefore also the compressor and turbine power are higher for air. In the Netherlands **214.6** MW of electricity will be generated with a total energy generation of 15.5 GWh in 3 days when argon is used in the second cycle. For air the power becomes 220.9 MW with a total amount of energy of 15.9 GWh in 3 days.

Table 6.5: Work done by components

Components	**Power [MW]**	**Flow [kg/s]**	**E_{3days} [GWh]**	**Power [MW]**	**Flow [kg/s]**	**E_{3days} [GWh]**
	2^{nd} **cycle argon**			2^{nd} **cycle air**		
Pump	0.01	225.8	0.01	0.0005	225.8	0.005
Turbine 1	-137.7	225.8	-9.91	-137.7	225.8	-9.91
Compressor 1	51.6	633.5	3.71	81.2	345.6	5.85
Turbine 2	-128.5	633.5	-9.25	-164.5	345.6	-11.84
Liquid air	-	225.8	10.73	149	225.8	10.73
Molten salt	164	375.3	11.81	227.6	520.9	16.39
Power output NL	-214.6	-	-15.45	-220.9	-	-15.91

In Equation (6.6) and Equation (6.7) the energy efficiencies of the electricity generation are calculated. All the work done by the compressors, turbines and pumps is divided by the total amount of heat added to the system. It can be seen that the energy efficiency where argon is used as transfer fluid is a lot higher. Therefore it would be the best option to use argon in the second cycle, however the costs of argon are higher than for air and the availability of argon compressors and argon turbines is lower than for air compressors and turbines. All the values in the equations can be found in Table 6.5. $Q_{MS,NL}$ is the energy of molten salt in the Netherlands, so the energy of molten salt in Morocco minus the heat losses during storage and transportation.

$$\eta_{generation,argon} = \frac{-(W_{Turb_1} + W_{Turb_2} + W_{Comp_1} + W_{Pump})}{Q_{liqair} + Q_{MS,NL}} = \frac{9.91 + 9.25 - 3.71 - 0.0005}{10.73 + 11.81} = 68.6\% \tag{6.6}$$

$$\eta_{generation,air} = \frac{-(W_{Turb_1} + W_{Turb_2} + W_{Comp} + W_{Pump})}{Q_{liqair} + Q_{MS,NL}} = \frac{9.91 + 11.84 - 5.85 - 0.0005}{10.73 + 16.39} = 58.7\% \tag{6.7}$$

In Equation (6.8) and Equation (6.9) the energy efficiencies of the whole cycle are shown. The energies taken as input are the heat of molten salt after the receiver of a CSP plant and the electricity generated by a PV system. The ouput is the electricity generated in the Netherlands. The values for the numerator can be found in Table 6.5. For the denominator, the energy needed to produce liquid air ($W_{LA,production}$) can be found in Table 6.3 and the heat of molten salt without heat losses ($Q_{MS,MA}$) is $11.81 + 0.18 =$ **11.99** GWh.

$$\eta_{wholecycle,argon} = \frac{-(W_{Turb_1} + W_{Turb_2} + W_{Comp_1} + W_{Pump})}{W_{LA,production} + Q_{MS,MA}} = \frac{9.91 + 9.25 - 3.71 - 0.0005}{16.44 + 11.98} = 54.4\% \tag{6.8}$$

$$\eta_{wholecycle,air} = \frac{-(W_{Turb_1} + W_{Turb_2} + W_{Comp} + W_{Pump})}{W_{LA,production} + Q_{MS,MA}} = \frac{9.91 + 11.84 - 5.85 - 0.0005}{16.44 + 16.61} = 48.1\% \tag{6.9}$$

6.1.4 Overview

In Figure 6.6 an overview of the energy losses is shown. In this figure the second cycle during electricity generation is argon. Molten salt is obtained immediately after the receiver of a CSP plant. To obtain 12 GWh of hot molten salt in 3 days, the heliostat field and tower need to have the same size as the heliostat field and tower for a 71 MW CSP plant. This is pumped onto a tanker together with liquid air, which is obtained from electricity by a PV system. To obtain 16 GWh of electricity, the size of the PV system must be 609 MW. During the production of liquid air 5.56 GWh will be lost. During storage and transportation molten salt will cool by 4.1 °C en lose 0.18 GWh of energy. For liquid air boil-off losses will occur with a total amount of 0.16 GWh. The total amount of electricity generated with one round-trip is 15.5 GWh. This equates to a power plant with a size of **214.6 MW**. For a power plant where air is used as second cycle the total amount of electricity generated with the energy of one round-trip is 12.3 GWh. The size of the power plant becomes 170.3 MW. In Appendix G an overview of a Sankey diagram with a total input of 100 MWh is shown. This is the same input as for the other Sankey diagrams presented in this thesis.

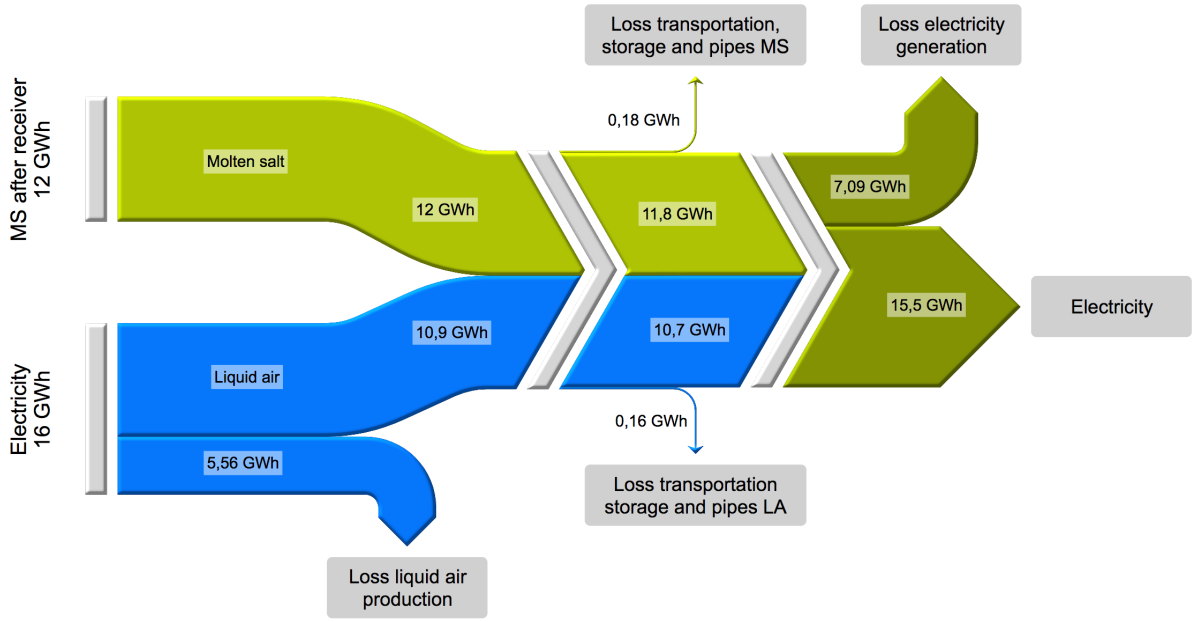

Figure 6.6: Energy transported by a tanker with 158000 DWT, 2^{nd} cycle argon

6.2 Costs

In this section the levelized costs of electricity (LCoE) of the liquid air combined with Solar Salt concept are calculated. First, all the capital costs and O&M costs are determined, see Section 6.2, with use of the inputs and assumptions which are stated in Section 6.2. The annualized capital costs are calculated with the capital costs, see Equation (6.10), and the LCoE is calculated by dividing the total costs per year with the total amount of electricity generated in one year, see Equation (6.11). The capital costs of

the components used to generate electricity from liquid air and Solar Salt; 3 heat exchangers, 2 turbines, 1 compressor and 1 pump together are 1000 €/kW. These costs are shown in Section 6.2 under the name power cycle. The capital costs of the power cycle are assumed to be 500 €/kW, this is the cost per kW for a combined cycle gas turbine [98] assumed that this is the same for the power cycle. In literature no storage tank costs of the liquid air could be found, it is assumed that the costs obtained for the hot storage tank are the same for the liquid air storage tank.

Table 6.6: Inputs/assumptions costs

Item	Unit	Value
Discount rate (r)	%	5
CRF	-	1.952
Lifetime	yr	30
Capacity factor	%	80
Heat_{CSP}	€/kWh	0.018
LCoE PV	€/kWh	0.022
Insurance & maintenance tanker	%	4
O&M storage	%	1
Power cycle	€/kW	500
Cost molten salt	€/kg	0.5
Hot storage	€/kWh	2.7
Liquid air storage	€/kWh	2.7
Cold storage	%	80% of hot storage
Rest storage	€/kWh	3.0

In Section 6.2 all the capital and O&M costs are stated. The capital and O&M costs for the heliostats, receiver and storage costs are included in the heat price of 0.018 €/kWh. According to Strahan (2013) [96] an air liquefaction plant with a production capacity of 19,300 ton/day will have a capital cost of 135 M€. The liquid air and hot Solar Salt tanks have an energy capacity of 3.6 GWh and 4.0 GWh, this leads to a capital cost of 9.7 M€and 10.8 M€, respectively. Cold storage is 80% of the costs for hot storage and this results in a capital cost of 8.8 M€. The storage tanks on the tanker have an energy capacity of 11.8 GWh and 10.7 GWh for Solar Salt and liquid air respectively, which results in costs of 32.4 M€and 29.4 M€. The total heat costs is the total heat in times the price of heat per kWh ($12 \cdot 0.018 = 21.6Me$, the total electricity costs to produce liquid air are $16 \cdot 0.022 = 35.2Me$. The operation and maintenance costs for liquid air production and electricity generation are assumed to be 2% of the liquid air production and electricity generation capital costs. All the components which are used to store Solar Salt or liquid air have a lower operation and maintenance cost, this is assumed to be 1% of the total capital costs for storage. Finally, the insurance and maintenance cost of the 4 tankers is set at 4% of the total capital costs. The capital costs of a tanker with a size of 158,000 DWT is 36.5 M€with fuel costs of 24.2 M€per trip, see Section 3.4.1.

Now all the capital costs are known, the annualized capital costs can be calculated. This is done by adding all the capital costs (CAPEX) which are stated in Section 6.2 times the capital recovery factor (CRF) and divide this by the lifetime of 30 years. This is done in Equation (6.10) and results in a annualized CAPEX of 59.9 M€.

$$\begin{aligned} CAPEX_{annualy} &= \frac{CAPEX \cdot CRF}{lifetime} \\ &= \frac{(CAPEX_{Morocco} + CAPEX_{transport} \cdot 4 + CAPEX_{Netherlands}) \cdot CRF}{lifetime} \\ &= 59.9 \ M€/yr \end{aligned} \tag{6.10}$$

With the annualized CAPEX known, the LCoE of the total system can be calculated. The annualized

Table 6.7: Capital costs

Capital costs								
Morocco			Transport			The Netherlands		
Component	Cost [M€]	#	Component	Cost [M€]	#	Component	Cost [M€]	#
Heliostats	Heat_{CSP}	1	Ship	36.5	4	Turbine		2
Receiver	Heat_{CSP}	1	MS storage	32.4	4	Compressor	107	1
Hot storage	Heat_{CSP}	1	LA Storage	29.4	4	HE's	(500 €/kW)	3
Cold storage	Heat_{CSP}	1	Molten salt	49.5	4	Pump		1
Rest storage	Heat_{CSP}					Rest storage	12	1
Pipes	1.8	2				LA storage	9.7	1
Molten salt	16.5	1				Hot storage	10.8	1
LA production	135 [96]	1				Cold storage	8.8	1
LA storage	9.7	1				Molten salt	16.5	1
O&M costs (yearly)								
Heat_{CSP}*	21.3		Fuel	24.2				
Storage**	5.3	1%	Crew	6				
LA production &			Insurance/					
Power block***	4.8	2 %	maintenance	6	4%			
LCoE_{PV}	35.2							
LCoE	**0.108 €/kWh** (with air: 0.154€/kWh)							

* Heat_{CSP} includes capital costs, O&M costs and personnel costs for part of the CSP plant in Morocco
** These are induced O&M and personnel costs due to the increase in size and number of storage tanks, larger quantities of molten salt and longer piping system in comparison with a CSP plant
*** O&M costs of the liquid air production and power block (2%)

CAPEX and all the O&M costs are added and divided by the total electricity generated over one year, the electricity generated in one year is the maximum power of the power cycle (214.6 MW) times the capacity factor (0.8) and the total amount of hours in a year (8766). The total LCoE becomes 0.108 €/kWh. This is lower than the requirement of 0.125 €/kWh and therefore it is possible to execute this concept.

$$\begin{aligned} LCoE &= \frac{CAPEX_{annually} + O\&M_{annually}}{Electricity_{annually}} \\ &= \frac{59.9 + 21.3 + 5.3 + 4.8 + 35.2 + 24.2 + 6 + 6}{0.296 \cdot 8766 \cdot 0.8} \\ &= 0.108 \ €/kWh \end{aligned} \tag{6.11}$$

6.3 Conclusion

A model of the liquid air production process has been made, because little research is done on the production of liquid air. A significant amount of electricity is saved by expanding the Joule-Thomson valve from 50 bar to 20 bar instead of 1 bar. The total energy efficiency of the liquid air production process is 66.2 %. With an electricity input of 609 MW for a maximum of 9 hours per day, the maximum liquid air production becomes 19.7 ton per day.

To generate electricity from liquid air and molten salt two options are shown. In one option argon is used as transfer fluid in the second cycle, in the other option air is used. The process where argon is used as transfer fluid leads to an energy efficiency of 68.6 % with an output power of 214.6 MW. This is

a lot higher than the energy efficiency and output power for the process with air, 58.7%. Also the mass ratio of liquid air : molten salt is defined in this process and is 1 : 1.67. With a production rate of 19.7 ton/day of liquid air and a mass ratio of 1 : 1.67 the ship must carry 58000 ton of liquid air and 99000 ton of molten salt, which results in a DWT of 158000 ton.

The total energy efficiency of the whole cycle from electricity and heated molten salt in Morocco to electricity in the Netherlands is 58.7 % for a second cycle with argon and 48.1% for a second cycle with air. The output power of the power plant in the Netherlands where argon is used as transfer fluid becomes 214.6 MW and the output power of the power plant with air is 170.3 MW.

These specifications finally lead to a LCoE of 0.108 €/kWh and 0.136 €/kWh for a cycle with argon and air respectively. The LCoE is below 0.125 €/kWh for the process with air, which means that this can be a potential business case. More research needs to be done on the capacity of large-scale liquid air production plants and large-scale liquid air storage. Also the availability of large argon turbines and compressors needs to be investigated. However, the LCoE could be brought down more if the input from PV and CSP is enlarged. Now the ship has a DWT of 158000 ton, but when this is increased by transporting more energy, the levelized costs of the ship will drop.

Chapter 7

Discussion

In this chapter the energy storage concepts which were elaborated upon are compared with each other. 3 totally different energy storage systems have been analyzed to find an energy efficient and cost effective solution to import solar energy from Morocco.

Liquid hydrogen, ammonia and methanol are all fuels with a high energy density. For these fuels the constraints are not the DWT of the tanker, capacity and price of storage tanks or the distance which has to be covered. These variables all have a small impact on the total efficiency and cost of the system compared to thermal energy storage and liquid air storage. For Solar Salt and liquid air this is different, these two energy storage systems are limited by their energy density and specific energy. The energy densities of hydrogen stored in liquid hydrogen, methanol or ammonia are approximately 10-25 times higher than the energy densities of Solar Salt and liquid air, the specific energy ratio between Solar Salt and liquid hydrogen is 270. A low energy density leads to high volumes and loads to store the same amount of energy generated by CSP systems and PV systems. These high loads and volumes are reflected in expensive storage tanks and tankers with a high DWT. Due to high storage costs compared to low amounts of energy transported the operation of the system become of significant importance. An increase in distance of the shipping route or operation with less tankers will have mayor effects on the price. For the chemically stored energy concepts an increase in distance or increase in the tanker operational costs will have much smaller consequences.

The problems for liquid hydrogen, ammonia and methanol are the expensive and energy intensive conversion processes: from electricity to hydrogen, hydrogen to fuel and fuel back to electricity. Nowadays the round-trip efficiencies, following the processes described in this thesis, lie between 14% - 20%. In combination with the high capital costs this leads to a high LCoE. The predictions made on the energy improvements and cost reductions in 2030 will still not reach the cost requirements set by this thesis. The extra energy losses obtained by transporting Solar Salt instead of using a regular CSP plant is only 1%. This is a huge difference compared to chemically stored energy. For the liquid air combined with Solar Salt concept a round-trip efficiency of 54.4% is achieved, this is the reason that this concept is the cheapest.

Thermal energy storage with Solar Salt as energy storage fluid is a technology with high maturity. Almost all the components during the process are well developed. Heating Solar Salt with the use of CSP plants is a conventional method and storing Solar Salt in thermally insulated storage tanks is often done. The only research which needs to be done is the implementation of storage tanks on tankers. The maturity of the liquid air combined with Solar Salt concept is notably lower, especially the high mass flows in different stages of the cycle need to be evaluated further; the liquid air production capacity and the power capacity of argon turbines. The bottlenecks for the chemical energy storage concepts lie in the capacity of fuel cells, the PEM fuel cell is commercially available, however the largest PEM fell cell plant nowadays is 2 MW. For liquid hydrogen there still are some problems constructing large liquid hydrogen

storage tanks. Finally the LCoE of the liquid air combined with Solar Salt concept is the lowest. The prices of chemically stored energy systems will drop significantly the coming years, but this would not be enough to compete with the other concepts on electricity storage if the specifications and assumptions in these thesis are followed. The Solar Salt concept can compete with the liquid air combined with Solar Salt concept if heat is delivered in the Netherlands.

Chapter 8

Conclusion & Recommendations

The two technologies which are used to generate electricity from solar energy are CSP plants and PV systems. For both CSP and PV systems a capacity of 2100 GWh/year is reasoned. CSP has a LCoE of 5.73 €ct/kWh and PV systems have an electricity price of 2.2 €ct/kWh. Due to the high irradiation, close distance and relatively stable country, Morocco is chosen to be the country where solar energy will be imported from. A HVDC submarine power cable between Morocco and the Netherlands is compared in proportion to the costs and distance of the NorNed cable. A HVDC submarine power cable over a distance of 2600 km results in a LCoE of 0.113 €/kWh.

It is concluded that storing electricity in chemical energy storage via the processes described in this thesis will lead to a too high LCoE. The electrolysis, Haber-Bosch process, carbon capture and fuel cell processes are simply to energy intensive. The most efficient and cost effective chemically energy stored based concept obtained is storing electricity in the form of liquid hydrogen. A round-trip efficiency of 27% with a LCoE of 0.491 €/kWh is obtained in 2015, from the predictions of 2030 a round-trip efficiency of 40% with a LCoE of 0.159 €/kWh is derived. The round-trip efficiencies of chemical energy storage have to increase to be able to store and transport solar energy in an economically feasible way. There are possibilities in direct fuel conversion technologies due to their high conversion efficiencies, however the technology readiness levels of these processes are still lower than 6, which means they are in the technology demonstration phase. More research is required, but direct fuel synthesis will play an important role in the future.

The thermal energy storage concept where Solar Salt is used as energy carrier has an energy efficiency from solar irradiation in Morocco to electricity in the Netherlands of 28%, which is very high; the conversion of solar irradiation to electricity performed by solar panels only is already ± 20%. A power output in the Netherlands of 296 MW is obtained with a high LCoE of 0.163 €/kWh, this is devoted to the high storage and transportation costs. The concept can be improved further if the specific energy is increased. Thermochemical energy storage and latent heat energy storage are promising thermal energy storage solutions to increase the specific energy. If heat is delivered in the Netherlands instead of electricity a heat price of 0.069 €/kWh can be realized. Subsidized solar heat is bought by the Dutch government for 0.095 €/kWh. This gives possibilities to effectuate a business case.

The energy output of liquid air and molten salt combined is 215 MW and the total energy efficiency from electricity and heated Solar Salt in Morocco to electricity in the Netherlands is 58.7 %. The LCoE is 0.108 €/kWh and stays well below the subsidized costs of 0.125 €/kWh. More research is needed in the power capacities of argon turbines and large-scale liquid air production and storage, but the concept shows a lot of potential.

Transporting solar energy from Morocco to the Netherlands by a tanker with an electricity input of 2100 GWh/year results in two potential business cases. Generating heat in the Netherlands by use

of Solar Salt as energy carrier and generating electricity by storing energy in liquid air and Solar Salt. Looking at the maturity and price margin compared to subsidized heat or electricity, it is concluded that storing heat in Solar Salt in Morocco and delivering heat in the Netherlands is the business case with the most potential.

Bibliography

[1] Solargis. Investigate your region with Solargis solar resource maps, 2017. URL http://solargis.com/products/maps-and-gis-data/free/download/world.

[2] Christoph Richts. The Moroccan Solar Plan - A comparative analysis of CSP and PV utilization until 2020. -, 2012.

[3] SurveyMonkey. 2016 SAM CSP Cost Survey: Power Towers, 2016. URL https://www.surveymonkey.com/r/CWLPVR6.

[4] IRENA. Renewable Energy Technologies Cost Analysis Series: Concentrating Solar Power. *Comprehensive Renewable Energy*, 3(2):595–636, 2012. ISSN 0094243X. doi: 10.1016/B978-0-08-087872-0.00319-X.

[5] PVeducation. Solar Cell Structure, 2017. URL http://www.pveducation.org/pvcdrom/solar-cell-structure.

[6] ModernPowerSystems. Recognising its true value: a WEC perspective, 2017. URL http://www.modernpowersystems.com/features/featurerecognising-its-true-value-a-wec-perspective-4816858/featurerecognising-its-true-value-a-wec-perspective-4816858-2.html.

[7] T M I Mahlia, T J Saktisahdan, A Jannifar, M H Hasan, and H S C Matseelar. A review of available methods and development on energy storage; technology update. *Renewable and Sustainable Energy Reviews*, 33:532–545, 2014. ISSN 13640321. doi: 10.1016/j.rser.2014.01.068. URL http://linkinghub.elsevier.com/retrieve/pii/S1364032114000902.

[8] M. N. Azpiazu, J. M. Morquillas, and A. Vazquez. Heat recovery from a thermal energy storage based on the Ca(OH)2/CaO cycle. *Applied Thermal Engineering*, 23(6):733–741, 2003. ISSN 13594311. doi: 10.1016/S1359-4311(03)00015-2.

[9] Linde. Liquid Air Energy Storage (LAES), 2017. URL http://www.linde-healthcare.com.sg/en/clean_technology/clean_technology_portfolio/energy_storage/liquid_air_energy_storage/index.html.

[10] Argo Rosin and Vanemteadur Tallinn. Energy storages. *Modern Electric, Hybrid Electric, and Fuel Cell Vehicles*, pages 300–332, 2012.

[11] DoE USA. Hydrogen production cost from solid oxide electrolysis. *Hydrogen and fuel cells program record 16014*, pages 1–4, 2016. URL http://hydrogen.energy.gov/pdfs/9014{_}hydrogen{_}storage{_}materials.pdf.

[12] Fornavn Etternavn. *Songwut Fornavn Etternavn Efficient Liquefaction Tittel på Hydrogen avhandlingen Processes Undertittel på avhandlingen Fornavn Songwut Etternavn Tittel på Hydrogen avhandlingen Efficient Liquefaction Processes Undertittel på avhandlingen Thesis for the de.* -, 2013. ISBN 9788247118696.

[13] Wikipedia. Proton-exchange membrane fuel cell, 2018. URL https://en.wikipedia.org/wiki/Proton-exchange_membrane_fuel_cell.

[14] Eric R Morgan. Techno-Economic Feasibility Study of Ammonia Plants Powered by Offshore Wind. *University of Massachusetts - Amherst, PhD Dissertations*, page 432, 2013. URL http://scholarworks.umass.edu/open{_}access{_}dissertations/697.

[15] Mar Pérez-Fortes, Jan C. Schöneberger, Aikaterini Boulamanti, and Evangelos Tzimas. Methanol synthesis using captured CO2as raw material: Techno-economic and environmental assessment. *Applied Energy*, 161:718–732, 2016. ISSN 03062619. doi: 10.1016/j.apenergy.2015.07.067. URL http://dx.doi.org/10.1016/j.apenergy.2015.07.067.

[16] Antoni Gil, Marc Medrano, Ingrid Martorell, Ana Lazaro, Pablo Dolado, Belen Zalba, and Luisa F. Cabeza. State of the art on high temperature thermal energy storage for power generation. Part 1-Concepts, materials and modellization. *Renewable and Sustainable Energy Reviews*, 14(1):31–55, 2010. ISSN 13640321. doi: 10.1016/j.rser.2009.07.035.

[17] MAN Diesel & Turbo. Propulsion Trends in Tankers. *MAN Diesel*, pages 1–15, 2005. doi: 5510-0031-01. URL papers2://publication/uuid/E2231138-C89F-4814-BB59-307D249B99F2.

[18] Md Mamoon Rashid, Mohammed K Al Mesfer, Hamid Naseem, and Mohd Danish. Hydrogen Production by Water Electrolysis: A Review of Alkaline Water Electrolysis, PEM Water Electrolysis and High Temperature Water Electrolysis. *International Journal of Engineering and Advanced Technology*, pages 2249–8958, 2015.

[19] Thomas R. Mancini, Jesse A. Gary, Gregory J. Kolb, and Clifford Kuofei Ho. Power Tower Technology Roadmap and cost reduction plan. -, 2011. ISSN 9781620814239. doi: 10.2172/1011644. URL http://www.osti.gov/servlets/purl/1011644-0d5QFT/.

[20] Manuel Romero Gómez, Ramón Ferreiro Garcia, Javier Romero Gómez, and José Carbia Carril. Thermodynamic analysis of a Brayton cycle and Rankine cycle arranged in series exploiting the cold exergy of LNG (liquefied natural gas). *Energy*, 66:927–937, 2014. ISSN 03605442. doi: 10.1016/j.energy.2013.12.036. URL http://dx.doi.org/10.1016/j.energy.2013.12.036.

[21] Gavin A. Schmidt. GISS Surface Temperature Analysis, 2017. URL https://data.giss.nasa.gov/gistemp/graphs/.

[22] CBS. Verbruik hernieuwbare energie toegenomen naar 5,8%, 2016. URL https://www.cbs.nl/nl-nl/nieuws/2016/21/verbruik-hernieuwbare-energie-toegenomen-naar-5-8-.

[23] European Commision. 2050 Energy strategy, 2017. URL https://ec.europa.eu/energy/en/topics/energy-strategy-and-energy-union/2050-energy-strategy.

[24] Copyright David and J C Mackay. *Sustainable Energy — without the hot air This Cover-sheet must not appear in the printed book .*, volume 78. Cambridge Ltd., 2009. ISBN 9780954452933. doi: 10.1109/PES.2004.1373296. URL www.withouthotair.com.

[25] RVO. SDE+ voorjaar 2017. *RVO*, pages 7–30, 2017. URL http://www.rvo.nl/subsidies-regelingen/publicaties-stimulering-duurzame-energieproductie.

[26] Hans van der Lugt. SDE+-budget voorjaarsronde 2017 blijft deels onbenut, 2017. URL http://energeia.nl/nieuws/103846-1709/sde-budget-voorjaarsronde-2017-blijft-deels-onbenut.

[27] Saurabh Mahapatra. Lowest-Ever Solar Price Bid (2.42¢/kWh) Dropped In Abu Dhabi By JinkoSolar & Marubeni Score, 2017. URL https://cleantechnica.com/2016/09/20/lowest-ever-solar-price-bid-2-42%C2%A2kwh-dropped-abu-dhabi-jinkosolar-marubeni-score/.

[28] Rashid Al. Mohammed bin Rashid Al Maktoum. -, page 2006, 2006.

[29] HelioCSP. Morocco shortlists five international bids for Noor Midelt PV-Concentrated Solar Power project, 2017. URL http://helioscsp.com/morocco-shortlists-five-international-bids-for-noor-midelt-pv-concentrated-solar-power-project/

[30] Susan Kreamer. SolarReserve Bids 24-Hour Solar At 6.3 Cents In Chile, 2017. URL https://cleantechnica.com/2017/03/13/solarreserve-bids-24-hour-solar-6-3-cents-chile/.

[31] The National. 24-hour solar power is possible for Mena, 2017. URL https://www.thenational.ae/business/24-hour-solar-power-is-possible-for-mena-1.40805.

[32] Jonathan Watts. Desert tower raises Chile's solar power ambition to new heights, 2015. URL https://www.theguardian.com/environment/2015/dec/22/desert-tower-raises-chiles-solar-power-ambition-to-new-heights.

[33] NREL. Concentrating Solar Power Projects Noor III, 2017. URL https://www.nrel.gov/csp/solarpaces/project_detail.cfm/projectID=4293.

[34] NREL. Concentrating Solar Power Projects Redstone Solar Thermal Power Plant, 2016. URL https://www.nrel.gov/csp/solarpaces/project_detail.cfm/projectID=4289.

[35] NREL. Concentrating Solar Power Projects Copiapo, 2015. URL https://www.nrel.gov/csp/solarpaces/project_detail.cfm/projectID=4299.

[36] CleanTechnica. Dubai Awards 700 Megawatt Solar CSP Contract For Mammoth Mohammed Bin Rashid Al Maktoum Solar Park, 2017. URL https://cleantechnica.com/2017/09/19/dubai-awards-700-mw-solar-csp-contract-mammoth-mohammed-bin-rashid-al-maktoum-solar-park/.

[37] HelioCSP. How Port Augusta Got the World's Cheapest Concentrated Solar Power, 2017. URL http://helioscsp.com/how-port-augusta-got-the-worlds-cheapest-concentrated-solar-power/.

[38] NewEnergyUpdate. Global CSP capacity forecast to hit 22 GW by 2025, 2017. URL http://analysis.newenergyupdate.com/csp-today/markets/global-csp-capacity-forecast-hit-22-gw-2025.

[39] T. Hirsch and A. Khenissi. A systematic comparison on power block efficiencies for CSP plants with direct steam generation. *Energy Procedia*, 49:1165–1176, 2013. ISSN 18766102. doi: 10.1016/j.egypro.2014.03.126. URL http://dx.doi.org/10.1016/j.egypro.2014.03.126.

[40] Solarinsure. Top 5 Largest Solar Power Plants of the World, 2017. URL https://www.solarinsure.com/largest-solar-power-plants.

[41] ESI-Africa. Successful bid for Scaling Solar yields low tariffs, 2016. URL https://www.esi-africa.com/news/neoen-successful-bid-for-scaling-solar-yields-low-tariffs/.

[42] CleanTechnica. Dubai Gets Record-Low Bid Of 2.99¢/kWh For 800 MW Solar PV Project, 2016. URL https://cleantechnica.com/2016/05/02/lowest-solar-price-dubai-800-mw-solar-project/.

[43] PV magazine. Sterling and Wilson wins contract to build 1.17 GW solar project in Abu Dhabi, 2017. URL https://www.pv-magazine.com/2017/06/20/sterling-and-wilson-wins-contract-to-build-1-17-gw-solar-project-in-abu-dhabi/.

[44] PVtech. Bids in 300MW Saudi solar tender breach two cents, 2017. URL https://www.pv-tech.org/news/technical-bids-for-300mw-of-solar-in-saudi-arabia-already-breach-2-cents.

[45] Reneweconomy. Chile solar auction sets new record low for solar PV, 2017. URL http://reneweconomy.com.au/chile-solar-auction-sets-new-record-low-for-solar-pv-85114/.

[46] Y Aldali and F Ahwide. Evaluation of A 50MW Two-Axis Tracking Photovoltaic Power Plant for AL-Jagbob , Libya : Energetic , Economic , and Environmental Impact Analysis. -, 7(12):811–815, 2013.

[47] Irena. USolar photovoltaic Summary Charts, 2017. URL http://www.irena.org/costs/Charts/Solar-photovoltaic.

[48] Roberto Rudervall, Jp Chapentier, and Raghuveer Sharma. High voltage direct current (HVDC) transmission systems technology review paper. *Energy Week*, pages 1–19, 2000. URL http://www2.internetcad.com/pub/energy/technology{_}abb.pdf.

[49] Wikipedia. NorNed, 2017. URL https://en.wikipedia.org/wiki/NorNed.

[50] Paola Bresesti, Wil L. Kling, Ralph L. Hendriks, and Riccardo Vailati. HVDC connection of offshore wind farms to the transmission system. *IEEE Transactions on Energy Conversion*, 22(1):37–43, 2007. ISSN 08858969. doi: 10.1109/TEC.2006.889624.

[51] D Kearney, B Kelly, R Cable, N Potrovitza, U Herrmann, P Nava, R Mahoney, J Pacheco, D Blake, and H Price. Overview on use of a Molten Salt HTF in a Trough Solar Field. *NREL Parabolic Trough Thermal Energy Storage Workshop*, 2003.

[52] Haisheng Chen, Thang Ngoc Cong, Wei Yang, Chunqing Tan, Yongliang Li, and Yulong Ding. Progress in electrical energy storage system: A critical review. *Progress in Natural Science*, 19(3): 291–312, 2009. ISSN 10020071. doi: 10.1016/j.pnsc.2008.07.014. URL http://dx.doi.org/10.1016/j.pnsc.2008.07.014.

[53] Gareth Brett and Matthew Barnett. The application of liquid air energy storage for large scale long duration solutions to grid balancing. *EPJ Web of Conferences*, 79(03002):1–9, 2014. ISSN 2100-014X. doi: 10.1051/epjconf/20137903002. URL http://dx.doi.org/10.1051/epjconf/20137903002.

[54] R Morgan, S Nelmes, E Gibson, and G Brett. An analysis of a large-scale liquid air energy storage system. *Proceedings of the Institution of Civil Engineers-Energy*, 168(2):135–144, 2015.

[55] T. Takaishi, R. Nakano, A. Numata, and K. Sakaguchi. Approach to High Efficiency Diesel and Gas Engines. *Mitsubishi Heavy Industries, Ltd. Technical Review*, 45(1):21, 2008.

[56] Yves Wild and Thermo King Corp. Determination of energy cost of electrical energy on board sea-going vessels. -, 2005.

[57] S.S. Kalligeros, F. Zannikos, E. Lois, and G. Anastopoulos. Monoglyceride Content in Marine Diesel Fuel-A Guide. *SAE Technical Papers*, 2014-Octob(January 2016), 2014. doi: 10.4271/2014-01-2775.

[58] Bunkerindex. Bunker Index NWE, 2015. URL http://www.bunkerindex.com/prices/bixfree.php?priceindex_id=10.

[59] Sara McAllister, Jyh-Yuan Chen, and A. Carlos Fernandez-Pello. *Fundamentals of Combustion Processes*. -, 2011. ISBN 978-1-4419-7942-1. doi: 10.1007/978-1-4419-7943-8. URL http://link.springer.com/10.1007/978-1-4419-7943-8.

[60] Xingwen Yu and Peter G. Pickup. Recent advances in direct formic acid fuel cells (DFAFC). *Journal of Power Sources*, 182(1):124–132, 2008. ISSN 03787753. doi: 10.1016/j.jpowsour.2008.03.075. URL http://link.springer.com/10.1007/978-1-4419-7943-8.

[61] Hasnain S.M. Review on sustainable thermal energy storage technologies, Part I: heat storage materials and techniques. *Energy Conversion and Management*, 39(11):1127–1138, 1998. ISSN 01968904. doi: 10.1016/S0196-8904(98)00025-9. URL http://www.sciencedirect.com/science/article/pii/S0196890498000259.

[62] Mar Pérez-Fortes, Jan C. Schöneberger, Aikaterini Boulamanti, Gillian Harrison, and Evangelos Tzimas. Formic acid synthesis using CO2as raw material: Techno-economic and environmental evaluation and market potential. *International Journal of Hydrogen Energy*, 41(37):16444–16462, 2016. ISSN 03603199. doi: 10.1016/j.ijhydene.2016.05.199.

[63] Richard A Rick Caulfield, Scott Willis, Bob Grimm, P O Box, Port Townsend, Physical Address, and Otto Street. Solid State Ammonia Synthesis (SSAS) Pilot Plant Demonstration System for Renewable Energy (RE) Firming Storage, Transmission, and Export Alaska Applied Sciences, Inc. -, pages 1–5, 2011.

[64] W. van Jong. Hydrogen - Energy from Gas. powerpoint, 2017.

[65] IEA. Technology Roadmap. *SpringerReference*, page 81, 2015. ISSN 03060012. doi: 10.1007/SpringerReference_7300. URL http://www.springerreference.com/index/doi/10.1007/SpringerReference{_}7300.

[66] Luca Bertuccioli, Alvin Chan, David Hart, Franz Lehner, Ben Madden, and Eleanor Standen. Study on development of water electrolysis in the EU. *Fuel Cells and hydrogen Joint Undertaking*, pages 1–160, 2014. URL http://www.fch-ju.eu/sites/default/files/studyelectrolyser{_}0-Logos{_}0{_}0.pdf.

[67] Hydrogenics. OnSite Hydrogen Generation HyLYZER ® PEM Electrolysis Technology. -, pages 1–8, 2017. URL http://www.hydrogenics.com/assets/pdfs/ANNEX1-HyLYZER-1.pdf.

[68] DOE. 3.1 Hydrogen Production. *Fuel Cell Technologies Office Multi-Year Research, Development and Demonstration Plant*, 11007:1–44, 2015. URL http://energy.gov/eere/fuelcells/downloads/fuel-cell-technologies-office-multi-year-research-development-and-22.

[69] Originator Chris Ainscough, David Peterson, and Eric Miller. Hydrogen production cost from PEM electrolysis. *Ainscough,Chris Petersonm, David Miller, Eric Satyapal, Sunita*, pages 1–11, 2014.

[70] R. Rivera-Tinoco, M. Farran, C. Bouallou, F. Auprêtre, S. Valentin, P. Millet, and J. R. Ngameni. Investigation of power-to-methanol processes coupling electrolytic hydrogen production and catalytic CO2 reduction. *International Journal of Hydrogen Energy*, 41(8):4546–4559, 2016. ISSN 03603199. doi: 10.1016/j.ijhydene.2016.01.059.

[71] Sune Dalgaard Ebbesen, Søren Højgaard Jensen, Anne Hauch, and Mogens Bjerg Mogensen. High temperature electrolysis in alkaline cells, solid proton conducting cells, and solid oxide cells. *Chemical Reviews*, 114(21):10697–10734, 2014. ISSN 15206890. doi: 10.1021/cr5000865.

[72] Yaser Khojasteh Salkuyeh, Bradley A. Saville, and Heather L. MacLean. Techno-economic analysis and life cycle assessment of hydrogen production from natural gas using current and emerging technologies. *International Journal of Hydrogen Energy*, 42(30):18894–18909, 2017. ISSN 03603199. doi: 10.1016/j.ijhydene.2017.05.219. URL http://dx.doi.org/10.1016/j.ijhydene.2017.05.219.

[73] E Tzimas, C Filiou, S D Peteves, and J Veyret. *Hydrogen Storage : State-of-the-Art and Future Perspective*. -, 2003. ISBN 9289469501.

[74] Wade A Amos. Costs of Storing and Transporting Hydrogen. *Other Information: PBD: 27 Jan 1999; PBD: 27 Jan 1999; PBD: 27 Jan 1999*, page Medium: ED; Size: vp., 1999. URL http://www.osti.gov/bridge/servlets/purl/6574-OBMlES/webviewable/.

[75] Christopher Yang and Joan Ogden. Determining the lowest-cost hydrogen delivery mode. *International Journal of Hydrogen Energy*, 32(2):268–286, 2007. ISSN 03603199. doi: 10.1016/j.ijhydene.2006.05.009.

[76] Fuel Cells and Nordic Countries. Integrated Design for Demonstration of Efficient Liquefaction of Hydrogen. *Hydrogen and Fuel Cells in the Nordic Countries, November 1, 2013*, 2013.

[77] Andreas Zuttel. Materials for hydrogen storage. *Materials Today*, 6(9):24–33, 2003. ISSN 13697021. doi: 10.1016/S1369-7021(03)00922-2.

[78] Nedstack. Nedstack product specifications, 2014. URL http://www.nedstack.com/wp-content/uploads/2017/05/nedstack_product-specifications-of-xxl-stacks.pdf.

[79] E. A. Brohi. Ammonia as fuel for internal combustion engines ? An evaluation of the feasibility of using nitrogen-based fuels in ICE. -, page 43, 2014. URL http://energy.gov/eere/sunshot/sunshot-initiative.

[80] C. Zamfirescu and I. Dincer. Ammonia as a green fuel and hydrogen source for vehicular applications. *Fuel Processing Technology*, 90(5):729–737, 2009. ISSN 03783820. doi: 10.1016/j.fuproc.2009.02.004.

[81] WorleyParsons. CCS learning from the LNG sector - A report for the GCCSI. -, 2013.

[82] M. B.V. Virji and R. H. Thring. Analysis of a 50 kWe indirect methanol proton exchange membrane fuel cell (PEMFC) system for transportation applicatio. *Proceedings of the Institution of Mechanical Engineers, Part D: Journal of Automobile Engineering*, 219(8):937–950, 2005. ISSN 09544070. doi: 10.1243/095440705X34694.

[83] V.K. Shen et all. NIST Standard Reference Simulation Website, 2018. URL `http://doi.org/10.18434/T4M88Q`.

[84] Dennis Y C Leung, Giorgio Caramanna, and M. Mercedes Maroto-Valer. An overview of current status of carbon dioxide capture and storage technologies. *Renewable and Sustainable Energy Reviews*, 39:426–443, 2014. ISSN 13640321. doi: 10.1016/j.rser.2014.07.093. URL `http://dx.doi.org/10.1016/j.rser.2014.07.093`.

[85] Methanex. Methanex posts regional contract methanol prices for North America, Europe and Asia., 2018. URL `https://www.methanex.com/our-business/pricing`.

[86] Chao Xu, Zhifeng Wang, Xin Li, and Feihu Sun. Energy and exergy analysis of solar power tower plants. *Applied Thermal Engineering*, 31(17-18):3904–3913, 2011. ISSN 13594311. doi: 10.1016/j.applthermaleng.2011.07.038. URL `http://dx.doi.org/10.1016/j.applthermaleng.2011.07.038`.

[87] Ulf Herrmann, Bruce Kelly, and Henry Price. Two-tank molten salt storage for parabolic trough solar power plants. *Energy*, 29(5-6):883–893, 2004. ISSN 03605442. doi: 10.1016/S0360-5442(03)00193-2.

[88] Concentrating Solar Power. Technology Roadmap Concentrating Solar Power. *Current*, 5:1–52, 2010. ISSN 1557170X. doi: 10.1787/9789264088139-en. URL `http://www.oecd-ilibrary.org/energy/technology-roadmap-concentrating-solar-power{%}7B{_}{%}7D9789264088139-en`.

[89] NuclearPower. Thermal Efficiency Improvement – Rankine Cycle, 2017. URL `https://www.nuclear-power.net/nuclear-engineering/thermodynamics/thermodynamic-cycles/rankine-cycle-steam-turbine-cycle/boiler-and-condenser-pressures-rankine-cycle/`.

[90] Siemens. A Full Range of World-class Industrial Steam Turbines. *Industrial Steam Turbines*, 1(1):1–8, 2009.

[91] Andrew Heshedahl Sudmant, Andy Gouldson, Sarah Colenbrander, Rory Sullivan, Faye McAnulla, and Niall Kerr. Understanding the case for low-carbon investment through bottom-up assessments of city-scale opportunities. *Climate Policy*, 17(3):299–313, 2017. ISSN 17527457. doi: 10.1080/14693062.2015.1104498.

[92] J. Hernández-Moro and J. M. Martínez-Duart. Analytical model for solar PV and CSP electricity costs: Present LCOE values and their future evolution. *Renewable and Sustainable Energy Reviews*, 20:119–132, 2013. ISSN 13640321. doi: 10.1016/j.rser.2012.11.082.

[93] Solar Paces Greenpeace International and Stella. Concentrating Solar Power Global Outlook 09. *Power*, page 88, 2009.

[94] Craig Turchi, Mark Mehos, Clifford K Ho, and Gregory J Kolb. Current and future costs for parabolic trough and power tower systems in the US market. *Renewable Energy*, page 11, 2010. URL `http://www.nrel.gov/docs/fy11osti/49303.pdf`.

[95] Vivek Chandra. Gas Pipelines, 2017. URL `http://www.natgas.info/gas-information/what-is-natural-gas/gas-pipelines`.

[96] David (ed.) Strahan. *Liquid Air in the energy and transport systems*. -, 2013. ISBN 9780957587229. URL `http://liquidair.org.uk/files/full-report.pdf`.

[97] Mohamed S El-Genk and Jean-Michel Tournier. Noble gas binary mixtures for gas-cooled reactor power plants. *Nuclear Engineering and Design*, 238(6):1353–1372, 2008.

[98] PA Pilavachi, CP Roumpeas, S Minett, and NH Afgan. Multi-criteria evaluation for chp system options. *Energy Conversion and Management*, 47(20):3519–3529, 2006.

[99] Energieleverancier. COpbrengst zonnepanelen, 2017. URL `https://www.energieleveranciers.nl/zonnepanelen/opbrengst-zonnepanelen`.

Appendices

Appendix A

Windturbines and solar panels part of the Netherlands

uren jaar	8766	
Energieverbruik NL	3000	PJ
Oppervlak NL	41500	km2
Windmolens		
Windspeed	6	m/s *
air density	1,3	kg/m3
capacity factor	50%	
Windmolens capacitei	2,21	W/m2
Oppervlake nodig	43105	km2
factor NL	104%	
Solar panels		
Solar panels energie	120	kWh/m2/year **
Oppervlake nodig	6944	km
factor NL	17%	

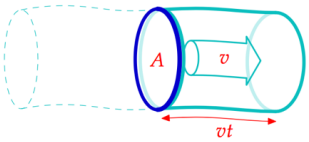

The kinetic energy of this piece of air is

$$\frac{1}{2}mv^2 = \frac{1}{2}\rho Avt\,v^2 = \frac{1}{2}\rho Atv^3. \tag{B.1}$$

So the power of the wind, for an area A – that is, the kinetic energy passing across that area per unit time – is

$$\frac{\frac{1}{2}mv^2}{t} = \frac{1}{2}\rho Av^3. \tag{B.2}$$

efficiency factor × power per unit area × area

$$= 50\% \times \frac{1}{2}\rho v^3 \times \frac{\pi}{4}d^2 \tag{B.4}$$

$$\frac{\text{power per windmill (B.4)}}{\text{land area per windmill}} = \frac{\frac{1}{2}\rho v^3 \frac{\pi}{8}d^2}{(5d)^2} \tag{B.7}$$

$$= \frac{\pi}{200}\frac{1}{2}\rho v^3 \tag{B.8}$$

$$= 0.016 \times 140\,\text{W/m}^2 \tag{B.9}$$

$$= 2.2\,\text{W/m}^2. \tag{B.10}$$

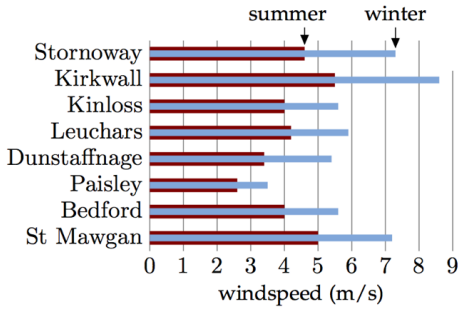

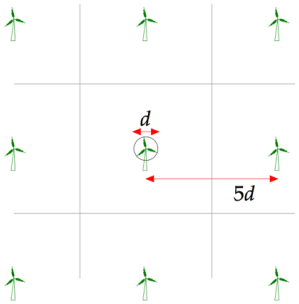

Figure A.1: Windturbines and solar panels part of the Netherlands

* The wind speed is taken the same as in England

** [99]

Appendix B

Irradiation

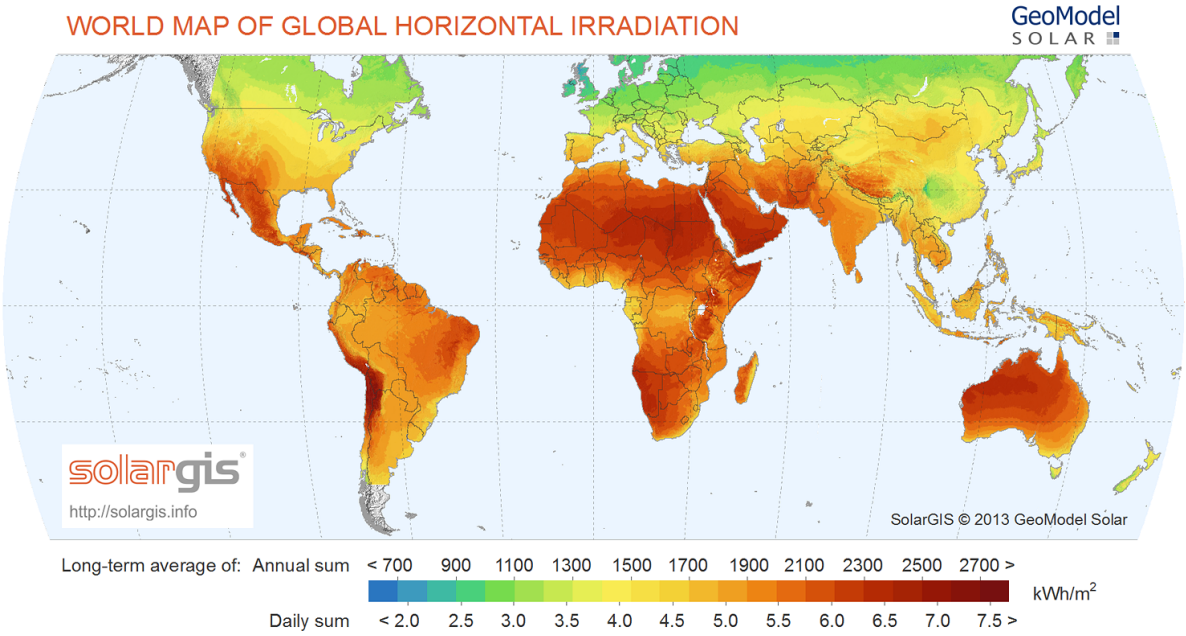

Figure B.1: Global Horizontal Irradiation World [1]

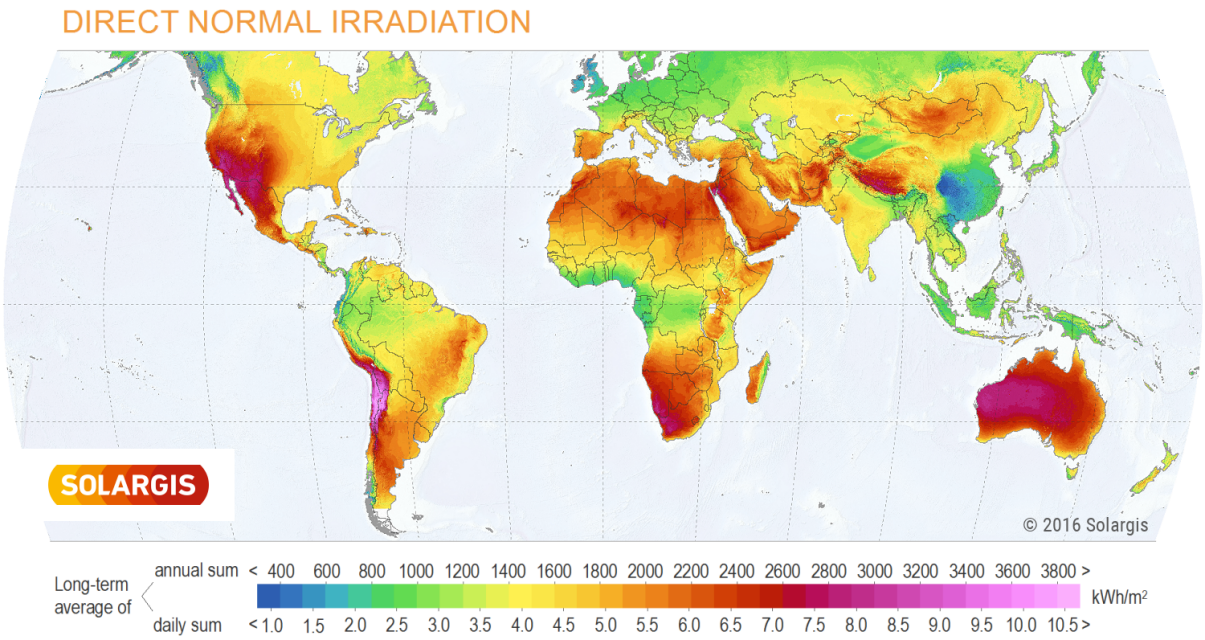

Figure B.2: Direct Normal Irradiation World [1]

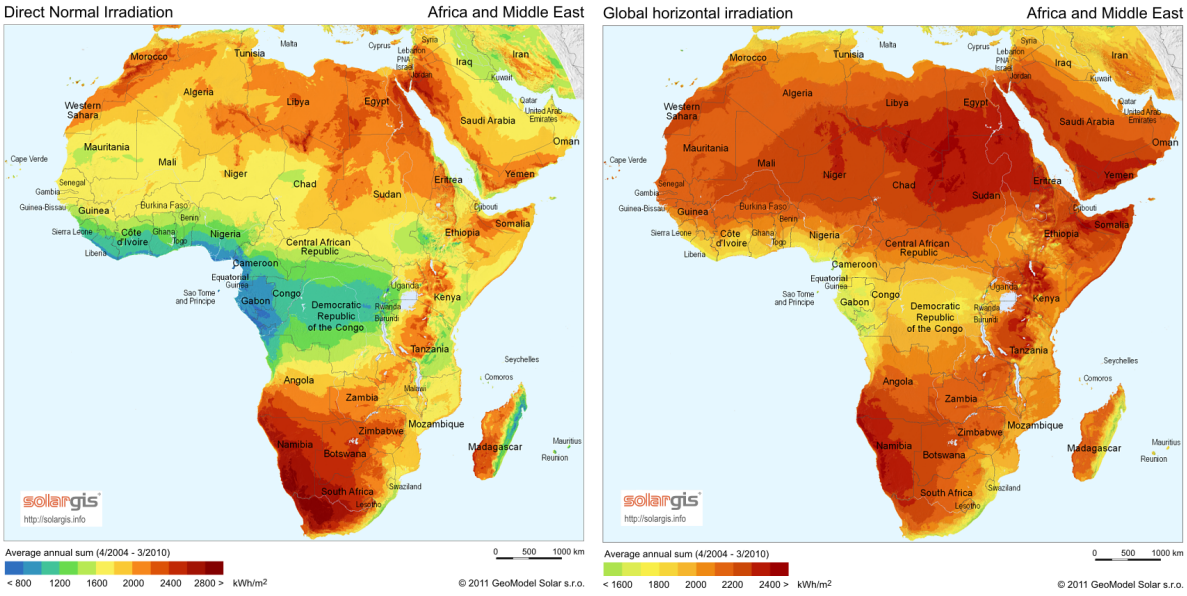

(a) DNI Africa and Middle East

(b) GHI Africa and Middle East

Figure B.3: DNI and GHI Africa and Middle East [1]

Solar radiation (yearly average)

G horizontal: 2195 kWh/m^2 (show MJ/m^2)

Diffuse horizontal: 867 kWh/m^2

Direct normal: 1975 kWh/m^2

Air temperature

Yearly: 27.7 °C (show F)

January: 18.3 °C

July: 35.2 °C

Terrain (SRTM3)

Altitude: 116 m (show ft)

Slope inclination: 0.5 ° (show %)

Slope azimuth: 132° (SE)

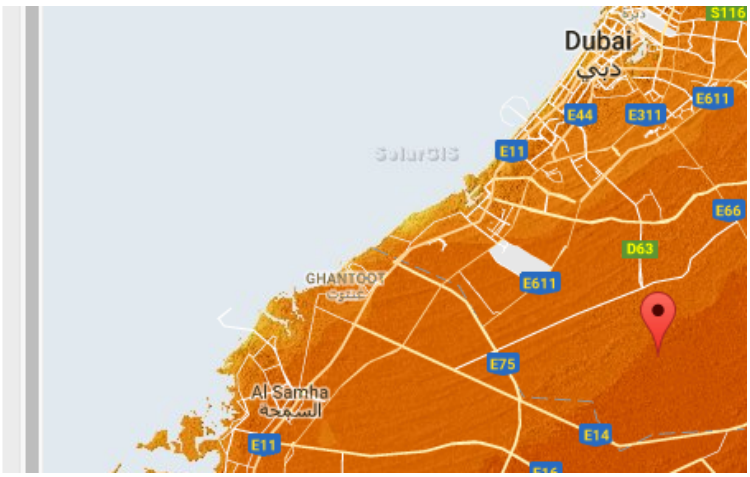

Figure B.4: Irradiation Dubai [1]

Solar radiation (yearly average)

G horizontal: 2088 kWh/m^2 (show MJ/m^2)

Diffuse horizontal: 640 kWh/m^2

Direct normal: 2281 kWh/m^2

Air temperature

Yearly: 18.8 °C (show F)

January: 11.5 °C

July: 27.1 °C

Terrain (SRTM3)

Altitude: 546 m (show ft)

Slope inclination: 2.6 ° (show %)

Slope azimuth: 211° (SW)

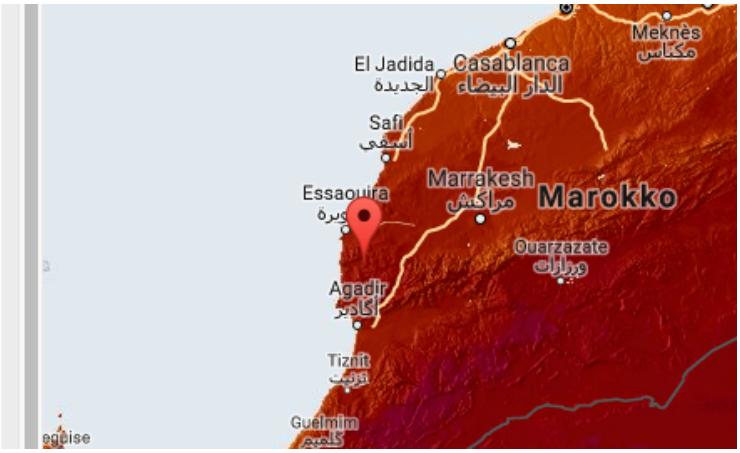

Figure B.5: Irradiation Agadir [1]

Appendix C

SOEC Efficiency Assumptions

Capital Costs				Notes
H2A Total Direct Capital Cost	$32.779.698	View/Edit		Click to enter details on the Cost Detail Sheet
H2A Carbon Sequestration Total Direct Capital Cost		Link to Detail Sheet		Click to enter details on the Carbon Sequestration calculation sheet.
Indirect Depreciable Capital Costs				
	Enter values in basis year (2012) dollars	**Combined Plant Scaling and Escalation Factor**	**Reference Year (2007) Dollars**	
Site Preparation ($) (may change to construction costs)	$723.584	0,91	$655.594	
Engineering & design ($)	$3.617.918	0,91	$3.277.970	
Process contingency ($)	$2.351.648	0,91	$2.130.682	
Project contingency ($)	$2.351.648	0,91	$2.130.682	
Other (Depreciable) capital ($)		0,91	$0	
One-time Licensing Fees ($)		0,91	$0	
Up-Front Permitting Costs ($) (legal and contractors fees included here)	$5.426.877	0,91	$4.916.955	
Total Depreciable Capital Costs			$45.891.581	
Non-Depreciable Capital Costs	**Enter values in basis year (2012) dollars**	**Combined Plant Scaling and Escalation Factor**	**Reference Year (2007) Dollars**	
Cost of land ($/acre)	$50.000	0,96	$48.081,85	
Land required (acres)	5	1	5	
Land Cost ($)			$240.409	
Other non depreciable capital costs		0,96	$0	
Total Non-Depreciable Capital Costs			$240.409,23	
Total Capital Costs	$46.131.990			

Figure C.1: Direct Capital Costs SOEC

Electrolyzer Stack	7.539.331	Based on 35.1kWh/kgH2, $430/kWinput in 2012$, 52,300TPD design capacity, 23%/77% stack/BOP cost split.	
Electrolyzer BoP	25.240.368	Based on 35.1kWh/kgH2, $430/kWinput in 2012$, 52,300TPD design capacity, 23%/77% stack/BOP cost split.	
	32.779.698		
Stack Cost (% SOEC Sys Cost)	23%		
BoP Cost (% SOEC Sys Cost)	77%		

Figure C.2: Capital Costs SOEC

Fixed Operating Costs	Enter values in basis year (2012) dollars	Combined Plant Scaling and Escalation Factor	Reference Year (2007) Dollars	
Total plant staff (number of FTEs employed by plant)	15	1	15	
Burdened labor cost, including overhead ($/man-hr)	$50	0,91	$45,57	
Labor cost, $/year			$1.421.818	
G&A rate (% of labor cost)	20%	☑ H2a Default		
G&A ($/year)			$284.364	
Licensing, Permits and Fees ($/year)		0,91	$0,00	
Property tax and insurance rate (% of total capital investment per year)	2%	☑ H2a Default		
Property taxes and insurance ($/year)			$ 922.640	
Rent ($/year)		0,96	$0,00	
Material costs for maintenance and repairs ($/year)		0,91	$0	
Production Maintenance and Repairs ($/year)	$1.085.375	0,91	$983.390,95	3%, same as PEM current central
Other Fees ($/year)		0,91	$0	
Other Fixed O&M Costs ($/year)		0,91	$0,00	
Total Fixed Operating Costs			$3.612.213	

Figure C.3: Fixed Operating Costs

Appendix D

PEM Efficiency Assumptions

Energy Efficiency Calculations			Central / Future	Basis for Assumptions
	H_2 Outlet Pressure	psi	1000	Industry feedback
Stack Electrical Usage				
	Cell voltage	volts/cell	1,577	Based on literature and industry input. 5% improvement for Future Cases compared to Current Cases (Current Cases 1.75 volts/cell) (assuming 1.6A/cm^2 current density).
	Voltage Efficiency	% LHV	78,0%	Equation: 1.23/cell voltage
	Dryer Loss	% of gross H_2	1,5%	The 3% Dryer loss comes from industry ("3-4%")for Current Cases. The reductions (1.5%) are estimates based on a lower flow of water required for full saturation at higher outlet pressures in Future Cases.
	Permeation Loss	% of gross H_2	2,0%	Based on back diffusion model (1.85x10-7cm^2/s back diffusion coefficient): Industry input is 0.7% at 450psi, model says 0.5% at 450psi for a 3µm thick membrane, 2.02% at 1,000psi for a 2µm thick membrane.
	Total Stack Energy Usage per mass net H_2	**$kWh_{elec}/kg_{Net\ H2}$**	**44,27**	
BOP Loads				
	Power Inverter Efficiency	%	97%	Based on industry input (97% for future performance).
	Inverter Electrical Load	$kWh_{elec}/kg_{Net\ H2}$	1,37	
	Dryer Thermal Load	$kWh_{therm}/kg_{Net\ H2}$	0,31	Based on Hysys Simulation.
	Dryer Efficiency	kWh_{elec}/kWh_{therm}	3,30	Based on industry input for the ratio of net electrical energy for the chiller. 10% improvement for Future Central (3.67kWhelec/kWhtherm for Current Case) .
	Dryer Electrical Load	$kWh_{elec}/kg_{Net\ H2}$	1,02	
	Misc Electrical Load	$kWh_{elec}/kg_{Net\ H2}$	1,08	Based on industry input for current. 30% improvement for Future Central Case Compared to Current Forecourt Case (1.2 $kWh_{elec}/kg_{Net\ H2}$ for Current Case).
	Total BOP Electrical Load	**$kWh_{elec}/kg_{Net\ H2}$**	**3,47**	
Summary				
	Stack Electrical Usage	**kWh_{elec}/kg_{H2}**	**44,27**	
	BOP Electrical Usage	**kWh_{elec}/kg_{H2}**	**3,47**	
Total System Electral Usage per mass net H_2		$kWh_{elec}/kg_{Net\ H2}$	**47,7**	

Figure D.1: kWh Electricity / kg Hydrogen PEM

Major pieces/systems of equipment	Baseline Costs 2012		Baseline Costs 2020		Comments
Uninstalled Cost - ($/kW) (with suggested subsystem breakdown, further breakdown desirable if available)	368	368		259	
Electricity Usage (kWh/kg)	47,73915483	47,73915483		47,73915483	
System Power (kW)	104.032	104.032		104.032	
Stacks	37%	$ 14.164.939,24	42%	$ 11.331.951,39	20% cost reduction compared to 2012
BoP Total	**63%**				
Hydrogen Gas Management System-Cathode system side	1%	$ 382.836,20	1%	$ 382.836,20	
Oxygen Gas Management System-Anode system side	1%	$ 382.836,20	1%	$ 382.836,20	
Water Reacant Delivery Management System	1%	$ 382.836,20	1%	$ 382.836,20	
Thermal Management System	7%	$ 2.679.853,37	10%	$ 2.679.853,37	
Power Electronics	44%	$ 16.844.792,61	31%	$ 8.422.396,30	50% cost reduction compared to 2012
Controls & Sensors	1%	$ 382.836,20	1%	$ 382.836,20	
Mechanical Balance of Plant-ss plumbing/copper cabling/Dryer valves...	2%	$ 765.672,39	3%	$ 765.672,39	
Item Breakdown- Other	3%	$ 1.148.508,59	4%	$ 1.148.508,59	
Item Breakdown-Assembly Labor	3%	$ 1.148.508,59	4%	$ 1.148.508,59	
	Total	$ 38.283.619,56	Total	$ 26.937.458,89	

Figure D.2: Direct Capital Costs PEM

Capital Costs				**Notes**	
H2A Total Direct Capital Cost	$26.937.459	View/Edit		**Click to enter details on the Cost Detail Sheet**	
H2A Carbon Sequestration Total Direct Capital Cost		Link to Detail Sheet		**Click to enter details on the Carbon Sequestration calculation sheet.**	
Indirect Depreciable Capital Costs					
	Enter values in basis year (2012) dollars	**Combined Plant Scaling and Escalation Factor**	**Reference Year (2007) Dollars**		
Site Preparation ($) (may change to construction costs)	$594.621	0,91	$538.749	2% of installed capital cost	
Engineering & design ($)	$2.378.485	0,91	$2.154.997	8% of installed capital cost	
Process contingency ($)		0,91	$0		
Project contingency ($)	$4.459.659	0,91	$4.040.619	15% of installed capital cost	
Other (Depreciable) capital ($)		0,91	$0		
One-time Licensing Fees ($)		0,91	$0		
Up-Front Permitting Costs ($) (legal and contractors fees included here)	$4.459.659	0,91	$4.040.619	15% of installed capital cost	
Total Depreciable Capital Costs			$37.712.442		
Non-Depreciable Capital Costs	**Enter values in basis year (2012) dollars**	**Combined Plant Scaling and Escalation Factor**	**Reference Year (2007) Dollars**		
Cost of land ($/acre)	$50.000	0,96	$48.081,85	Norsk Hydro presentation 2004. Land needed for 100,000 kg/day plant stated to be 2.71 Hectares (257m x 105m), or 6.9 acres	
Land required (acres)	5	1	5		
Land Cost ($)			$240.409		
Other non depreciable capital costs		0,96	$0		
Total Non-Depreciable Capital Costs			$240.409,23		
Total Capital Costs	$37.952.852				

Figure D.3: Capital Costs PEM

Fixed Operating Costs				
	Enter values in basis year (2012) dollars	**Combined Plant Scaling and Escalation Factor**	**Reference Year (2007) Dollars**	
Total plant staff (number of FTEs employed by plant)	4	1	4	
Burdened labor cost, including overhead ($/man-hr)	$50	0,91	$45,57	
Labor cost, $/year			$379.152	
G&A rate (% of labor cost)	20%			
G&A ($/year)			$75.830	
Licensing, Permits and Fees ($/year)		0,91	$0,00	
Property tax and insurance rate (% of total capital investment per year)	2%			
Property taxes and insurance ($/year)			$ 759.057	
Rent ($/year)		0,96	$0,00	
Material costs for maintenance and repairs ($/year)		0,91	$0	
Production Maintenance and Repairs ($/year)	$891.932	0,91	$808.123,77	3% of installed capital cost
Other Fees ($/year)		0,91	$0	
Other Fixed O&M Costs ($/year)		0,91	$0,00	
Total Fixed Operating Costs			$2.022.163	

Figure D.4: Fixed Operating Costs PEM

Appendix E

Methanol process

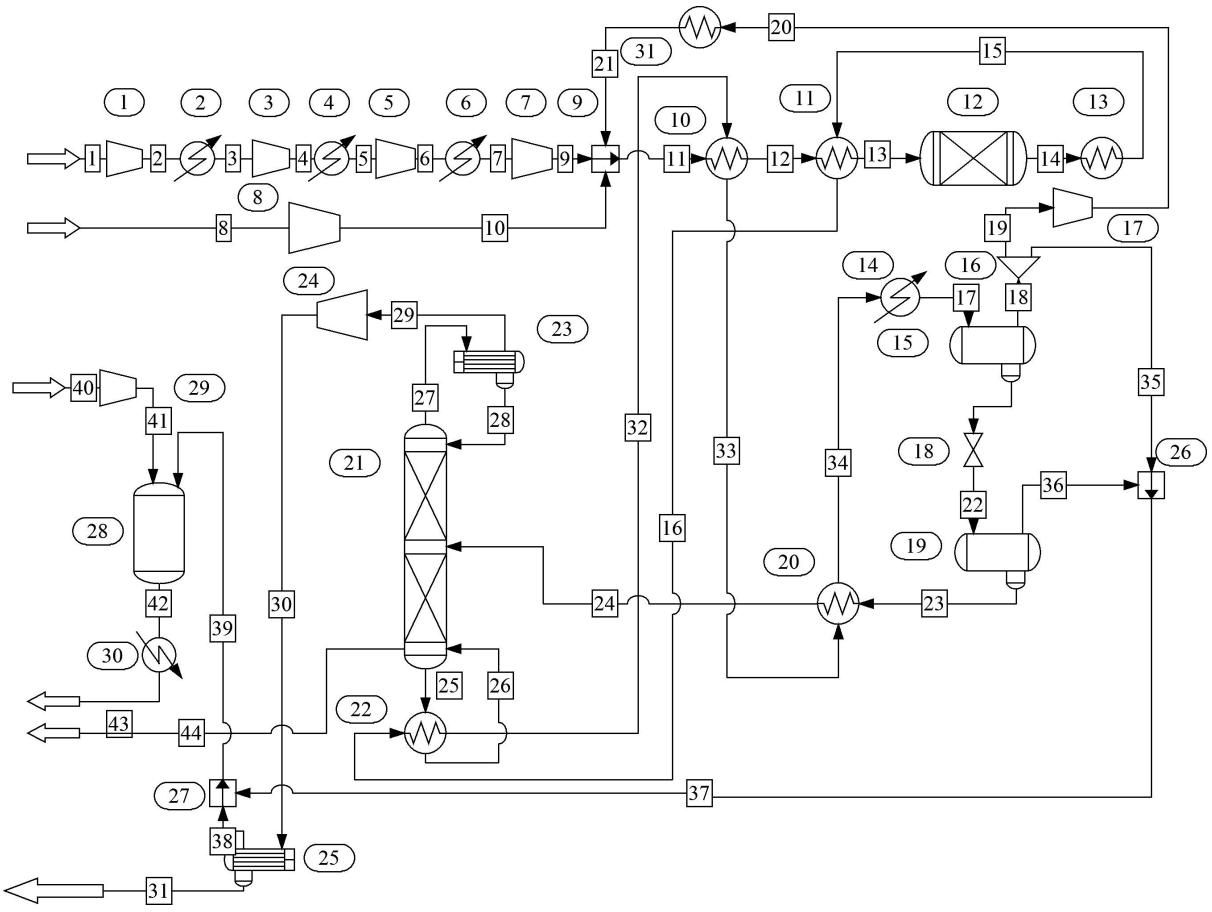

Figure E.1: Methanol Process [15]

Table 1
Technological metrics evaluation for the MeOH CCU-plant.

Mass balance (t/t_{MeOH})	
Inlet CO_2	1.460
Inlet H_2	0.199
Inlet air to furnace	0.813
Outlet MeOH	1
Outlet H_2O	0.569
Flue gas from furnace	0.905
Energy balance ($MW\ h/t_{MeOH}$)	
Electricity consumption	0.169
Heating needs	0.439
Cooling needs	0.862
CO_2convR (%)	21.97
CO_2convP (%)	93.85
Gross CO_2used (t/t_{MeOH})	1.370
Net CO_2used (t/t_{MeOH})	1.234

Table 4
Main metrics comparison between MeOH CCU-plant and the weighted-average conventional synthesis plant in Europe.

	CCU-plant	Conventional plant [45]
Electricity needs ($MW\ h/t_{MeOH}$)	0.169	0.147
Water needs (tH_2O/tMeOH)	26.39	90
Capital costs (€/(t_{MeOH}/yr)	451.16	846.73
Variable costs (€/t_{MeOH})	641.48	358.08
Fixed costs (€/t_{MeOH})	24.57	42.84
Direct CO_2 emissions (tCO_2/t_{MeOH})	0.090	0.695
Indirect CO_2 emissions (tCO_2/t_{MeOH})	0.136	0.073
Inlet CO_2 (tCO_2/t_{MeOH})	1.460	

Appendix F

Steam turbine

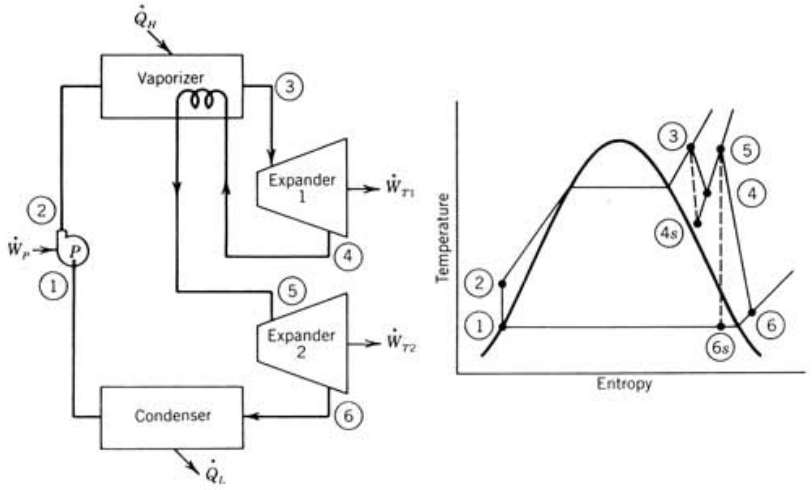

Figure F.1: Rankine cycle with reheat process

Table F.1: Rankine cycle with reheat values

nr	T [K]	p [bar]	h [kJ/kg]	s [kJ/kg K]
1	309	0.059	151	0.519
2	309	165	166	0.513
3	831	165	3453	6.481
4	580	29.762	3010	6.567
5	831	29.762	3586	7.395
6	309	0.059	2407	7.818

Appendix G

Sankey Diagram Liquid Air & Molten Salt Combined 100 MWh input

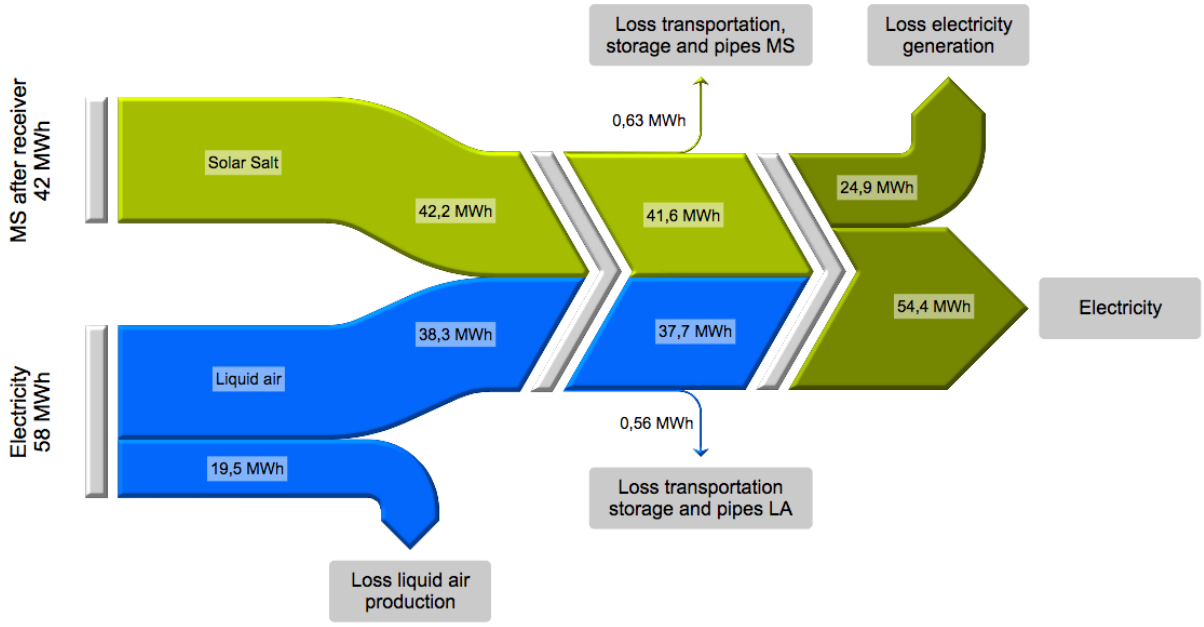

Figure G.1: Energy flow diagram with a total input of 100 MWh, 2^{nd} cycle argon